

Adaptive Learning and Robust Model Predictive Control for Uncertain Dynamic Systems

by

Kunwu Zhang

B.Sc., Hubei University of Science and Technology, 2013

M.Sc., University of Victoria, 2016

A Dissertation Submitted in Partial Fulfillment of the
Requirements for the Degree of

DOCTOR OF PHILOSOPHY

in the Department of Mechanical Engineering

© Kunwu Zhang, 2021

University of Victoria

All rights reserved. This dissertation may not be reproduced in whole or in part, by
photocopying or other means, without the permission of the author.

Adaptive Learning and Robust Model Predictive Control for Uncertain Dynamic Systems

by

Kunwu Zhang

B.Sc., Hubei University of Science and Technology, 2013

M.Sc., University of Victoria, 2016

Supervisory Committee

Dr. Yang Shi, Supervisor
(Department of Mechanical Engineering)

Dr. Daniela Constantinescu, Departmental Member
(Department of Mechanical Engineering)

Dr. Pan Agathoklis, Outside Member
(Department of Electrical and Computer Engineering)

ABSTRACT

Recent decades have witnessed the phenomenal success of model predictive control (MPC) in a wide spectrum of domains, such as process industries, intelligent transportation, automotive applications, power systems, cyber security, and robotics. For constrained dynamic systems subject to uncertainties, robust MPC is attractive due to its capability of effectively dealing with various types of uncertainties while ensuring optimal performance concerning prescribed performance indices. But most robust MPC schemes require prior knowledge on the uncertainty, which may not be satisfied in practical applications. Therefore, it is desired to design robust MPC algorithms that proactively update the uncertainty description based on the history of inputs and measurements, motivating the development of adaptive MPC. This dissertation investigates four problems in robust and adaptive MPC from theoretical and application points of view. New algorithms are developed to address these issues efficiently with theoretical guarantees of closed-loop performance.

Chapter 1 provides an overview of robust MPC, adaptive MPC, and self-triggered MPC, where the recent advances in these fields are reviewed. Chapter 2 presents notations and preliminary results that are used in this dissertation. Chapter 3 investigates adaptive MPC for a class of constrained linear systems with unknown model parameters. Based on the recursive least-squares (RLS) technique, we design an online set-membership system identification scheme to estimate unknown parameters. Then a novel integration of the proposed estimator and homothetic tube MPC is developed to improve closed-loop performance and reduce conservatism.

In Chapter 4, a self-triggered adaptive MPC method is proposed for constrained discrete-time nonlinear systems subject to parametric uncertainties and additive disturbances. Based on the zonotope-based reachable set computation, a set-membership parameter estimator is developed to refine a set-valued description of the time-varying parametric uncertainty under the self-triggered scheduling. We leverage this estimation scheme to design a novel self-triggered adaptive MPC approach for uncertain nonlinear systems. The resultant adaptive MPC method can reduce the average sampling frequency further while preserving comparable closed-loop performance compared with the periodic adaptive MPC method.

Chapter 5 proposes a robust nonlinear MPC scheme for the visual servoing of quadrotors subject to external disturbances. By using the virtual camera approach, an image-based visual servoing (IBVS) system model is established with decoupled image kinematics and quadrotor dynamics. A robust MPC scheme is developed to maintain the visual target stay within the field of view of the camera, where the tightened state constraints are constructed

based on the Lipschitz condition to tackle external disturbances.

In Chapter 6, an adaptive MPC scheme is proposed for the trajectory tracking of perturbed autonomous ground vehicles (AGVs) subject to input constraints. We develop an RLS-based set-membership based parameter to improve the prediction accuracy. In the proposed adaptive MPC scheme, a robustness constraint is designed to handle parametric and additive uncertainties. The proposed constraint has the offline computed shape and on-line updated shrinkage rate, leading to further reduced conservatism and slightly increased computational complexity compared with the robust MPC methods.

Chapter 7 shows some conclusion remarks and future research directions.

Table of Contents

Supervisory Committee	ii
Abstract	iii
Table of Contents	v
List of Tables	ix
List of Figures	x
Acronyms	xii
Acknowledgements	xiv
Dedication	xv
1 Introduction	1
1.1 MPC Overview	1
1.2 Robust MPC: Overview	2
1.2.1 Robust MPC with a worst-case objective function	3
1.2.2 Robust MPC with a nominal objective function	4
1.3 Adaptive MPC	6
1.3.1 Overview	6
1.3.2 Categories of adaptive control	7
1.3.3 Literature review	8
1.4 Self-Triggered MPC	21
1.5 Research Motivations and Contributions	23
2 Preliminary Results	26
2.1 Notations	26

2.2	Stability Theorem	27
2.2.1	Stability and asymptotic stability	27
2.2.2	Robust stability	28
2.3	MPC Design Strategy	30
2.3.1	Control invariance	30
2.3.2	Standard MPC	31
2.3.3	Adaptive min-max MPC	32
2.4	System definition	34
2.4.1	Set-membership parameter estimation with periodic state measurement	34
2.4.2	Zonotopic set computation	35
3	Adaptive MPC for A Class of Constrained Linear Systems with Parametric Uncertainties	36
3.1	Introduction	36
3.2	Problem Formulation	38
3.3	Uncertainty Estimation	38
3.3.1	Parameter estimation	38
3.3.2	Uncertainty set estimation	40
3.4	Adaptive Model Predictive Control	41
3.4.1	Error tube and constraint satisfaction	41
3.4.2	Construction of terminal sets	43
3.4.3	Construction of the cost function	45
3.4.4	Adaptive MPC algorithm	46
3.5	Simulation Results	50
3.6	Conclusion	51
4	Self-Triggered Adaptive Model Predictive Control of Constrained Nonlinear Systems: A Min-Max Approach	53
4.1	Introduction	53
4.2	Problem Formulation and Control objective	55
4.3	Self-Triggered Adaptive Min-Max MPC	56
4.3.1	Zonotope-based set-membership parameter estimator	56
4.3.2	ST-AMPC algorithm	59
4.3.3	Recursive feasibility and closed-loop stability	61

4.4	Illustrative Example	64
4.5	Conclusion	66
5	Robust Nonlinear Model Predictive Control Based Visual Servoing of Quadrotor UAVs	69
5.1	Introduction	69
5.2	System Modeling	71
5.2.1	Quadrotor dynamics	71
5.2.2	Image feature and IBVS dynamics	73
5.2.3	Control objective	74
5.3	Controller Design	75
5.3.1	Robust NMPC scheme	76
5.3.2	Feasibility and stability analysis	79
5.4	Simulation and Experiment	83
5.4.1	Numerical simulation	83
5.4.2	Experimental test	84
5.5	Conclusion	86
6	Trajectory Tracking Control of Autonomous Ground Vehicles Using Adaptive Learning MPC	88
6.1	Introduction	88
6.2	Problem Formulation	89
6.2.1	AGV kinematics	89
6.2.2	Tracking problem formulation	91
6.2.3	Control objective	92
6.3	Adaptive Learning MPC Algorithm	94
6.3.1	Parameter estimation	94
6.3.2	Adaptive MPC algorithm	96
6.4	Theoretical Analysis	98
6.4.1	Parameter selection	99
6.4.2	Recursive feasibility	100
6.4.3	Closed-loop stability	104
6.5	Numerical Example	107
6.6	Conclusion	110
7	Conclusion and Future Work	111

7.1 Conclusion	111
7.2 Future Directions	113
A Publications	115
Bibliography	117

List of Tables

Table 3.1	The comparison of system performance.	50
Table 4.1	Closed-loop performance comparison.	67
Table 6.1	The comparison of system performance.	110

List of Figures

Figure 1.1	The schematic diagram of MPC. The blue and red lines indicate the trajectories of pass states and inputs, while the green and yellow lines are trajectories of future states and inputs, respectively.	2
Figure 1.2	Adaptive control system architectures with indirect and direct adaption.	7
Figure 1.3	Adaptive control system architectures with indirect and direct adaptation.	8
Figure 3.1	The time evolution of the system state x_1	51
Figure 3.2	The time evolution of the system state x_2	51
Figure 3.3	Trajectories of control input u	52
Figure 3.4	The estimated uncertainty set Θ obtained at $k = 0, 3, 7, 20$	52
Figure 4.1	Trajectories of uncertainties.	65
Figure 4.2	Trajectories of system state x_t and triggering time instant t_k	67
Figure 4.3	Control input u_t	67
Figure 4.4	Comparison of uncertainty estimation at triggering time instants $t_k = 1, 5, 7, 36, 66, 79$	68
Figure 5.1	Reference coordinate frames.	72
Figure 5.2	The dual-loop control structure.	75
Figure 5.3	The trajectories of (a) ground target points in the real image plane and (b) the quadrotor in the inertia frame.	84
Figure 5.4	Time evolutions of (a) image moments s , (b) linear velocities in the virtual camera frame \mathbf{v}^v , (c) control inputs \mathbf{u} and (d) desired attitudes $\boldsymbol{\eta}_d$	85
Figure 5.5	The schematic diagram of the experimental setup.	86
Figure 5.6	The experimental trajectories of (a) image moments s , (b) linear velocities in the virtual camera frame \mathbf{v}^v , (c) control inputs \mathbf{u} and (d) desired Euler angles $\boldsymbol{\eta}_d$ for the inner loop.	87

Figure 5.7	The processing of images captured by the onboard camera at different time instants.	87
Figure 6.1	The structure of an AGV system.	91
Figure 6.2	Trajectories of the AGV's head point $\mathbf{p}_h(k)$	108
Figure 6.3	Control inputs $\mathbf{u}(k)$	108
Figure 6.4	Tracking errors $\mathbf{p}_e(k)$ and input errors $\mathbf{u}_e(k)$	109
Figure 6.5	Trajectories of the tracking errors $\mathbf{p}_e(k)$	109
Figure 6.6	Parameter estimation $\hat{r}(k)$ and $\sigma(k)$	110

Acronyms

AGVs autonomous ground vehicles

ARX autoregressive exogenous

CE certainty-equivalence

CLF control Lyapunov function

DARX dynamic auto-regressive with exogenous input

DP dynamic programming

FIR finite-impulse-response

FOV field of view

GP Gaussian process

GPS global positioning system

IBVS image-based visual servoing

IOSS input-output-to-state stability

ISpS input-to-state practically stable

ISS input-to-state stable

LMI linear matrix inequality

LPV linear parameter varying

LS least-squares

LTI linear time-invariant

MIMO multi-input and multi-output

MPC model predictive control

MPCI model predictive control and identification

NMPC nonlinear MPC

NN neural network

NPC neural predictive control

OCP optimal control problem

OED optimal experiment design

PE persistency of excitation

RCI robust control invariant

RHC receding horizon control

RLS recursive least-squares

RPI robust positive invariant

SPC subspace predictive control

SSDP successive semidefinite programming

SSF separable state feedback

ST-AMPC self-triggered adaptive MPC

ST-RMPC self-triggered robust MPC

UAVs unmanned aerial vehicles

VTOL vertical take-off and landing

ACKNOWLEDGEMENTS

Firstly, I would like to express my sincerest thanks to my supervisor, Dr. Yang Shi, a decent and professional scholar, for his continuous and intensive help, guidance, and encouragement during my Master's and PhD's study. He has been a great mentor in mapping my PhD journey, advising on academic research as well as career development, and connecting me with valuable resources I need to solve problems. His sense and passion for conducting world-class research and innovating in scientific research drive me to achieve better and higher. He always appreciates me on my every little progress/achievement and encourages me with great patience when I suffer from frustrations. I greatly appreciate him and feel extremely fortunate to be one of his students!

Next, I would like to thank the committee members, Dr. Daniela Constantinescu and Dr. Pan Agathoklis, for their insightful comments. They have been continuously supporting and helping me since my PhD Candidacy exam. I also would like to thank the external examiner, Dr. Jinfeng Liu, for his constructive suggestions in improving my dissertation.

Moreover, I'm privileged to know and work with my group members and friends from the Applied Control and Information Processing Lab (ACIPL) at the University of Victoria (UVic). Past senior students or current professors, Prof. Mingxi Liu, Prof. Xiaotao Liu, Prof. Bingxian Mu, Prof. Chao Shen, and Prof. Yuanye Chen, will be my role models. I am particularly grateful to Dr. Jicheng Chen, Dr. Changxin Liu, Tianyu Tan, Qian Zhang, Henglai Wei, Dr. Qi Sun, Xinxin Shang, Dr. Songlin Zhuang, Yaning Guo, Haoqiang Ji, Qi Zhou, Chen Ma, Huaiyuan Sheng, Zhuo Li, Xiang Sheng, Zhang Zhang, Chonghan Ma, Tianxiang Lu, Binyan Xu, Yufan Dai, and Yue Song, for their suggestions and comments that have greatly helped improve me. I want to thank you all for the sincere friendship and happy time we have spent.

Finally, I would like to thank my parents and uncle for their love and support.

Victoria, B.C., Canada

October, 2021

To my beloved parents

Chapter 1

Introduction

This chapter provides the introductory knowledge of [model predictive control \(MPC\)](#), robust MPC, and adaptive MPC. Then an overview of recent developments of adaptive MPC is presented, followed by the motivation and contribution of this thesis. The organization of this thesis is given at the end of this chapter.

1.1 MPC Overview

Recent decades have witnessed the phenomenal success of MPC in a wide spectrum of domains, such as process industries, intelligent transportation, automotive applications, power systems, cyber security and robotics [1–7]. This is because MPC offers a systematic and efficient way for complex systems to deal with hard system constraints while ensuring the optimal performance concerning prescribed performance indices [8–11]. MPC generates the control inputs by repeatedly solving a constrained and finite-horizon [optimal control problem \(OCP\)](#) in a receding-horizon fashion. Therefore, MPC is also called [receding horizon control \(RHC\)](#).

In the standard MPC framework, the control actions are obtained by solving the finite horizon OCP at each sampling instant based on the current measurement of the state x_k . Solving this OCP yields an optimal control sequence $\{u_{l|k}^*\}$ including N control actions, where N is the prediction horizon and $u_{l|k}^*$ denotes the prediction of the control input u_{k+l} . Then the first element of this optimal control sequence is applied to the system, i.e., $u_k = u_{0|k}^*$, as shown in Figure 1.1. Repeating this computation process at the next sampling time instant based on the new measurements yields new optimal control actions. Therefore, MPC is naturally the feedback control law implemented implicitly, which is different

from conventional feedback control strategies that provide offline computed control laws. Specifically, if the control actions are computed by solving the open-loop OCP, the corresponding MPC formulation is referred to as the *open-loop MPC* formulation. With this flexible formulation and simple concept, MPC provides an effective and efficient methodology to deal with system constraints and has become an attractive multivariable optimal control method.

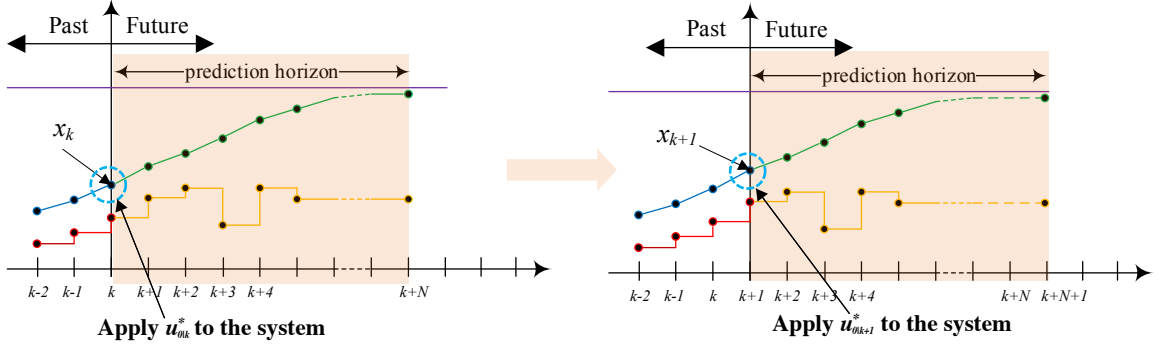


Figure 1.1: The schematic diagram of MPC. The blue and red lines indicate the trajectories of pass states and inputs, while the green and yellow lines are trajectories of future states and inputs, respectively.

As introduced in [11], an alternative to the solution obtained by solving the open-loop OCP for the MPC problem is to use **dynamic programming (DP)**. Compared with the open-loop OCP solution where the decision variable is a sequence of control actions $u_{l|k}^*$, the DP solution considers a sequence of control policies $\tau_{l|k}(\cdot)$ as the decision variable. Therefore, this MPC formulation is also referred to as the *closed-loop MPC* formulation or the *feedback MPC* formulation. Note that, without considering uncertainties, the open-loop and closed-loop MPC formulations are equivalent, i.e., $u_{0|k}^* = \tau_{0|k}(x_k)$.

1.2 Robust MPC: Overview

When uncertainties are present, the superiority of feedback control for handling uncertainties renders the closed-loop MPC formulation superior to the open-loop MPC formulation, which, however, makes the associated OCP much more complicated, especially for high-dimensional systems [2]. Although standard closed-loop MPC has a certain level of robustness against sufficiently small uncertainties due to its receding-horizon nature [12], its robustness may still be inadequate for practical applications because of its deterministic formulation of the OCP. Motivated by this fact, robust MPC has been developed to offer

computationally tractable MPC frameworks for handling system uncertainties in a systematic way.

According to the objective function to be minimized in the OCP, existing results on robot MPC can be briefly classified into two categories: Robust MPC with the maximized objective function and robust MPC with the nominal objective function. In the following, we present a brief review of several representative results on each category of robust MPC schemes.

1.2.1 Robust MPC with a worst-case objective function

The first category is to consider the worst-case objective function that is maximized over all possible uncertainties. This is achieved by formulating a min-max OCP, which is also referred to as min-max MPC [13, 14]. Therefore, min-max MPC can efficiently handle various types of uncertainties, including additive disturbances and parametric uncertainties. The min-max MPC approach is first proposed in [15] for the single-input-single-output system, and further extended to general linear systems [16, 17] and [linear parameter varying \(LPV\)](#) systems [18].

An open-loop min-max MPC scheme is proposed by [19] for a stable nonlinear system. This scheme may have a relatively high computational burden. In addition, the resulting controller may be conservative due to the small region of attraction and the open-loop prediction. To deal with the conservative issue, the feedback (or closed-loop) min-max MPC scheme is developed for the constrained nonlinear systems in [13, 20]. In this setup, the feedback is incorporated into the predictions. Therefore, the optimal solution, which is a sequence of control laws depending on the predicted system states, is obtained by solving the min-max optimization problem. It is shown that the resulting closed-loop system by applying the feedback min-max MPC method is [input-to-state practically stable \(ISpS\)](#). Another alternative approach called multi-stage MPC [21] is to explicitly take into account available new measurements at future sampling time instants. This is achieved by approximating the enumeration of the uncertainty realization as a scenario tree. However, the computational complexity of the aforementioned min-max MPC methods restricts their practical applications. Several methods for reducing the computational burden have been reported in the literature. For example, instead of considering the worst-case realization of the uncertainty, [17] solves the min-max optimization problem by only considering the extreme disturbance realizations. Therefore, the computational load can be significantly reduced. But this method is only suitable for low-dimensional systems and very short prediction

horizons. By designing a specific feedback policy in [22], the min-max MPC optimization problem is equivalently transferred to a convex and tractable optimization problem, thereby improving the computational efficiency. An overview of results on min-max MPC can be found in [14].

1.2.2 Robust MPC with a nominal objective function

An alternative to the worst-case objective function is the nominal cost function, as used in standard MPC. The robust MPC methods falling within this category usually rely on the tightened system constraints to guarantee constraint satisfaction for all possible uncertainties. Depending on the decision variable of the MPC optimization problem, the constraint tightening strategies in robust MPC can be classified as the open-loop methods and closed-loop methods.

Tube-based MPC

A typical example of MPC methods using the closed-loop constraint tightening strategies is tube-based MPC. As aforementioned, the closed-loop MPC is superior to open-loop control for uncertain systems. The main difficulty of closed-loop MPC is the high computational complexity arising from the use of control policy as the decision variable of the MPC optimization problem. Tube-based MPC is developed to address this problem by sacrificing, to some extent, optimality for simplicity. This is achieved by employing the parameterization of the locally stabilizing feedback control law in the MPC OCP. In addition, this feedback control law is also employed to construct the tightened state constraints such that the trajectories related to all possible realization of uncertainties are restricted within a small neighborhood of the designed nominal trajectory. Therefore, tube-based MPC has a similar order of computational complexity to standard MPC while providing less conservative closed-loop performance. The concept of tubes is originally presented in [23, 24], and tube-based MPC is explicitly proposed in [25, 26].

The essential idea of tube-based MPC is to tighten the system constraint \mathcal{X} based on a new system model stabilized by a feedback controller that the constraint satisfaction is guaranteed for all possible realization of uncertainties. This is achieved by constructing a positive invariant set \mathcal{S} [27] for the error between the real system state x_{k+l} and the predicted state $x_{l|k}$ based on the local feedback control law. For example, in [26], the state constraint and the input constraint are tightened as $\mathcal{X}_T = \mathcal{X} \ominus \mathcal{S}$ and $\mathcal{U}_T = \mathcal{U} \ominus K\mathcal{S}$, respectively, where K is a stabilizing feedback gain and $v_{k+l|k}$ is the control variable and \ominus is

the Pontryagin set subtraction. Then the closed-loop stability can be ensured by choosing a suitable objective function. Later in [28], an extension of the tube-based MPC method [26] is proposed by considering the initial condition of the nominal state trajectory as the decision variable of the MPC optimization problem, leading to the guarantee of robust exponential stability. This tube-based MPC method [26] is extended to solve the output feedback problem for constrained linear time-invariant systems [28] and time-varying systems [29]. A nonlinear version of the tube-based MPC is discussed in [30].

In the aforementioned tube-based MPC methods, the feedback gain, K , and the positive invariant set \mathcal{S} are calculated offline. As a result, the state cross-section \mathcal{X}_T and the control cross-section \mathcal{U}_T are determined offline and fixed during the online optimization problem. Therefore, this framework has the same order of computational complexity compared with standard MPC, which is referred to as “rigid tube-based MPC”. However, when considering parametric uncertainties, it is difficult to approximate the effects of state-dependent uncertainties on prediction accurately, thus resulting in a conservative performance of rigid tube-based MPC. This consideration motivates the development of dynamic tube-based methods including homothetic tube-based MPC [31–33], elastic tube-based MPC [34, 35] and [separable state feedback \(SSF\) tube-based MPC](#) [36–38], where the tube cross-sections are constructed, optimized, and updated in an online manner. This is achieved by considering the tube parameters as the decision variables of the MPC optimization problem. In homothetic tube-based MPC, the shapes of the state cross-sections $\mathcal{X}_{T,k}$ and the control cross-sections $\mathcal{U}_{T,k}$ are determined offline, but the size of each tube cross-section is determined by a scalar to be updated online. But in elastic tube-based MPC, the tube parameter is a vector. Therefore, the shape and size of each tube cross-section in elastic tube-based MPC can be optimized online. SSF tube-based MPC parameterizes the prediction of states and control inputs based on the sequences of partial states and control inputs. As a result, the tube cross-sections $\mathcal{U}_{T,k}$ and $\mathcal{X}_{T,k}$ are the collections of the tube cross-sections associated with partial states and control inputs. Compared with elastic tube-based MPC, SSF tube-based MPC allows the further optimized shape of each tube cross-section, thereby leading to improved performance. Note that, in the aforementioned dynamic tube-based MPC methods, the optimal tube cross-sections are constructed by introducing extra decision variables into the MPC optimization problem, which inevitably increases the computational complexity of the MPC algorithm. Consequently, a judicious trade-off between computational complexity and conservatism needs to be considered for the practical implementation of dynamic tube-based MPC.

Open-loop constraint tightening

Essentially, tube-based MPC is a kind of feedback MPC framework synthesized with the constraint tightening strategy. Indeed, tube-based MPC relies on the suitable parameterization of the control input to construct the bounded tube cross-sections. Finding such a control parameterization is relatively easy for linear systems. However, this is difficult for nonlinear systems due to the intrinsic complexity of nonlinearities. An alternative to tube-based MPC for nonlinear systems is to incorporate the constraint tightening strategy into the open-loop MPC framework, which is referred to as the constraint tightening method. For example, [39, 40] construct the sets for the error between the real system state and the predicted system state based on the Lipschitz constant and then employ these sets to tighten the state constraint. Instead of designing the error sets, [41] proposes a robustness constraint for the predicted states based on the Lipschitz constant. Then the authors develop a robust distributed MPC scheme for a large-scale nonlinear system, where the predicted state trajectory is bounded via a monotonically decreasing function. Compared with tube-based [nonlinear MPC \(NMPC\)](#) methods, although these constraint tightening schemes [39–41] may have relatively conservative control performance due to the open-loop fashion, the optimization problems arising from these MPC schemes are less complicated. Therefore, these open-loop constraint tightening strategies are promising for practical applications with limited computational power.

1.3 Adaptive MPC

1.3.1 Overview

Compared with standard MPC, robust MPC focuses on ensuring the theoretical properties of controlled systems, such as the stability, feasibility, and constraint satisfaction, for all possible realizations of uncertainties. The techniques used for dealing with uncertainties in robust MPC frameworks usually require extensive offline computation, such as the calculation of terminal ingredients and tightened constraints, based on the *a priori* knowledge of uncertainties. The system uncertainties should be bounded and have a deterministic description to enable the worst-case analysis. As a result, the performance of robust MPC is inherently conservative when the uncertainty bound is inaccurate or time-varying, especially for parametric uncertainties due to the difficulty of accurately estimating the impacts of parametric uncertainties when the system state evolves over time. Therefore, adaptive

MPC, which aims at systematically refining the description of uncertainties online in the robust MPC framework, e.g., [42–44], has emerged as a promising solution for handling uncertainties with inaccurate prior knowledge.

1.3.2 Categories of adaptive control

As the seamless integration of MPC and system identification, adaptive MPC inherently shares some general features of adaptive control schemes. Before delving into details of adaptive MPC, we first recall several categorizations of adaptive control approaches in the following to help understand the merits of adaptive MPC schemes.

From the perspective of control input effects, the adaptive MPC control schemes can be categorized into dual methods and non-dual methods, as shown in Figure 1.2. Adaptive dual control aims to cautiously drive the system output to its desired value and sufficiently excite the system to accelerate the system identification process, thereby compromising parameter estimate convergence and control performance [45]. As a result, the dual control is active for both control and estimation purposes, which is also referred to as the active learning method. On the other hand, most adaptive non-dual control methods are based on the *certainty-equivalence (CE) principle*, in which the parameter estimates are directly used in the control system design as if they are the true system parameters [46, 47]. From the estimation perspective, the estimation in the non-dual method is open-loop and relies on the *persistency of excitation (PE)* of system states to ensure the estimation performance. Therefore, the non-dual method is also named as the passive learning method. As a result, the adaptive non-dual control method is relatively easier to implement but more conservative compared with the dual control method.

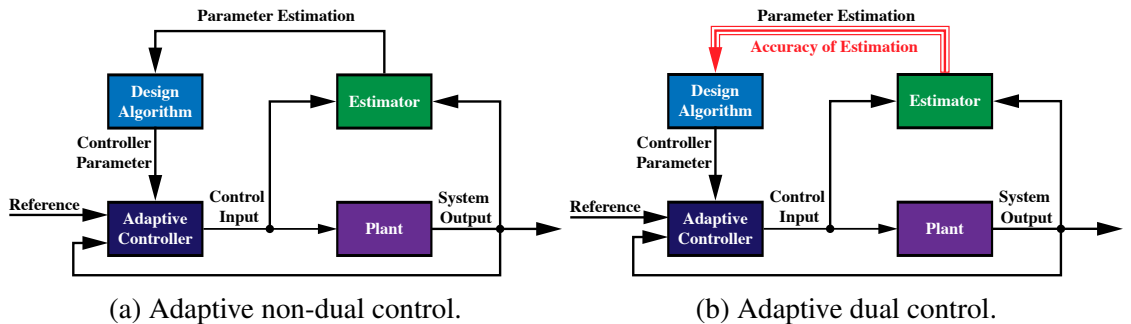


Figure 1.2: Adaptive control system architectures with indirect and direct adaption.

From the perspective of control system architecture, adaptive control methods can be grouped into direct and indirect methods. As shown in Figure 1.3a, in the indirect adaptive

control framework, the estimator updates the system parameter. The adaptation process is decomposed into separate steps for parameter estimation and controller parameter calculation. The direct adaptive control illustrated in Figure 1.3b employs a direct estimator for unified parameter estimation and controller parameter updates. Direct adaptive control usually relies on a nested bi-level optimization problem for simultaneous system identification and control parameter updates, thereby potentially outperforming indirect methods. But designing such a bi-level optimization problem is relatively complicated, especially for nonlinear systems. Therefore, indirect adaptive control methods are more readily applicable to complicated applications.

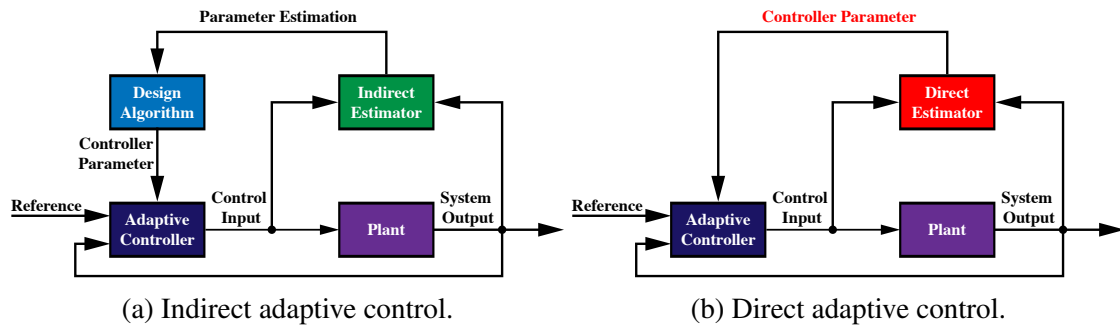


Figure 1.3: Adaptive control system architectures with indirect and direct adaptation.

1.3.3 Literature review

As an emerging topic, many research efforts have been devoted to the development of adaptive MPC, intending to guarantee the closed-loop properties, including closed-loop stability and recursive feasibility, and estimation convergence. Based on the categorizations of adaptive control presented in the previous subsection, the recent results on adaptive MPC can be categorized into three main groups: Active learning-based adaptive MPC, passive learning-based adaptive MPC, and data-driven MPC. An overview of recent results on each category is presented in the following.

Active learning-based adaptive MPC

In adaptive control, the informative operating data can be obtained by actively probing the uncertain system. This probing effect is also referred to as excitation, experimentation, exploration, or active learning [48]. Therefore, the active learning-based adaptive MPC methods focus on improving system learning by increasing the amount of information generated by the control inputs. A common solution to generate the informative operating data

is by guaranteeing the system excitation [49]. Another solution is via [optimal experiment design \(OED\)](#) under the closed loop [50].

Adaptive MPC with persistent excitation. In adaptive MPC, the probing feature of the control inputs is added by reformulating the MPC optimization problem or by imposing the system excitation on control inputs directly. Although adding this probing feature to control inputs inevitably leads to the undesired system excitation deteriorating control performance, this probing effect can improve system learning and further enhance future control performance. Therefore, the active learning-based method potentially improves the control performance compared with the methods without involving active learning. A more detailed discussion about the exploration-exploitation trade-off in MPC with active learning can be found in a recent survey paper [51].

The idea of adding the excitation constraint in the optimization problem is originally proposed in [52], where a simultaneous [model predictive control and identification \(MPCI\)](#) approach is developed for processes modeled by [finite-impulse-response \(FIR\)](#) models. The unknown system parameters are identified based on the [least-squares \(LS\)](#) technique. The excitation constraint in [52] has a form of quadratic matrix inequalities, thereby leading to a non-convex optimization problem. Later in [53], the approach in [52] has been extended to handle [dynamic auto-regressive with exogenous input \(DARX\)](#) processes, where an excitation constraint depending on process inputs only is developed. The authors in [53] also propose a [successive semidefinite programming \(SSDP\)](#) algorithm to solve the non-convex optimization online. The theoretical analysis of the optimality of this SSDP algorithm is presented in [54]. In [55], an extension of the MPCI method [53] is proposed to reduce the computational complexity by expressing the PE constraint in the frequency domain. A [neural network \(NN\)](#) based nonlinear adaptive MPC algorithm is proposed in [56], where the nonlinear process is modeled by a dynamic radial basis function network and then identified by an adaptive fuzzy means algorithm. This adaptive MPC optimization problem is augmented by a PE constraint presented in [52] for the output of hidden nodes to improve the estimation performance.

A multiobjective optimization-based adaptive MPC framework is proposed in [57], where the PE condition is considered as the primary objective. This formulation can avoid the potential feasibility problem caused by the excitation constraint while ensuring sufficient system excitation. In [58, 59], a two-phase optimization-based adaptive MPC algorithm is proposed. In the first phase, a set of exciting control inputs with acceptable closed-loop performance is obtained by solving the nominal MPC problem. Among them,

the control input that maximizes the measure of the information matrix will be implemented to the system. This adaptive MPC algorithm can provide a certain level of probing effect while ensuring the loss of closed-loop performance within a prescribed range.

Due to the inherent advantage of MPC, the excitation constraint can be exactly handled, while the loss of control performance can be minimized. Generally, the input excitation level is decided by a tuning parameter. Therefore, it is difficult to systematically decide whether the input excitation is necessary, which inevitably increases the conservatism of adaptive MPC. To address this issue, the authors in [60] propose an adaptive MPC strategy where the PE constraint is inactive over the prediction horizon. Compared with the MPC methods, e.g., [52, 53], a backward-looking input excitation constraint is designed in [60] such that the PE constraint is only imposed on the first element in the control sequence. Therefore, there always exists a periodic feasible input sequence that guarantees the recursive feasibility of the adaptive MPC algorithm in [60].

Based on the idea of zone-tracking MPC presented in [61], a stabilizing adaptive MPC scheme is proposed in [62]. The main feature of this work is to steer the system state into the invariant set such that the system can be excited safely without destroying the closed-loop stability. This invariant set is constructed based on the target excitation condition. Therefore, the conflict between the system excitation and stabilization can be mitigated while the recursive feasibility is guaranteed. In [63, 64], an integration of tube-based MPC [28] and PE constraint presented in [60] is proposed. Under the assumption that the excitation feature of control inputs cannot be eliminated by the feedback control policy in tube-based MPC, this formulation inherits the closed-loop properties of tube-based MPC. The authors in [65] propose an MPC strategy with looking-forward PE. The main feature of this method is to track a periodic PE reference trajectory, allowing to preserve the system excitation without relying on the non-convex PE constraint. The periodic PE reference trajectory is generated around the steady state such that the persistently exciting control inputs can be implemented safely. Under the assumption that reference tracking control law and the reference state satisfy the incremental stability condition, the adaptive MPC scheme in [65] can drive the system state to the PE reference trajectory exponentially.

MPC with integrated experiment design. The objective of experiment design is to maximize the information generated by the experiment. A distinguishing feature of MPC with integrated experiment design is to take the estimation accuracy into account in the MPC formulation such that the generated control inputs have dual effects for regulating and probing the closed-loop system [66]. Instead of exciting all directions in PE constraint based adap-

tive MPC, OED-based adaptive MPC excites directions affected by uncertainties, providing less conservative control performance.

In [67], an adaptive MPC scheme is proposed based on the CE-based MPC formulation, where a standard MPC cost function is augmented with a term related to the predicted covariance matrix to minimize the variance of the parameter estimates. As a result, the system probing is only performed when the estimation error is large or when the observed information is insufficient for system identification. Therefore, it is not necessary to persistently excite the control inputs. This method has been extended in [48] for orthonormal basis-function models. Compared with [67], the method in [48] depends on the future control inputs for the exact propagation of the conditional distribution of the uncertain parameters over the prediction horizon, thereby avoiding heuristic additions to the cost function. The authors in [68] propose a Lyapunov-based MPC approach for constrained linear uncertain systems described by a polytopic Linear Difference Inclusion. The cost function in this work is modified by adding a term related to the predicted parameter estimation error covariance. Therefore, the control inputs that minimize the objective function can excite the system. In addition, by combining the **robust control invariant (RCI)** set with the Lyapunov-based constraint, a feasible set is designed in [68] to guarantee the recursive feasibility and asymptotic stability.

A CE-based MPC formulation is augmented with OED is proposed in [69, 70] for nonlinear systems subject to process disturbances and measurement noises. A so-called self-reflective MPC scheme is presented in this work with the modified objective function, where the information of adjoint forward and backward propagation of states is employed in MPC to compute second-order moment expansions of the expected loss of optimality of the CE-based MPC. Consequently, both the control performance and the approximation of expected loss can be minimized. An integrated OED-based MPC for nonlinear systems subject to an uncertain model structure is presented in [71], where the cost function is modified to include and optimize a measure of the Bayes risk of choosing incorrect models. Therefore, the future uncertainty of the model structure is explicitly considered in [71], which mitigates the conflict between system probing and control. In [72] the authors present a multiobjective economic MPC formulation for nonlinear systems. In this formulation, the learning cost is considered as the objective function to improve system learning, and the primary MPC cost is bounded by an average constraint. Therefore, a simple trade-off between the control performance and learning performance can be achieved while the guaranteed safety and closed-loop performance are preserved.

Passive learning-based adaptive MPC

A distinguishing feature of passive learning-based adaptive MPC is that the control inputs have no probing effects for system learning. Therefore, there is no conflict between the probing activity and control activity of the control inputs. The uncertainty reduction is a side-effect of the control action. Literature in this category aims at reducing the conservatism of MPC algorithms based on system learning with guaranteed non-increasing estimation errors. Based on different MPC formulations, a review of several representative results on passive learning-based adaptive MPC is presented in the following.

MPC with the updated model. An early work on adaptive MPC is proposed in [73] by directly augmenting a standard NMPC formulation with an LS-based parameter estimator. A controllable perturbation of parameter estimation is designed to generate sufficient information for the convergence of model adaption. It is shown in [73] that the asymptotic stability can be guaranteed when the estimation error converges to zero. For unconstrained systems subject to unknown system parameters, in [74], an integrated perturbation analysis strategy and sequential quadratic programming technique are proposed for improving the computational efficiency of adaptive MPC. The parameter estimate in this formulation is considered as the perturbation in the optimization problem. Based on the neighboring extremals approach [75], the solution to the MPC optimization problem is computed with a predictor-corrector form, where the correction term is calculated based on the Hamiltonian for the optimization problem. This allows for achieving high computational efficiency when the perturbations arising from parameter estimates are small.

In [76, 77], an adaptive MPC formulation with a [control Lyapunov function \(CLF\)](#) based constraint is proposed for unconstrained nonlinear systems subject to unknown parameters. This Lyapunov-based constraint is constructed based on an [input-to-state stable \(ISS\)](#) controller associated with the parameter updating law and imposed on the first element of the control sequence [77] or the terminal state [76]. This kind of CLF-based adaptive MPC formulation inherits the guaranteed closed-loop stability of the ISS controller. But this method relies on the existence of the ISS controller. Designing such an ISS controller is difficult for constrained systems.

For unconstrained linear systems, an adaptive MPC approach is proposed in [78] for linear systems subject to unknown state and input matrices, where the closed-loop stability and bounded estimation error can be guaranteed via imposing additional constraints on control inputs. This approach has been extended to handle input constraints [79] and

incremental input constraints [80] by appropriately tightening the input constraint. Based on the ISS stabilizing MPC method [81], an adaptive MPC scheme is developed in [82] for input-constrained neutrally stable linear systems. The prediction model is updated by employing the switching logic presented in [83] to minimize the output errors.

When considering state and input constraints, a so-called indirect adaptive MPC method is proposed in [84] for state and input-constrained linear systems, where an RCI set is employed to ensure the recursive feasibility. By designing the terminal cost function and terminal constraint using a parameter-dependent Lyapunov function [85], the closed-loop system is ISS with respect to the estimation error. This method is extended to handle constrained linear systems subject to both unknown state and input matrices in [86] by using a less conservative RCI set. The authors have further proved that the closed-loop system is asymptotically stable when the estimation error is sufficiently small. In [87, 88], a decreasing horizon tube-based MPC method [89] is augmented by a parameter estimator presented in [78]. The tube cross-sections are designed based on the outer approximation of the reachable set for the disturbance arising from the model mismatch. Consequently, the resultant adaptive MPC scheme inherits the closed-loop properties of the original tube-based MPC method. A combination of the min-max MPC method [90] and the parameter estimator proposed in [78] is provided in [91], where the robust constraint satisfaction is guaranteed via the min-max optimization. An extension of the adaptive MPC method [78] is proposed in [92], where a Levenberg–Marquardt algorithm is employed to improve the performance of parameter estimation.

In [93, 94], the unmodeled dynamics is represented as the external disturbance. Then an adaptive MPC algorithm is developed by augmenting the standard tube-based MPC formulation [28] with a suitable system identification method. The authors in [95] consider a constrained nonlinear system subject to additive disturbances. By approximating the nonlinear system as an uncertain Quasi-Linear Parameter Varying system, a tube-based adaptive MPC algorithm is developed for the regulation problem.

MPC with the updated model and constraints. The aforementioned works only employ the identified model in MPC to improve the prediction accuracy. The constraints used for ensuring closed-loop stability and recursive feasibility are developed offline based on the initial knowledge of the uncertainty. Therefore, these methods are relatively conservative when the estimation error becomes small.

A promising solution to this issue is to update the constraints in the MPC optimization problem by efficiently using the information generated from system learning. In [96], the

authors consider a class of constrained continuous-time linear systems with a controllable canonical form. An adaptive MPC formulation is developed by augmenting a comparison-based MPC method [97] with an online parameter estimator. The comparison model is updated by using the parameter estimation and then employed to tighten the state and input constraints such that the recursive feasibility can be ensured. The closed-loop stability is guaranteed by updating the feedback gain based on the parameter estimate. This method is extended to tackle single-input single-output discrete-time linear systems in [98].

The set-membership system identification is also widely employed in adaptive MPC. Compared with the point-estimation of unknown parameters, the set-membership estimation method aims to update the parameter estimate as well as the set description of uncertainties. Early works on augmenting robust MPC with set-membership system identification are presented in [99, 100]. The authors in [100] propose a set-valued adaptation strategy for both point estimation and set estimation. The set of parametric uncertainty being adapted is described as a ball whose center and radius are updated based on the available measurements. A Lipschitz-based internal model is established in this method to generate an uncertainty cone around the nominal state based on the estimated uncertainty set. Then by restricting this uncertainty cone within the state constraint and the terminal constraint, robust constraint satisfaction and closed-loop stability can be guaranteed. A similar adaptive MPC method is presented in [99] with reduced conservatism by considering the worst-case realization of uncertainty via the min-max optimization. But the methods in [99, 100] rely on an assumption on the terminal ingredients. This assumption is relaxed in [101, 102], where the terminal constraint and the terminal cost function are parameterized as the functions of parameter estimates rather than the functions of the estimated uncertainty set. The extensions of the min-max method [99] and the Lipschitz-based approach [100] are presented in [102] with a rigorous analysis of closed-loops stability and recursive feasibility, which is further extended to continuous-time nonlinear systems with exogenous disturbances [103] and economic objective function [104], and discrete-time nonlinear systems [105]. In [106, 107], the authors propose a min-max adaptive MPC scheme for nonlinear systems subject to external disturbances, where a piecewise constant adaptive law is employed to contract a set-valued description of additive disturbances. The min-max adaptive MPC for constrained linear systems can be found in [108].

Recently, in [109] an output feedback MPC strategy with set-membership identification is presented for stable **multi-input and multi-output (MIMO)** systems subject to measurement noises. A set of admissible models consistent with available measurements and uncertainty descriptions is updated online and employed in MPC to improve the knowledge of

the system dynamics. This model set is also used to tighten the input and output constraints. Based on these tightened constraints and the equality terminal constraint, the recursive feasibility of the resultant adaptive MPC algorithm can be guaranteed. The method [109] is applied to FIR systems with chance constraints in [110] by approximating the chance constraints as the deterministic constraints. An extension of [110] is presented in [111], where the sparsity information of the unknown system parameters is employed to improve the closed-loop performance. Another extension of the result [109] is presented in [112] for time-varying MIMO systems. Based on the upper bound of the parameter's changing rate, the estimated admissible model sets can be inflated over the prediction horizon. Therefore, the time-varying nature of the MIMO system can be handled. In [113], a learning MPC formulation [114] for iterative tasks is augmented with the set-membership system identification method presented in [109].

The authors in [115] firstly propose a homothetic method strategy integrated with set-membership identification. One distinguishing feature of this method is that a parameterization of the state tubes is involved in MPC such that the state tubes are constructed online and optimized with respect to the set-valued description of uncertainty. Then by designing a λ -contractive and invariant terminal set in [115], the recursive feasibility of the adaptive MPC algorithm and practical stability of the closed-loop system can be guaranteed. The results in [115] are extended and refined in [42] by developing a set-membership strategy including both point estimation and set estimation. The min-max cost is replaced by a CE cost to reduce the computational complexity. The formulation allows for the guaranteed finite gain ℓ_2 stability, which is novel in the literature on adaptive MPC.

In [116], an adaptive MPC scheme is presented where a set-membership parameter estimation with reduced computational complexity is developed by computing a hypercube to bound the parametric uncertainty. This method is based on the robust MPC method in [33], where the shape of the tube is fixed while the size of the tube is propagated by a scalar function in MPC. Therefore, the resulting adaptive MPC scheme is relatively conservative but has reduced computational complexity compared with the method in [42]. In [43], a tube-based adaptive MPC algorithm is presented for the nonlinear system by augmenting the robust MPC method [33] and the set-membership system identification strategy presented in [116]. Similar to [42], the state tube is constructed based on an incremental Lyapunov function and a contraction rate for the nominal system. But the propagation of tube size in MPC is based on the parameter estimate, thereby leading to improved closed-loop performance. The formulations in [43, 116] can ensure finite gain ℓ_2 stability of the closed-loop system.

For adaptive MPC methods in [42, 115, 116], the shapes of tubes are decided offline and the sizes of tubes are optimized online. Later in [44, 117, 118], a more flexible representation of the tube cross-section is considered, where both the shape and size of state tubes are optimized online based on a tube-based MPC formulation presented in [35]. A class of linear systems subject to parametric and additive uncertainties is considered in [117], where the tube-based MPC formulation [35] is augmented with a set-membership identification system identification method [119] and the PE constraint presented in [60]. A min-max cost function is considered in this formulation to reduce the conservatism. By designing an upper bound for the terminal tube parameter and the terminal state in [117], the resulting adaptive MPC algorithm is recursively feasible, and the closed-loop system is ISS. The results in [117] are extended in [118] with reduced computational complexity by convexifying the PE constraint. In addition, the point estimation of the unknown parameter is calculated in [118]. Therefore, the min-max cost is replaced by a CE cost to reduce the computational complexity further. Instead of designing the state tubes, the authors in [44] construct the tube for the disturbances arising from the parametric uncertainty. A set-membership parameter estimator derived from [105] is employed to update the uncertainty set. The terminal constraints and the cost function are updated in [44] based on the estimated uncertainty set to improve the closed-loop performance.

A recent result on combining stochastic MPC with set-membership system identification is presented in [120], where a class of linear systems subject to hard constraints and chance constraints is considered. The parameter estimator used in this work is derived from the set-membership scheme presented in [109] and extended to handle the time-varying unknown parameters. A tightened deterministic constraint is developed by using Bonferroni's inequality [121] to ensure the satisfaction of chance constraints. The recursive feasibility and closed-loop stability are guaranteed by choosing the appropriate terminal ingredients.

Data-driven MPC

Most of the aforementioned results on adaptive MPC methods are *model-based* which rely on the *a priori* knowledge of the system model structure. Indeed, the system identification has to be conducted before the calculation of control inputs based on the input and state history. However, it may be difficult or even impossible to conduct the system identification in some practical problems since the data may not be informative enough. In contrast, *data-driven* control aims to compute the optimal control input compatible with the collected data, thereby can be applied without the *a priori* knowledge of the system model [122].

Therefore, data-driven MPC is also of interest in adaptive MPC to enable a model-free operation [123].

In this subsection, an overview of recent development on data-driven MPC is presented. We firstly review the existing results on *indirect data-driven MPC* which have a two-step formulation consisting of sequential system identification and model-based control. Then we focus on *direct data-driven MPC* where the MPC optimization problem is formulated from the collected data directly without conducting the system identification.

Indirect data-driven MPC. In indirect data-driven MPC, the system model is firstly identified, then the control input is calculated based on the identified model. Identifying the system model from data has been extensively studied in the field of system identification, e.g., [124, 125]. Due to the inherent features of data-driven learning algorithms, data-driven MPC has attracted increasing attention in recent years [123]. The first work on data-driven MPC is proposed in [126] for unconstrained **linear time-invariant (LTI)** systems by integrating MPC with a subspace identification algorithm [127]. Therefore, this formulation is also named **subspace predictive control (SPC)**. Since predicting future behaviors in SPC is achieved based on the low-rank Hankel matrix constructed directly from the collected data, the parametric representation of the dynamic system is not required. Later in [128], the SPC method [126] is extended to handle the input and output constraints by formulating a proper quadratic programming problem. A disturbance compensation mechanism is also developed in [128] to handle the measured disturbances. In [129], an SPC scheme is developed for Hammerstein LTI systems, where a set of kernel matrices are constructed to approximate the Hammerstein nonlinearities. A comprehensive introduction to SPC can be found in [130], and application of SPC to some industry issues can be found in [131, 132]. Note that the aforementioned SPC methods only show empirical success. It is still difficult to theoretically guarantee their closed-loop performance. For unconstrained LTI systems, the authors in [133] propose a necessary and sufficient small-gain stability condition for the closed-loop system. But for the general constrained LTI systems, ensuring the recursive feasibility and closed-loop stability is still a challenging problem.

Similar to subspace identification, the **Gaussian process (GP)** has also attracted increasing attention in data-driven MPC. Compared with the subspace identification, the GP model can be used to describe nonlinear systems, thereby potentially having broader applications [134]. The use of the GP model for the prediction in MPC optimization is firstly presented in [135]. Later, the GP regression is incorporated with explicit MPC [136], one-step MPC [137] and fault-tolerant MPC [138]. The combination of Sparse Spectrum GP regression

and stochastic MPC is presented in [139]. Based on Pontryagin’s maximum principle, the authors in [140] propose a new integration of GP and stochastic MPC with guaranteed optimality. Instead of using the GP model to describe the dynamic system, in [141] the GP regression is used to learn and compensate the periodic time-vary disturbance. This result is further refined in [142] for nonlinear systems subject to chance constraints.

For the modeling of complex nonlinear systems, NN is also an attractive tool. Many research efforts have been made to incorporate the NN model into the MPC framework, which is referred to as **neural predictive control (NPC)**. The early results on this topic aim to use NN to model the nonlinear term in the system model such that the linear MPC can be applied, e.g., [143, 144]. Later in [145] a recurrent NN is employed to establish the prediction model for nonlinear systems. The authors in [146] combine the offline step test data and online collected data to establish the prediction model in NMPC based on the feedforward NN. In [147], an NPC scheme is developed for the path planning of mobile robots, where a multi-layer wavelet NN is employed to model the car-like mobile robot. The combinations of continuous-time recurrent NN and NMPC are proposed in [148]. The authors in [149] develop an NPC scheme based on two recurrent NNs, including the echo state network and the simplified dual network. The echo state network is used for identifying the dynamic model used in MPC, while the simplified dual network is adopted to solve the MPC optimization problem with the guarantee of optimality. In [150], the self-organizing recurrent radial basis function based recurrent NN is leveraged within the NMPC framework, where both the structure and the parameter of the NN are updated concurrently to improve the modeling accuracy. This result is further extended in [151] with improved computation efficiency by using the multistructure radial basis function.

The aforementioned works investigate the point estimate of the dynamic model from collected data. An alternative to this strategy is to derive a set-membership description of the dynamic system from data. The main advantage of this framework is the guarantee of bounded prediction error. Therefore, it is promising to incorporate data-driven set-membership identification into the MPC framework. The authors in [152] investigate a linear system with an **autoregressive exogenous (ARX)** structure. A feasible parameter set is built from data and *a priori* knowledge of the unknown regressor. Then a set-valued description of the dynamic system is derived and then incorporated into the tube-based MPC framework. The closed-loop stability and recursive feasibility can be guaranteed by constructing the error tube and designing suitable ingredients. Instead of assuming a specific form of the system, [153] uses the data-driven model for the set-valued description of the dynamic model, where the set propagation is computed based on the matrix zonotope

recursion. It is further shown that this data-driven MPC scheme [153] is equivalent to the standard MPC method in the absence of measurement noises.

Direct data-driven MPC. Compared with the indirect data-driven MPC methods, direct data-driven MPC unifies the system identification and control input calculation via formulating a nested bi-level optimization problem from data, thereby having a simpler formulation. Recently, behavioral system theory has attracted increasing attention in data-driven control, in which the dynamic systems can be abstracted as a set of trajectories [154]. Compared with the subspace methods extracting the parametric model from a data Hankel matrix, the behavioral system theory methods aim to find the low-dimensional feature from the data Hankel matrix, thereby naturally being attractive for data-driven control.

In data-driven control, one crucial question is how to efficiently describe dynamic behaviors of the system using the data directly. For nonlinear systems, this problem is still challenging. But for LTI systems, there is a fundamental result which is the so-called *fundamental lemma* proposed by Willems *et al.* [155]. This result stipulates that all possible finite-length trajectories of the LTI system can be obtained from a given finite set of trajectories generated under the persistently exciting control inputs. Consequently, this result illustrates a sufficient condition to uniquely identify the LTI model, thereby providing a theoretic underpinning for results on subspace identification [156, 157] and data-driven control [130, 133, 158].

The first work on the behavioral system theory based data-driven MPC is proposed in [159] for unconstrained LTI systems, where a minimal image representation of the dynamic system is used for the prediction. But in [159] the data Hankel matrix is constructed based on current time data instead of the persistently exciting data. Therefore, the closed-loop stability cannot be guaranteed. Later in [160], a data-driven MPC scheme, which is the so-called DeePC, is presented for constrained LTI systems, where the image feature vector is considered as the decision variable of the MPC optimization problem. Compared with the method [159], the data Hankel matrix in [160] is constructed based on given trajectories with persistently exciting control inputs, resulting in better prediction performance. In addition, it is proved that for controllable LTI systems, the closed-loop behavior of DeePC [160] is equivalent to the standard MPC algorithm.

The recent extensions of DeePC scheme are presented in [161–164]. In [161], a stochastic DeePC is proposed for LTI systems subject to stochastic disturbances, where the cost function is modified by adding heuristic regularization terms. Then the formulated DeePC optimization problem is solved by using the distributionally robust optimization technique

[165] to handle the stochastic disturbance. The result in [161] is later extended in [162] with the theoretical guarantees of constraint satisfaction and probabilistic performance under the assumption on the Lipschitz continuity of the objective function. In [163, 164], a robust DeePC scheme is developed for LTI systems subject to bounded measurement noises. By adding the quadratic regulation terms to the objective function, the DeePC optimization problem can be reformulated as the min-max optimization problem to handle the disturbances. In [164], the authors theoretically show that this min-max formulation enables a robust performance guarantee under different types of uncertainty sets. Note that in [161–164], the performance guarantee is theoretically investigated from the optimization perspective, i.e., deriving an upper bound for the optimal value of the objective function. But the stability of the closed-loop system and the recursive feasibility of the MPC algorithm are not discussed.

Recently, there are some results exploring the analysis of closed-loop properties for data-driven MPC [166–171]. The first result on data-driven MPC with guarantees of closed-loop stability and recursive feasibility is presented in [166], where an equality terminal constraint is considered in the MPC optimization problem. By designing a specific Lyapunov function consisting of the optimal value function and an **input-output-to-state stability (IOSS)** Lyapunov function [172], it proves that the closed-loop system is exponentially stable. An extension of this data-driven MPC scheme is also proposed in [166] for input-constrained LTI systems, in which a slack variable is introduced to compensate the disturbances. In order to preserve the closed-loop properties, an extended state including the past n -step inputs and outputs is constructed, leading to a so-called n -step MPC formulation with the periodic operation. Consequently, the closed-loop stability and recursive feasibility can be guaranteed periodically. The data-driven MPC scheme [166] is further extended to the robust constraint satisfaction [168] and the setpoints tracking [167]. The authors in [169] investigate the data-driven MPC for nonlinear affine systems. By approximating the nonlinear affine system as the image representation based data-driven model, the method [168] is applied to handle the model deviation.

Note that in [166–169] an equality terminal constraint is employed to guarantee the closed-loop stability, which, however, may lead to the conservative control performance. To address this issue, the result [170] investigates the design of general terminal ingredients, i.e., the terminal cost and the terminal set constraint, for data-driven MPC. Similar to [166], the extended states consisting of the past inputs and outputs are introduced to reformulate the LTI systems. As shown in [173], this new system can be further represented as a linear fractional transformation to compute the terminal cost function and terminal constraint.

Another result on reducing the conservatism of the equality terminal constraint in data-driven MPC is presented in [171]. If the uncertainty is sufficiently small, by choosing a sufficiently long prediction horizon, the closed-loop stability and recursive feasibility can be ensured without relying on terminal ingredients.

Direct data-driven MPC usually has an implicit identification step that generates a prediction model similar to the one used in indirect data-driven MPC. This intermediate step of system identification makes indirect data-driven MPC less sensitive to noisy data. Therefore, several results have appeared in literature exploring the relation and comparison between indirect and direct data-driven MPC [174–176]. For LTI systems, the authors in [174] prove that SPC and DeePC are equivalent in deterministic cases, and the numerical example shows SPC can outperform DeePC in the presence of additive Gaussian noise. A similar conclusion is derived in [175], in which DeePC is proved to be the convex relaxation of SPC for the regulation problem. The result [175] further suggests that the indirect method can outperform the direct method for LTI systems with “variance errors”, i.e., the additive disturbances whose probability distribution are known, and the direct method is recommended for “biased errors”, i.e., the model mismatch caused by using the linear model obtained from data to describe a nonlinear system with noise-free measurements. The performance comparison between indirect and direct data-driven MPC for stochastic LTI systems with different sizes of data set is presented in [176], where the convergence rate of identification and suboptimality gap between the data-driven method and the model-based method are used as the indices. A compromise between indirect and direct data-driven MPC is reported in [177]. This result presents a two-step framework. But the prediction is achieved by using the prediction matrix built from the data instead of the identification of a state-space or FIR model. Therefore, the pre-assumption on the system model is not required in [177].

1.4 Self-Triggered MPC

The problem of addressing the computation and communication constraints in networked dynamic systems has attracted increasing attention in recent years [178]. Compared with the control methods with periodic execution, event-based aperiodic control, where the control input is not calculated and transmitted until a certain well-defined event occurs, has proved to be effective in achieving the trade-off between the closed-loop performance and the overall communication load. Therefore, numerous research efforts have been made to explore event-based aperiodic control for networked dynamic systems. According to dif-

ferent triggering mechanisms in the existing literature, there are two main categories [178]: Event-triggered control and self-triggered control. In the former, the event is generally triggered at time instants when the system outputs or states satisfy a certain condition, e.g., leaving a prescribed set. As a result, the continuous state or output measurement of the system is required in event-triggered control to determine the computation of control inputs and transmission of new measurements. For self-triggered control, the next sampling time instant and the control input are determined simultaneously based on the measurements obtained only at triggering time instants, thereby potentially allowing a further reduction in overall communication load. A comprehensive introduction to event-triggered and self-triggered control can be found in [178].

While event-based aperiodic control methods have become increasingly popular in recent years, there are relatively few results on communication-efficient control of constrained dynamic systems. MPC, which has proved to be effective in handling system constraints for complicated systems [179], is a natural and promising framework to achieve these objectives. In event-triggered MPC, the new control inputs are only computed and transmitted if a performance criterion is violated, which allows the communication and computational power to be saved while almost preserving the control performance [180–182]. Self-triggered MPC pre-determines the execution of control inputs and time instants of state measurements based on the prediction from the plant model. As a result, self-triggered MPC only samples at the triggering time instants, thereby requiring less overall information from the system.

Some results addressing self-triggered MPC have been reported in the literature, e.g., [183–190]. For deterministic systems, a self-triggered MPC scheme is developed in [183] for input-constrained nonlinear affine systems, where the control inputs are implemented in a sample-and-hold fashion by discretizing the optimal control trajectory into several control input samples with optimal sampling intervals. In [187], the authors propose a self-triggered MPC method that jointly designs the triggering behavior and control inputs for constrained nonlinear systems such that the maximum sampling interval and the optimal control inputs can be simultaneously obtained by solving an optimization problem. When considering the system with uncertainties, a tube-based self-triggered MPC algorithm is presented in [189] for linear systems subject to additive disturbances. But the sampling interval is determined based on the tube cross-sections associated with the maximum admissible sampling interval, leading to a conservative region of attraction for the self-triggered MPC algorithm. To address this issue, in [190], the integration of self-triggered MPC with homothetic tubes is proposed, where the tube cross-sections are optimized online based on

the length of the sampling interval to reduce the conservatism. The probabilistic constraints and stochastic disturbances are considered in [184, 185]. To relieve the computational burden, the authors in [186] have proposed an adaptive mechanism for the prediction horizon in the dual-mode MPC framework. By incorporating the self-triggering mechanism into the min-max MPC strategy, a recent work in [188] provides a novel **self-triggered robust MPC (ST-RMPC)** algorithm for general nonlinear systems considering both parametric uncertainties and additive disturbances.

1.5 Research Motivations and Contributions

Although numerous results on robust MPC and adaptive MPC have been reported in the literature, there are still many problems that need to be further investigated. As aforementioned, adaptive MPC aims to achieve a dual control objective, including regulation and system identification. Specifically, the control signals should guarantee that the system output can cautiously track the desired values while sufficiently exciting the system to accelerate the system identification process [191]. But synthesizing system identification with MPC definitely introduces new theoretical and practical problems. Similar to most adaptive control methods, a persistent excitation of the system is required to achieve the satisfactory performance of system identification, which, however, is usually conflicted with the control objective [192]. How to achieve the exploration-exploitation trade-off in adaptive MPC is still challenging. In addition, due to the recursive updates of the system model in MPC, it is difficult to guarantee the stability of the closed-loop system and the recursive feasibility of the adaptive MPC algorithm, especially for complicated nonlinear systems. Motivated by these issues, this dissertation focuses on designing robust and adaptive MPC. The detailed motivations and objectives of each chapter are presented in the following.

- **Chapter 2** presents the notations and preliminary results that are useful throughout this dissertation.
- **Chapter 3** studies adaptive MPC for constrained linear systems subject to parametric uncertainties. The tube-based MPC strategy is one of the most attractive approaches for linear systems to handle uncertainties since it can efficiently deal with uncertainties while having a comparable computational complexity to standard MPC [2]. Several results on adaptive MPC have been developed based on the tube-based MPC technique, e.g., [42, 63, 64, 87, 88, 115, 116]. However, these results are developed based on the rigid tube methods with fixed shapes and sizes, e.g.,

[63, 64] or the homothetic tube method with dynamic sizes but fixed shapes, e.g., [42, 87, 88, 115, 116]. Therefore, these results may be conservative under recursive updates of the uncertainty set. To address this issue, we propose an adaptive MPC scheme based on the elastic tube method in Chapter 3, where both the size and shape of the tube cross-sections are optimized via the MPC optimization problem. We theoretically show the perturbed closed-loop system is asymptotically stable under standard assumptions. Numerical simulations and comparisons are given to illustrate the efficacy of the proposed method.

- **Chapter 4** investigates self-triggered MPC for constrained discrete-time nonlinear systems subject to parametric uncertainties and additive disturbances. Some results on ST-RMPC have been proposed in the literature, e.g., [184–186, 188–190]. But these results on self-triggered MPC handle the uncertainties by considering its worst-case realization based on *a priori* knowledge of the uncertainty bound. Inherently, those methods become conservative when the uncertainty is over-estimated and time-varying. In Chapter 4, we develop an **self-triggered adaptive MPC (ST-AMPC)** scheme based on the min-max MPC framework for uncertain nonlinear systems. A set-membership parameter estimator is developed based on the zonotope-based indirect polytopic set computation such that the proposed estimator can be used for the system with the aperiodic self-triggered sampling. It is theoretically shown that the resulting ST-AMPC method is recursively feasible, and the closed-loop system is ISpS at triggering time instants. A numerical example and comparison study are presented to illustrate the advantages of the proposed method.
- **Chapter 5** presents a robust MPC scheme for the visual servoing of quadrotors subject to external disturbances. In recent years, quadrotor **unmanned aerial vehicles (UAVs)** have received considerable attention in many fields, such as agriculture, industry, and transportation, due to their high maneuverability, agile mobility, and **vertical take-off and landing (VTOL)** capability [193–196]. The navigation of quadrotors usually relies on the position information measured by the **global positioning system (GPS)** or other positioning systems. However, the position information may be unavailable in some indoor or cluttered urban areas. For the quadrotor equipped with a camera, visual servoing provides an alternative solution to this problem, where the image data are employed as the feedback to regulate the quadrotor’s pose with respect to a predefined visual target, allowing the navigation of quadrotors in GPS-denied environments. The implementation of the visual servoing usually requires

that the visual target always stays in the **field of view (FOV)** of the camera during the visual servoing process, which is also referred to as the visibility constraint. To address this issue, the MPC-based visual servoing method is a promising solution. In Chapter 5, we investigate the **image-based visual servoing (IBVS)** of quadrotors subject to external disturbances based on robust MPC. A constraint tightening strategy is developed based on the Lipschitz condition to handle the external disturbances. The sufficient conditions on guaranteeing the recursive feasibility and closed-loop stability are established in this chapter. Numerical simulation and experimental validation are provided to illustrate the efficacy of the proposed method.

- **Chapter 6** explores the trajectory tracking of perturbed **autonomous ground vehicles (AGVs)** based on adaptive MPC. Over the past decades, AGVs have received considerable attention in modern military and civilian areas due to their high maneuverability, agile mobility, and low cost, e.g., [197–199]. Compared with other control strategies, MPC is an attractive control paradigm since it can systematically and efficiently deal with system constraints. Numerous results on MPC-based trajectory tracking control of AGV have been developed in the literature. When considering uncertainties, most MPC-based trajectory tracking strategies assume that the AGV system is perfectly modeled and is only perturbed by external disturbances such as the wheel slipping and measurement noises. But the presence of model mismatch is also inevitable in practical problems. In Chapter 6, we develop an adaptive MPC scheme for the trajectory tracking of AGV subject to unknown parameters. A set-membership based parameter estimator is developed based on the **recursive least-squares (RLS)** technique to identify the unknown system parameter with non-increasing estimation error. Then a robustness constraint is introduced into the MPC optimization to handle parametric and additive uncertainties. Sufficient conditions on ensuring the recursive feasibility of the proposed adaptive MPC method are developed. We further prove that the closed-loop tracking system is ISS under recursive updates of the system model. A numerical example and comparison study are provided to show the efficacy of the proposed method.
- **Chapter 7** concludes this dissertation and presents our future research directions.

Chapter 2

Preliminary Results

This chapter introduces the main notations and preliminary results on closed-loop stability and LS that are useful via the dissertation.

2.1 Notations

We use the symbols \mathbb{R} and \mathbb{N} to denote the sets of all real numbers and non-negative integers, respectively. Let $\mathbb{R}_{>0}$, $\mathbb{R}_{\geq 0}$ and $\mathbb{N}_{>0}$ represent the set of all positive real numbers, non-negative real numbers, and positive integers. We define $\mathbb{N}_{[a,b]} := \{x \in \mathbb{N} : a \leq x \leq b, b \geq a\}$.

The set $\mathbb{B}^m = \{b \in \mathbb{R}^m : \|b\|_\infty \leq 1\}$ is called a unit hypercube of dimension m . Given two sets $X \subseteq \mathbb{R}^n$ and $Y \subseteq \mathbb{R}^n$, their Pontryagin difference is denoted by $X \ominus Y = \{z \in \mathbb{R}^n : z + y \in X, \forall y \in Y\}$, and their Minkowski sum is $X \oplus Y = \{x + y : x \in X, y \in Y\}$. Given a continuous function $\Pi(\cdot)$ and a set S , we adopt $\Pi(S)$ to denote the set-valued operation $\{\Pi(s) : s \in S\}$. We use the notations $\blacklozenge(S)$ and $\blacksquare(S)$ to denote the zonotopic and the box overbounding of S , respectively. Given a matrix $H \in \mathbb{R}^{n \times m}$, a set $\mathbb{H} \subseteq \mathbb{R}^m$ and a vector $h \in \mathbb{R}^m$, we define $H\mathbb{H} := \{Hh : h \in \mathbb{H}\}$ and $h - \mathbb{H} := \{h - \hat{h} : \hat{h} \in \mathbb{H}\}$. Given a set $\mathcal{A} \subseteq \mathbb{R}^n$ and a vector $z \in \mathbb{R}^n$, we use the notation $|z|_{\mathcal{A}} = \inf_{\bar{z} \in \mathcal{A}} \|z - \bar{z}\|$ to denote the distance from z to \mathcal{A} .

Given a vector $z \in \mathbb{R}^n$, we use $\|z\|$ and $\|z\|_\infty$ to represent the Euclidean norm and the infinity norm of z , respectively. For a matrix $Z \in \mathbb{R}^{n \times n}$, its maximum and minimum eigenvalues are denoted by $\lambda_{\max}(Z)$ and $\lambda_{\min}(Z)$, respectively. We adopt $\text{col}(z_1, z_2, \dots, z_n)$ to denote the column operation $[z_1^T, z_2^T, \dots, z_n^T]^T$ for column vectors z_1, z_2, \dots, z_n . The notation $\{z_i\}_{i=1}^n$ denotes the sequence $\{z_1, z_2, \dots, z_n\}$ with n elements. Given a positive inte-

ger n , we use I_n to denote an identity matrix of size $n \times n$. Let $z_1 = [z_{11}, z_{21}, \dots, z_{n1}]^T$ and $z_2 = [z_{12}, z_{22}, \dots, z_{n2}]^T$ be two n -dimensional column vectors, we write $z_1 \leq z_2$ ($z_1 \geq z_2$) when $z_{i1} \leq z_{i2}$ ($z_{i1} \geq z_{i2}$) for all $i \in \mathbb{N}_{[1, N]}$. Given two matrices $Z_1, Z_2 \in \mathbb{R}^{n \times n}$, $Z_1 \prec Z_2$ means that the matrix $Z_1 - Z_2$ is negative definite.

2.2 Stability Theorem

In this subsection, we review some preliminary results on the stability properties of discrete-time systems. In the following, we recall several definitions, assumptions, and theorems from [200] and [11].

2.2.1 Stability and asymptotic stability

Consider a deterministic, discrete-time autonomous system

$$x_{k+1} = f(x_k), \quad (2.1)$$

where $x_k \in \mathbb{R}^n$ is the system state. Given the initial condition $x_0 = x$, we use $\Phi(k, x)$ to denote the solution of (2.1) at time k , i.e., $x_k = \Phi(k, x)$.

Before introducing the concepts and preliminary results of stability, we firstly recall some definitions.

Definition 2.1 (Positive invariant set). [11, Definition B.2] A closed set $\mathcal{A} \subset \mathbb{R}^n$ is positive invariant for the system (2.1) if $x_{k+1} \in \mathcal{A}$ for all $x_k \in \mathcal{A}$.

Definition 2.2 (Class \mathcal{K} , \mathcal{K}_∞ , \mathcal{KL} , and \mathcal{PD} functions). [11, Definition B.3]

- a) A function $\alpha : \mathbb{R}_{\geq 0} \rightarrow \mathbb{R}_{\geq 0}$ is called \mathcal{K} -function if it is continuous, strictly increasing and $\alpha(0) = 0$.
- b) A function $\beta : \mathbb{R}_{\geq 0} \rightarrow \mathbb{R}_{\geq 0}$ is called \mathcal{K}_∞ -function if it is \mathcal{K} -function and $\beta(x) \rightarrow \infty$ as $x \rightarrow \infty$.
- c) A function $\gamma : \mathbb{R}_{\geq 0} \times \mathbb{R}_{\geq 0} \rightarrow \mathbb{R}_{\geq 0}$ is called \mathcal{KL} -function if $\gamma(\cdot, t)$ is a \mathcal{K} -function for each fixed $k \geq 0$ and $\gamma(x, \cdot)$ is decreasing with $\gamma(x, t) \rightarrow 0$ as $t \rightarrow \infty$ for each fixed $x \geq 0$.
- d) A function $\delta : \mathbb{R}_{\geq 0} \rightarrow \mathbb{R}_{\geq 0}$ is called \mathcal{PD} -function (positive definite function) if $\delta(0) = 0$ and $\delta(x) > 0$ for all $x > 0$.

The definition of asymptotic stability is given as follows.

Definition 2.3 (Asymptotic stability). [11, Definition B.11] Suppose that the set $\Omega \subseteq \mathbb{R}^n$ is positive invariant and the set $\mathcal{A} \subseteq \Omega$ is closed and positive invariant for the system (2.1). Then \mathcal{A} is asymptotically stable in Ω for the system (2.1) if there exists a \mathcal{KL} -function $\gamma(\cdot, \cdot)$ such that

$$|\Phi(k, x)|_{\mathcal{A}} \leq \gamma(|x|_{\mathcal{A}}, k) \quad (2.2)$$

for all $x \in \Omega$ and $k \in \mathcal{N}$. The set Ω is also called the region of attraction of set \mathcal{A} for the system (2.1).

The asymptotic stability can be established based on the Lyapunov stability theorem, which is presented in the following.

Definition 2.4 (Lyapunov function). [11, Definition B.12] Suppose that the set $\Omega \subseteq \mathbb{R}^n$ is positive invariant and the set $\mathcal{A} \subseteq \Omega$ is closed and positive invariant for the system (2.1), and $f(\cdot)$ is locally bounded. A function $V : \Omega \rightarrow \mathbb{R}_{\geq 0}$ is called a Lyapunov function in Ω for the system (2.1) and set \mathcal{A} if there exist \mathcal{K}_{∞} -functions α_1, α_2 and a continuous \mathcal{PD} function α_3 that the following conditions

$$V(x) \geq \alpha_1(|x|_{\mathcal{A}}), \quad (2.3a)$$

$$V(x) \leq \alpha_2(|x|_{\mathcal{A}}), \quad (2.3b)$$

$$V(f(x)) - V(x) \leq -\alpha_3(|x|_{\mathcal{A}}) \quad (2.3c)$$

hold for all $x \in \Omega$.

Theorem 2.1 (Lyapunov function for asymptotic stability). [11, Theorem B.18] Given the positive invariant sets Ω and \mathcal{A} for the system (2.1), if there exists a Lyapunov function in Ω for the system (2.1) and \mathcal{A} , then \mathcal{A} is asymptotically stable in Ω for the system (2.1).

Note that for the regulation problem without considering uncertainties, if the point x^* is the equilibrium point for the system (2.1), then $\mathcal{A} = \{x^*\}$.

2.2.2 Robust stability

We now review the stability concepts and properties for discrete-time uncertain systems described by

$$x_{k+1} = f(x_k, w_k), \quad (2.4)$$

where $x_k \in \mathbb{R}^n$ is the system state and $w_k \in \mathbb{R}^n$ is the uncertainty belonging to the compact set \mathcal{W} . Let $\Phi(k, x, \mathbf{w}_k)$ denote the solution of (2.4) at time k , i.e., $x_k = \Phi(k, x, \mathbf{w}^k)$, under the initial condition $x_k = x$ and $\mathbf{w}^k = \{w_i\}_{i=0}^{k-1}$.

We first recall the definition of the robust positive invariant set.

Definition 2.5 (Robust positive invariant set). [11, Definition B.2] *A closed set $\Omega \subset \mathbb{R}^n$ is robust positive invariant (RPI) for the system (2.4) if $x_{k+1} \in \Omega$ for all $x_k \in \Omega$ and $w_k \in \mathcal{W}$.*

Support that $f(0, 0) = 0$ and \mathcal{W} contains the origin, and Ω is the RPI set for the system (2.4). The definitions of input-to-state stability, input-to-state practical stability, ISS-Lyapunov function, and ISpS-Lyapunov function are given as follows.

Definition 2.6 (ISS). [11, Definition B.45] *The system (2.4) is ISS if there exist a \mathcal{KL} -function $\beta(\cdot, \cdot)$ and a \mathcal{K} -function $\sigma(\cdot)$ such that, for all $x \in \Omega$ and $w_i \in \mathcal{W}, i \in \mathbb{N}_{[0, k]}$, the following condition holds*

$$\|\Phi(k, x, \mathbf{w}_k)\| \leq \beta(\|x\|, k) + \sigma(\bar{w}), \quad (2.5)$$

where $\bar{w} = \sup_{w_k \in \mathcal{W}} \|w_k\|$.

Definition 2.7 (ISpS). [201] *The system (2.4) is ISpS if there exist a \mathcal{KL} -function $\beta(\cdot, \cdot)$, a \mathcal{K} -function $\sigma(\cdot)$, and a constant $\delta \geq 0$ such that, for all $x \in \Omega$ and $w_i \in \mathcal{W}, i \in \mathbb{N}_{[0, k]}$, the following condition holds*

$$\|\Phi(k, x, \mathbf{w}_k)\| \leq \beta(\|x\|, k) + \sigma(\bar{w}) + \delta, \quad (2.6)$$

where $\bar{w} = \sup_{w_k \in \mathcal{W}} \|w_k\|$.

Definition 2.8 (ISS-Lyapunov function). [11, Definition B.46] *A function $V : \Omega \rightarrow \mathbb{R}_{\geq 0}$ is an ISS-Lyapunov function for the system (2.4) in Ω if there exist \mathcal{K}_{∞} -functions $\alpha_1, \alpha_2, \alpha_3$ and a \mathcal{K} function σ that the following conditions*

$$\alpha_1(\|x\|) \leq V(x) \leq \alpha_2(\|x\|), \quad (2.7a)$$

$$V(f(x, w)) - V(x) \leq -\alpha_3(\|x\|) + \sigma(\bar{w}) \quad (2.7b)$$

hold for all $x \in \Omega$ and $w \in \mathcal{W}$, where $\bar{w} = \sup_{w_k \in \mathcal{W}} \|w_k\|$.

Definition 2.9 (ISpS-Lyapunov function). [202, Definition 6] *A function $V : \Omega \rightarrow \mathbb{R}_{\geq 0}$ is an ISpS-Lyapunov function for the system (2.4) in Ω if there exist \mathcal{K}_{∞} -functions $\alpha_1, \alpha_2, \alpha_3$,*

a constant $\delta \geq 0$, and \mathcal{K} functions σ_1, σ_2 that the following conditions

$$\alpha_1(\|x\|) \leq V(x) \leq \alpha_2(\|x\|) + \delta, \quad (2.8a)$$

$$V(f(x, w)) - V(x) \leq -\alpha_3(\|x\|) + \sigma(\bar{w}) \quad (2.8b)$$

hold for all $x \in \Omega$ and $w \in \mathcal{W}$, where $\bar{w} = \sup_{w_k \in \mathcal{W}} \|w_k\|$.

Similarly, the input-to-state stability and input-to-state practical stability can be established by following the following theorems.

Theorem 2.2 (Lyapunov function for input-to-state stability). *[11, Lemma B.47] Suppose that f is continuous. If there exists a continuous ISS-Lyapunov function in Ω for the system (2.4), then the system (2.1) is ISS in Ω .*

Theorem 2.3 (Lyapunov function for input-to-state stability). *[202, Theorem 1] If there exists a continuous ISpS-Lyapunov function in Ω for the system (2.4), then the system (2.1) is ISpS in Ω .*

2.3 MPC Design Strategy

2.3.1 Control invariance

Before presenting the MPC design strategy, we first recall several definitions related to the control invariant set.

Deterministic systems

Consider a general deterministic, discrete-time system

$$x_{k+1} = f(x_k, u_k), \quad (2.9)$$

where $x_k \in \mathbb{R}^{n_x}$ and $u_k \in \mathbb{R}^{n_u}$ are the system state and input, respectively. The system is subject to the following state and input constraints:

$$x_k \in \mathcal{X}, u_k \in \mathcal{U}. \quad (2.10)$$

It is assumed that the origin is the equilibrium point of the system in (2.9), and the system state is accessible for all $k \in \mathbb{N}$. The definition of control invariant set is presented in the following.

Definition 2.10 (Control invariant set). [11, Definition 2.10] A set $\Omega \subseteq \mathcal{X}$ is called the control invariant for the system (2.9) subject to constants (2.10) if, for all $x_k \in \Omega$, there exists a $u_k \in \mathcal{U}$ such that $x_{k+1} = f(x_k, u_k) \in \Omega$.

Uncertain systems

Consider a general uncertain, discrete-time system

$$x_{k+1} = f(x_k, u_k, w_k), \quad (2.11)$$

where $x_k \in \mathbb{R}^{n_x}$ and $u_k \in \mathbb{R}^{n_u}$ are the system state and input, respectively. $w_k \in \mathbb{R}^n$ is the uncertainty belonging to the compact set \mathcal{W} . The system is subject to constraints (2.10). In the following, we recall several well-established definitions that are widely used in robust MPC.

Definition 2.11 (Robust control invariant set). [11, Definition 3.6] A set $\Omega \subseteq \mathcal{X}$ is called the robust control invariant (RCI) for the system (2.11) subject to constants (2.10) if, for all $w_k \in \mathcal{W}$, there exists a $u_k \in \mathcal{U}$ such that $x_{k+1} = f(x_k, u_k) \in \Omega$ for every $x_k \in \Omega$.

Definition 2.12 (Minimal RPI set). [203, Definition 2] A set $\Omega \subseteq \mathcal{X}$ is called the minimal RPI (mRPI) set for the system (2.11) subject to constants (2.10) if it is contained in every RPI set of the system (2.11).

Definition 2.13 (Maximal RPI set). [?] A set $\Omega \subseteq \mathcal{X}$ is called the maximal RPI (MRPI) set for the system (2.11) subject to constants (2.10) if it contains every RPI set of the system (2.11).

Definition 2.14 (l -step robust stabilizable set). [?] Let $\Omega \subseteq \mathcal{X}$ denote the RPI set for the system (2.11) subject to constants (2.10). A set $X_l(\Omega)$ is called the l -step robust stabilizable set for the system (2.11) subject to constants (2.10) if, for all $x_k \in X_l(\Omega)$, there exists a sequence of admissible control inputs $\{u_i\}_{i=k}^{k+s}$, $s \in \mathbb{N}_{[0,l]}$ such that $x_{k+s} \in X_l(\Omega)$ for all $w_{k+i} \in \mathcal{W}$, $i \in \mathbb{N}_{[0,s]}$. The initial condition $X_l(\Omega) = \Omega$.

2.3.2 Standard MPC

Suppose that the control objective is to stabilize the system in (2.9) to the origin. The main insight of MPC is to solve an online optimization problem to obtain the control actions that optimize the future output behaviors with respect to a prescribed performance index, where

a dynamic model is employed to predict the future system output. In particular, the optimal control input is obtained by solving the following optimization problem.

$$V_N(x_k) = \min_{\mathbf{u}_k} J_N(x_k, \mathbf{u}_k) = \sum_{l=0}^{N-1} \ell(x_{l|k}, u_{l|k}) + \ell_f(x_{N|k}), \quad (2.12a)$$

$$\text{s.t.} \quad x_{l+1|k} = f(x_{l|k}, u_{l|k}), \quad l \in \mathbb{N}_0^{N-1} \quad (2.12b)$$

$$x_{l|k} \in \mathcal{X}, u_{l|k} \in \mathcal{U}, \quad l \in \mathbb{N}_0^{N-1} \quad (2.12c)$$

$$x_{N|k} \in \mathcal{X}_f \quad (2.12d)$$

$$x_{0|k} = x_k \quad (2.12e)$$

where N is the prediction horizon; $\mathbf{u}_k = \{u_{i|k}\}_{i=0}^{N-1}$ is the sequence of control inputs; $x_{l|k}$ denotes the predicted system state at time $l+k$ based on the plant in (2.9), current system state x_k , and control inputs $\{u_{i|k}\}_{i=0}^{l-1}$; \mathcal{X}_f is the terminal constraint; $\ell : \mathbb{R}^{n_x} \times \mathbb{R}^{n_u} \rightarrow \mathbb{R}_{\geq 0}$ and $\ell_f : \mathbb{R}^{n_x} \rightarrow \mathbb{R}_{\geq 0}$ are the functions of stage cost and terminal cost, respectively. As shown in Figure 1.1, at the current time instant k , the optimization problem (2.12) is solved to obtain the optimal control sequence \mathbf{u}_k^* , and the first element in the sequence is implemented to the system in (2.9), i.e., $u_k = u_{0|k}^*$. At next time instant, we repeat the above procedure based on the new measurement x_{k+1} to obtain control input u_{k+1} .

2.3.3 Adaptive min-max MPC

In this subsection, similar to [102], we present an adaptive MPC scheme based on the well-established closed-loop min-max MPC approach proposed in [202]. Consider a discrete-time nonlinear system subject to the parametric uncertainty and the additive disturbance

$$x_{k+1} = \mathcal{F}(x_k, u_k, v_k, d_k) \triangleq f(x_k, u_k) + g(x_k, u_k)v_k + d_k, \quad (2.13)$$

where $x_k \in \mathbb{R}^{n_x}$ and $u_k \in \mathbb{R}^{n_u}$, $v_k \in \mathcal{V} \subset \mathbb{R}^{n_v}$ and $d_k \in \mathcal{D} \subset \mathbb{R}^{n_x}$ are the system state, the control input, the parametric uncertainty, and the additive disturbance, respectively. Both v_k and d_k are unknown and time-varying, and \mathcal{V} and \mathcal{D} are known zonotopes. The definition of zonotope can be found in Definition 2.15. $f : \mathbb{R}^{n_x} \times \mathbb{R}^{n_u} \rightarrow \mathbb{R}^{n_x}$ and $g : \mathbb{R}^{n_x} \times \mathbb{R}^{n_u} \rightarrow \mathbb{R}^{n_x \times n_v}$ are nonlinear functions satisfying conditions $f(0, 0) = 0$ and $g(0, 0) = 0$. The system is subject to constraints $x_k \in \mathcal{X}$ and $u_k \in \mathcal{U}$ for all $t \in \mathbb{N}$, where \mathcal{X} and \mathcal{U} are compact sets containing the origin. It is assumed that x_k is always measurable. For the uncertainties d_k and v_k , we assume that there exist constants $\bar{d}, \bar{v}, \bar{\delta} \in \mathbb{R}_{>0}$ such that

$\|d_k\| \leq \bar{d}$, $\|v_k\| \leq \bar{v}$, and $\|v_{k+1} - v_k\| \leq \bar{\delta}$. for all all $d_k \in \mathcal{D}$ and $v_k, v_{k+1} \in \mathcal{V}$.

Let $x_{l|k}$ denote the prediction of the state x_{l+k} which is made at the time instant k . Given the prediction horizon $N \in \mathbb{N}_{>0}$, we suppose that the predicted state trajectory $x_{l|k}$, $l \in \mathbb{N}_{[0,N]}$, of the system (4.1) is generated by the control policy $\mu_{l|k} : \mathbb{R}^{n_x} \rightarrow \mathbb{R}^{n_u}$, parametric uncertainties $v_{l|k}$ and additive disturbances $d_{l|k}$ with $l \in \mathbb{N}_{[0,N-1]}$ and $x_{0|k} = x_k$. Then the cost function for min-max MPC is given by

$$\bar{J}_N(\mathbf{x}_{k,N}, \boldsymbol{\mu}_{k,N}, \mathbf{w}_{k,N}) = \sum_{l=1}^{N-1} \ell(x_{l|k}, \mu_{l|k}(x_{l|k})) + \ell_f(x_{N|k}),$$

where $\mathbf{x}_{k,N} = \{x_{l|k}\}_{l=0}^N$, $\boldsymbol{\mu}_{k,N} = \{\mu_{l|k}(x_{l|k})\}_{l=0}^{N-1}$ and $\mathbf{w}_{k,N} = \{v_{l|k}, d_{l|k}\}_{l=0}^{N-1}$; $\ell : \mathbb{R}^{n_x} \times \mathbb{R}^{n_u} \rightarrow \mathbb{R}_{\geq 0}$ and $\ell_f : \mathbb{R}^{n_x} \rightarrow \mathbb{R}_{\geq 0}$ are stage cost function and terminal cost function satisfying the condition $\ell(0, 0) = 0$ and $\ell_f(0) = 0$. Then the optimal control policy sequence $\boldsymbol{\mu}_{k,N}^*$ can be obtained by solving the following optimal control problem \mathcal{P}_0 [202]

$$\begin{aligned} \mathcal{P}_0 : V_N(x_k) = & \min_{\boldsymbol{\mu}_{k,N}} \max_{\mathbf{w}_{k,N}} \bar{J}_N(\mathbf{x}_{k,N}, \boldsymbol{\mu}_{k,N}, \mathbf{w}_{k,N}), \\ \text{s.t. } & x_{l+1|k} = \mathcal{F}(x_{l|k}, \mu_{l|k}(x_{l|k}), v_{l|k}, d_{l|k}), \\ & x_{0|k} = x_k, x_{l|k} \in \mathcal{X}_{N-l}, \mu_{l|k}(x_{l|k}) \in \mathcal{U}, \forall (v_{l|k}, d_{l|k}) \in \mathcal{V}_{l|k} \times \mathcal{D}, l \in \mathbb{N}_{[0,N]}, \end{aligned} \quad (2.14)$$

where the set $\mathcal{X}_i = \{x \in \mathbb{R}^{n_x} : \exists \mu(x) \in \mathcal{U} \text{ such that } \mathcal{F}(x, \mu(x), \mathcal{V}, \mathcal{D}) \subset \mathcal{X}_{i-1}\}$, $i \in \mathbb{N}_{[0,N]}$ is the i -step robust stabilizable set, as defined in Definition 2.14, with $\mathcal{X}_0 = \mathcal{X}_f$ and \mathcal{X}_f is the terminal set. $\mathcal{V}_{l|k} = (\mathcal{V}_k \oplus l\bar{\delta}\mathbb{B}^{n_v}) \cap \mathcal{V}$ is the prediction of the bounding set \mathcal{V}_{l+k} . Note that $\mu_{l|k}(\cdot)$ is the control policy which is the function depending on the predicted system state $x_{l|k}$, which leads to the closed-loop min-max MPC formulation [11]. Therefore, solving the optimal control problem \mathcal{P}_0 by means of the dynamic programming method, the following recursion equation for the optimal cost function can be obtained [204]

$$V_i(x_k) = \min_{\mu(\cdot) \in \mathcal{U}} \left\{ \max_{(v,d) \in \mathcal{V}_{N-i|k} \times \mathcal{D}} \{V_{i-1}(\mathcal{F}(x_k, \mu(x_k), v, d)) + \ell(x_k, \mu(x_k))\} \text{ such that } \mathcal{F}(x_k, \mu(x_k), v, d) \in \mathcal{X}_{i-1}, \mu(x_k) \in \mathcal{U}, \forall (v, d) \in \mathcal{V}_{N-i|k} \times \mathcal{D} \right\} \quad (2.15)$$

with the initial condition $V_0(x_k) = \ell_f(x_k)$ and $i \in \mathbb{N}_{[1,N]}$. Then similar to [202], the following assumptions on the cost function and terminal set are made in this work

Assumption 2.1. *There exist a local controller $\kappa_f : \mathbb{R}^{n_x} \rightarrow \mathbb{R}^{n_u}$, a \mathcal{K}_∞ -function $\alpha(\cdot)$, some \mathcal{K} functions $\sigma_1(\cdot), \sigma_2(\cdot), \sigma_3(\cdot)$ and a robust invariant set \mathcal{X}_f such that*

$$1) \mathcal{F}(x_k, \kappa_f(x_k), v_k, d_k) \in \mathcal{X}_f, \forall (x_k, v_k, d_k) \in \mathcal{X}_f \times \mathcal{V} \times \mathcal{D}.$$

- 2) $\kappa_f(x_k) \subseteq \mathcal{U}$ for all $x_k \in \mathcal{X}_f$.
- 3) $\ell(x_k, u_k) \geq \sigma_1(\|x_k\|)$ for all $x_k \in \mathcal{X}$ and $u_k \in \mathcal{U}$.
- 4) $\sigma_2(\|x_k\|) \leq \ell_f(x_k) \leq \sigma_3(\|x_k\|)$ for all $x_k \in \mathcal{X}_f$.
- 5) $\ell_f(\mathcal{F}(x_k, \kappa_f(x_k), v_k, d_k)) - \ell_f(x_k) \leq -\ell(x_k, \kappa_f(x_k)) + \alpha(\bar{d}), \forall (x_k, v_k, d_k) \in \mathcal{X}_f \times \mathcal{V} \times \mathcal{D}$.

As shown in [202, Theorem 2], if Assumption 2.1 holds, without considering the update of bounding set, i.e., $\mathcal{V}_k = \mathcal{V}, \forall t \in \mathbb{N}$, the periodic closed-loop system under the feedback control law $u_k = \mu_{0|k}^*(x_k)$ is ISpS, where $\mu_{0|k}^*(x_k)$ is the optimal control policy obtained by solving the optimal control problem \mathcal{P}_0 .

2.4 System definition

2.4.1 Set-membership parameter estimation with periodic state measurement

Consider the nonlinear system (2.13). At time instant t , given the system state x_{k-1} and the control input u_{k-1} , the parameter set \mathcal{L}_k , which encloses uncertain parameter v_{k-1} consistent with the observation of system state x_k , can be described as follows:

$$\mathcal{L}_k = \{v \in \mathbb{R}^{n_v} : y_k - g(x_{k-1}, u_{k-1})v \in \mathcal{D}\}. \quad (2.16)$$

where $y_k = x_k - f(x_{k-1}, u_{k-1})$.

As mentioned before, v_k has a maximum change rate $\bar{\delta}$ and $v_k \in \mathcal{V}$ for all $t \in \mathbb{N}$. Let \mathcal{V}_{k-1} denote the bounding set for the unknown parameter v_{k-1} , based on (2.16), the membership set of the unknown parameter v_k can be derived by

$$\mathcal{V}_k = ((\mathcal{V}_{k-1} \cap \mathcal{L}_k) \oplus \bar{\delta}\mathbb{B}^{n_v}) \cap \mathcal{V}, \quad (2.17)$$

where the initial condition $\mathcal{V}_0 = \mathcal{V}$. With this, it can be guaranteed that $v_k \in \mathcal{V}_k$ for all $t \in \mathbb{N}$. In addition, since \mathcal{V} and \mathcal{D} are convex polytopes, \mathcal{V}_k can be computed by following (2.17) directly. To reduce the computational complexity of the MPC problem, we remove the redundant constraints in \mathcal{V}_k by solving linear programming problems [205].

2.4.2 Zonotopic set computation

We first recall the following definition of the zonotope.

Definition 2.15 (Zonotope of order m [206]). *A zonotope of order m is a set of n -dimensional vectors defined by $\mathcal{Z} = p \oplus S\mathbb{B}^m$, where $p \in \mathbb{R}^n$ is the center of the zonotope and $S \in \mathbb{R}^{n \times m}$ is the generator matrix.*

Consider the system (2.13). Let \hat{X}_k denote the outer bound of exact uncertain state set [206] X_k for the state x_k . Given $X_{k+1} = \mathcal{F}(x_k, u_k, \mathcal{V}_k, \mathcal{D})$, it can be obtained that $X_{k+1} \subseteq \mathcal{F}(\hat{X}_k, u_k, \mathcal{V}_k, \mathcal{D})$. Suppose that \hat{X}_k is a zonotope with a form $\hat{X}_k = p_k^x \oplus S_k^x \mathbb{B}^{n_k^x}$, where $p_k^x \in \mathbb{R}^{n_x}$ is the center vector and $S_k^x \in \mathbb{R}^{n_x \times n_k^x}$ is the generator matrix. Recalling the zonotopic set computation method in [206], we define an inclusion function $\mathcal{G}_{\mathcal{F}}(\hat{X}_k, u, \mathcal{V}, \mathcal{D})$ associated with system model in (2.13) as the

$$\mathcal{G}_{\mathcal{F}}(\hat{X}_k, u, \mathcal{V}, \mathcal{D}) = \diamond(\nabla_x \mathcal{F}(\blacksquare(\hat{X}_k), u, \mathcal{V}, \mathcal{D})(\hat{X}_k - p_k^x)) \oplus \blacklozenge(\mathcal{F}(p_k^x, u, \mathcal{V}, \mathcal{D})),$$

where $\diamond(\cdot)$ is Zonotope inclusion function given in [206, Theorem 3]. If \mathcal{V}_k and \mathcal{D} are zonotopic, one has [206, Theorem 4]

$$X_{k+1} \subseteq \mathcal{F}(\hat{X}_k, u_k, \mathcal{V}_k, \mathcal{D}) \subseteq \mathcal{G}_{\mathcal{F}}(\hat{X}_k, u_k, \mathcal{V}_k, \mathcal{D}).$$

Therefore, by choosing $\hat{X}_{k+1} = \mathcal{G}_{\mathcal{F}}(\hat{X}_k, u_k, \mathcal{V}_k, \mathcal{D})$, it can be guaranteed that $X_{k+1} \subseteq \hat{X}_{k+1}$ for all $k \geq 0$.

Chapter 3

Adaptive MPC for A Class of Constrained Linear Systems with Parametric Uncertainties

3.1 Introduction

This chapter studies adaptive MPC for constrained linear systems subject to parametric uncertainties. A computationally tractable adaptive MPC algorithm is proposed based on the techniques of tube MPC and RLS. Similar to [102], an RLS-based parameter estimator is developed to simultaneously update the point estimate of unknown parameters and the set description. In [102], only the estimated set description of uncertainties is used to update the min-max optimization problem. The proposed method is developed based on tube-based MPC to take full advantage of the estimation information, i.e., point and set descriptions of uncertainties, to improve the closed-loop performance. In addition, the min-max optimization problem in [102] is a non-convex and computationally complicated. Alternatively, the proposed work employs the tube MPC technique to handle the uncertainty, which has a comparable computational complexity to standard MPC.

As reviewed in Chapter 1, there are several results on tube-based adaptive MPC reported in the literature, e.g., [42, 63, 64, 87, 88, 115, 116]. However, the results [63, 64] are developed based on the rigid tubes, where the tube cross-sections are computed offline based on the initial knowledge of uncertainties, leading to relatively conservative control performance. There are some novel adaptive MPC strategies [42, 87, 88, 115, 116] combining the homothetic tube MPC technique with the set-membership identification, where

the sequence of state tubes $\{\mathcal{X}_{l|k}\}$ is developed with the form $\mathcal{X}_{l|k} = z_{l|k} + \sigma_{l|k}\mathcal{X}_0$ to guarantee the robust constraint satisfaction. Here, $z_{l|k}$ is the nominal system state, \mathcal{X}_0 is a given set, and $\sigma_{l|k}$ is a scalar to be optimized by the MPC optimization problem. It can be seen that the tube cross-sections are shaped by the set \mathcal{X}_0 , translated and scaled by the MPC optimization problem. The set \mathcal{X}_0 is calculated offline according to the initial knowledge of the uncertainty set, which may be conservative under recursive updates of the uncertainty set. Inspired by the tube MPC approach in [35], we construct the homothetic tubes in this work, where both the size and shape of the tube cross-sections are optimized via the MPC optimization problem. Consequently, it will promisingly lead to control performance improvement by using the proposed method.

In this chapter, we propose a computationally tractable adaptive MPC algorithm based on elastic tubes. We extend the robust MPC framework in [35] to allow for online model adaptation while guaranteeing closed-loop stability and recursive feasibility. Compared with the methods in [42, 115], the proposed approach introduces additional decision variables in the MPC optimization problem to optimize both the shape and size of the tube cross-sections, resulting in reduced conservatism.

The **main contributions** are two-fold:

- An online strategy for estimating unknown parameters and updating set descriptions of uncertainties is proposed based on the RLS technique, which is further employed to construct the elastic tube cross-sections to ensure robust constraint satisfaction. By deriving non-increasing properties on the proposed estimation routine, the resulting tube-based adaptive MPC scheme is recursively feasible under recursive model updates while providing less conservative performance compared with the robust tube MPC method. Furthermore, we theoretically show the perturbed closed-loop system is asymptotically stable under standard assumptions.
- To provide a trade-off between the computational complexity and conservatism, a specialization of the proposed adaptive method is also given with reduced computational complexity and comparable control performance. A numerical example and comparison study are given to illustrate the benefits of the proposed method.

3.2 Problem Formulation

Consider a discrete-time linear time-invariant (LTI) system with an unknown parameter $\theta \in \mathbb{R}^{n_\theta}$

$$x_{k+1} = A(\theta)x_k + B(\theta)u_k, \quad (3.1)$$

subject to a mixed constraint

$$\mathcal{M} = \{(x_k, u_k) | Fx_k + Gu_k \leq \mathbf{1}\}, \quad (3.2)$$

where $x_k \in \mathbb{R}^{n_x}$ and $u_k \in \mathbb{R}^{n_u}$ are the system state and input, respectively. The matrices $A(\theta)$ and $B(\theta)$ are the real affine functions of θ , i.e., $A(\theta) = A_0 + \sum_{i=1}^{n_\theta} A_i \theta_i$, $B(\theta) = B_0 + \sum_{i=1}^{n_\theta} B_i \theta_i$. $\theta = \text{col}(\theta_1, \theta_2, \dots, \theta_{n_\theta})$ is the vector of unknown parameters, which is assumed to be uniquely identifiable [207]. It is assumed that the parameter θ is bounded by a given set $\Theta_0 = \{\theta | \|\theta\| \leq r_0\}$ which contains the real parameter θ^* .

In this chapter, the goal is to design a state feedback control law for the perturbed and constrained system (3.1) while ensuring the desirable closed-loop performance and robust constraint satisfaction by means of adaptive MPC. In particular, we consider the following parameterization of the control input

$$u_k = Kx_k + v_k, \quad (3.3)$$

where $v_k \in \mathbb{R}^{n_u}$ is the decision variable of the MPC optimization problem; $K \in \mathbb{R}^{n_u \times n_x}$ is a prestabilizing state feedback gain such that $\phi(\theta) = A(\theta) + B(\theta)K$ is quadratically stable for all $\theta \in \Theta_0$.

3.3 Uncertainty Estimation

This section introduces an online parameter estimation scheme based on the RLS technique with guaranteed non-increasing estimation errors. Then an approach for approximating the feasible solution set (FSS) is presented. Finally, we conclude this section by analyzing the performance of the proposed estimation scheme.

3.3.1 Parameter estimation

Let $g(x_k, u_k)\theta = \sum_{i=1}^{n_\theta} (A_i x_k + B_i u_k)\theta_i$, then we can formulate a regressor model $y_k = g(x_k, u_k)\theta^*$ with $y_k = x_{k+1} - A_0 x_k - B_0 u_k$ to estimate θ^* by using the standard RLS

method. But the convergence of this solution relies on persistent excitation of $g(x_k, u_k)$, which cannot be guaranteed if $x_k = 0$ and $u_k = 0$. Similar to [103], we introduce the following filter w_k for the regressor $g(x_k, u_k)$ to improve the convergence performance,

$$w_{k+1} = g(x_k, u_k) - K_e w_k, \quad (3.4)$$

where $w_0 = 0$ and K_e is a Schur stable gain matrix. Let \hat{x}_k denote the system state estimated at time $k - 1$, based on (3.1) and (3.4), a state estimator at time k is designed as follows:

$$\hat{x}_{k+1} = A_0 x_k + B_0 u_k + g(x_k, u_k) \hat{\theta}_{k+1} + K_e \tilde{x}_k + K_e w_k (\hat{\theta}_k - \hat{\theta}_{k+1}), \quad (3.5)$$

where $\tilde{x}_k = x_k - \hat{x}_k$ is the state estimation error. Then subtracting (3.1) from (3.5) yields

$$\tilde{x}_{k+1} = g(x_k, u_k) \tilde{\theta}_{k+1} - K_e \tilde{x}_k - K_e w_k (\hat{\theta}_k - \hat{\theta}_{k+1}). \quad (3.6)$$

In order to establish an implicit regression model for $\hat{\theta}$, we introduce an auxiliary variable η_k in the following

$$\eta_k = \tilde{x}_k - w_k \tilde{\theta}_k. \quad (3.7)$$

Then by substituting (3.4)-(3.6) into (3.7), one gets

$$\eta_{k+1} = -K_e \eta_k. \quad (3.8)$$

Based on this implicit regression model, we develop the following parameter estimator by using the standard RLS algorithm [208]

$$\hat{\theta}_{k+1} = \hat{\theta}_k + \Gamma_{k+1}^{-1} w_k^T (\tilde{x}_k - \eta_k), \quad (3.9a)$$

$$\Gamma_{k+1} = \lambda \Gamma_k + w_k^T w_k, \quad (3.9b)$$

where $\Gamma_0 = \beta I_{n_\theta}$; β is the positive scalar, and $\lambda \in (0, 1)$ is the forgetting factor. Then it follows from [208] that the non-increasing estimation error is guaranteed, and the convergence of parameter estimates $\hat{\theta}_k$ can be achieved if the sequence w_k is persistently exciting.

By using the proposed estimation mechanism (3.9), the convergence of the estimation error $\tilde{\theta}_k$ relies on the persistently exciting sequence of w_k instead of $g(x_k, u_k)$. Suppose that the system is stable when $k \geq t_s$, $t_s \in \mathbb{N}_0^\infty$, and $w_{t_s} \neq 0$. According to (3.4), we have $w_{k+1} = -K_e w_k$ for all $k \geq t_s$. Let $\mathbf{w}_k = \{w_k, w_{k+1}, \dots, w_{k+N_p-1}\}$

with $N_p \in \mathbb{N}_0^\infty$. Then it can be derived that $\mathbf{w}_k \mathbf{w}_k^\top = \mathcal{K}_e w_k w_k^\top \mathcal{K}_e^\top$ for $k \geq t_s$, where $\mathcal{K}_e = \text{col}(I, -K_e, (-K_e)^2, \dots, (-K_e)^{N_p-1})$. Since K_e is Schur stable, it is possible to find $N_p, l_p \in \mathbb{N}_0^\infty, t_d \in \mathbb{N}_{t_s}^\infty, \rho_0 > 0$ and $\rho_1 > 0$ such that $\rho_1 I_{N_p N_x} > \sum_{j=0}^{l_p-1} (\mathbf{w}_{k+j} \mathbf{w}_{k+j}^\top) > \rho_0 I_{N_p N_x}$ for all $k \in \mathbb{N}_{t_s}^{t_d}$. Therefore, the sequence \mathbf{w}_k satisfies the PE condition during a certain period when the system is stable. In addition, it can be derived from (3.9) that $\hat{\theta}_{k+1} \approx \hat{\theta}_k, \Gamma_{k+1} \approx \lambda \Gamma_k$ and the corresponding $\hat{\Theta}_k \approx \hat{\Theta}_{k+1}$ when w_k is sufficiently small. Since w_k is decreasing when the system (3.1) is stable, $\hat{\Theta}_k$ will converge to a fixed set in finite time.

3.3.2 Uncertainty set estimation

To bound the unknown parameters, we introduce the following ellipsoidal uncertainty set

$$\hat{\Theta}_k = \{\theta \mid \|\theta - \hat{\theta}_k\|_{\Gamma_k} \leq \mathcal{V}_k\}. \quad (3.10)$$

where $\mathcal{V}_k > 0$ is the bound of the estimation error. According to (3.9b), we define the propagation of \mathcal{V}_k as $\mathcal{V}_{k+1} = \lambda \mathcal{V}_k$ with $\mathcal{V}_0 = \bar{\Lambda}(\Gamma_0) r_0^2$, where $\bar{\Lambda}(\Gamma_0)$ is the maximal eigenvalue of Γ_0 .

Let Θ_k denote the FSS of unknown parameters. Since unknown parameters are uniquely identifiable and stay in the *a priori* known set Θ_0 , Θ_k must be the subset of Θ_0 . Therefore, for all $k \geq 1$, Θ_k is computed as follows

$$\Theta_k = \Theta_{k-1} \cap \hat{\Theta}_k. \quad (3.11)$$

By choosing suitable $\hat{\theta}_0, \Gamma_0$ and \mathcal{V}_0 , $\hat{\Theta}_0$ can be equivalent to Θ_0 . The following lemma shows the performance of uncertainty set estimation.

Lemma 3.1. *Let Θ_k denote the estimated uncertainty set updated by following (3.4)-(3.11) at each time instant. Suppose that $\theta^* \in \Theta_0$, then we have $\theta^* \in \Theta_k$ for all $k \geq 0$.*

Proof. To prove this lemma, we firstly show that $\theta^* \in \hat{\Theta}_k$ for all $k \geq 0$. Let $\mathcal{V}(\tilde{\theta}_k) = \tilde{\theta}_k^\top \Gamma_k \tilde{\theta}_k$, then it follows from [208] that $\mathcal{V}(\tilde{\theta}_k)$ is non-increasing and $\mathcal{V}(\tilde{\theta}_k) \leq \lambda \mathcal{V}(\tilde{\theta}_{k-1})$. When $k = 0$, the condition $\mathcal{V}(\tilde{\theta}_0) = \tilde{\theta}_0^\top \Gamma_0 \tilde{\theta}_0 \leq \mathcal{V}_0$ holds by using $\|\tilde{\theta}_0\| \leq r_0$. When $k > 0$, we still have $\mathcal{V}_k \geq \mathcal{V}(\tilde{\theta}_k)$ since $\mathcal{V}_k = \lambda^k \mathcal{V}_0$ and $\mathcal{V}(\tilde{\theta}_k) \leq \lambda^k \mathcal{V}(\tilde{\theta}_0)$. Therefore, one gets $\mathcal{V}(\tilde{\theta}_k) \leq \mathcal{V}_k$ for all $k \geq 0$. Then according to (3.10), it can be derived that $\theta^* \in \hat{\Theta}_k$ for all $k \geq 0$. Suppose that $\theta^* \in \Theta_k$. At next time instant, we have $\theta^* \in \hat{\Theta}_{k+1}$, which implies

that $\theta^* \in \Theta_k \cap \hat{\Theta}_{k+1} = \Theta_{k+1}$. Hence, it can be concluded that $\theta^* \in \Theta_k$ for all $k \geq 0$ if $\theta^* \in \Theta_0$. \square

Generally, the tightened state constraints are widely employed in robust MPC to guarantee recursive feasibility and closed-loop stability. These constraints are designed based on the given bounds of uncertainties. Hence, having an accurate description of the uncertainty is crucial to obtain the desired closed-loop performance. By incorporating the proposed parameter estimator, it is possible to use the estimated parameters and uncertainty sets at each time instant to obtain more accurate predictions and less conservative tightened state constraints in robust MPC and thus improving the control performance. In the following section, a computationally tractable integration of tube MPC and the proposed estimator is presented.

3.4 Adaptive Model Predictive Control

In this section, we present a computationally tractable adaptive MPC algorithm based on the homothetic tube MPC technique. Let $x_{l|k}$ denote the predicted real system state l steps ahead from time k and $x_{l|k} = z_{l|k} + e_{l|k}$, where $z_{l|k}$ and $e_{l|k}$ are the predicted nominal system state and the error state, respectively. Our objective is to design a sequence of state tubes $\{\mathcal{X}_{l|k}\}$ for robust constraint satisfaction, i.e., the following conditions hold for some $u_{l|k}$:

$$x_k \in \mathcal{X}_{0|k} \tag{3.12a}$$

$$A(\theta)x + B(\theta)u_{l|k} \in \mathcal{X}_{l+1|k}, \forall x \in \mathcal{X}_{l|k}, \theta \in \Theta_{k+1} \tag{3.12b}$$

$$(x, u_{l|k}) \in \mathcal{M}, \forall x \in \mathcal{X}_{l|k} \tag{3.12c}$$

Instead of designing the state tube $\mathcal{X}_{l|k}$ directly, in this work we construct the tube cross section $S_{l|k}$ for the error state $e_{l|k}$. Therefore, the state tube can be established indirectly as $\mathcal{X}_{l|k} = z_{l|k} \oplus S_{l|k}$. In the following, we present how to design the homothetic tubes according to the estimation of uncertainties.

3.4.1 Error tube and constraint satisfaction

As mentioned in Section 3.3.1, we predict $\hat{\theta}_{k+1}$ and Θ_k at time k based on the state estimation error \tilde{x}_k . Hence the system matrices $A(\hat{\theta}_{k+1})$ and $B(\hat{\theta}_{k+1})$ are considered in the

following for predicting the nominal system state at time k :

$$z_{l+1|k} = A_{k+1}z_{l|k} + B_{k+1}u_{l|k} \quad (3.13)$$

where $A_{k+1} = A(\hat{\theta}_{k+1})$ and $B_{k+1} = B(\hat{\theta}_{k+1})$; N is the prediction horizon and $l \in \mathbb{N}_0^{N-1}$.

Then subtracting (3.1) from (3.13) results in

$$\begin{aligned} e_{l+1|k} &= x_{l+1|k} - z_{l+1|k} \\ &= \phi^* e_{l|k} + \Delta\phi_{k+1}z_{l|k} + \Delta B_{k+1}v_{l|k}, \end{aligned} \quad (3.14)$$

where $\phi^* = A(\theta^*) + B(\theta^*)K$, $\phi_{k+1} = A_{k+1} + B_{k+1}K$, $\Delta\phi_{k+1} = \phi^* - \phi_{k+1}$ and $\Delta B_{k+1} = B(\theta^*) - B_{k+1}$. Since Θ_k is compact and convex, we can find a polytope to over approximate Θ_k by following the algorithm in [209]. Let $\bar{\Theta}_k$ denote the polytopic over approximation of Θ_k , and $\text{Pol}(\cdot)$ is the polytopic approximation operator from the algorithm in [209]. Hence $\bar{\Theta}_k$ can be directly calculated as $\bar{\Theta}_k = \text{Pol}(\Theta_k)$. Due to the recursive set intersection in (3.11), we calculate $\bar{\Theta}_k$ indirectly to reduce the computational load, i.e., $\bar{\Theta}_k = \text{Pol}(\hat{\Theta}_k) \cap \bar{\Theta}_{k-1}$ with $\bar{\Theta}_0 = \text{Pol}(\Theta_0)$. Suppose that $\bar{\Theta}_k$ can be equivalently represented by a convex hull $Co(\hat{\theta}_k^j)$, where $j \in \mathbb{N}_0^{n_c}$ and n_c is an integer denoting the number of extreme points in the convex hull. Hence, a set for the system pair $(A(\theta), B(\theta))$ at time k can be approximated by using a convex hull $Co(A_k^j, B_k^j)$, where $A_k^j = A(\hat{\theta}_k^j)$ and $B_k^j = B(\hat{\theta}_k^j)$.

Inspired by the previous work [35], we consider a polytopic tube with the form $S_{l|k} = \{e_{l|k} | Ve_{l|k} \leq \alpha_{l|k}\}$ for the error $e_{l|k}$ to handle multiplicative uncertainties, where $V \in \mathbb{R}^{n_v \times n_x}$ is a matrix describing the shape of $S_{l|k}$; $\alpha_k \in \mathbb{R}^{n_v \times 1}$ is the tube parameter to be optimized. The following proposition shows a sufficient condition for the robust satisfaction of constraint (3.2).

Proposition 3.1. *Let $S_{l|k} = \{e_{l|k} | Ve_{l|k} \leq \alpha_{l|k}\}$. Suppose that $e_{l|k} \in S_{l|k}$, then $e_{l+1|k} \in S_{l+1|k}$. In addition, the constraint (3.2) is satisfied at each time instant if the following conditions hold:*

$$\mathbf{1} \geq \begin{cases} H\alpha_{l|k} + (F + GK)z_{l|k} + Gv_{l|k}, l \in \mathbb{N}_0^{N-1} \\ H\alpha_{l|k} + (F + GK)z_{l|k}, l \in \mathbb{N}_N^\infty \end{cases} \quad (3.15a)$$

$$\alpha_{l+1|k} \geq H_{k+1}^j \alpha_{l|k} + V(\Delta\phi_{k+1}^j z_{l|k} + \Delta B_{k+1}^j v_{l|k}), l \in \mathbb{N}_0^\infty, j \in \mathbb{N}_0^{n_c} \quad (3.15b)$$

where $\phi_k^j = A_k^j + B_k^j K$, $\Delta\phi_{k+1}^j = \phi_{k+1}^j - \phi_{k+1}$ and $\Delta B_{k+1}^j = B_{k+1}^j - B_{k+1}$; H and H_{k+1}^j

are non-negative matrices satisfying the conditions $HV = F + GK$ and $H_{k+1}^j V = V\phi_{k+1}^j$.

Proof. Consider the uncertain input matrix $B(\theta)$ in the system (3.1), this proof is completed by following the proof of Proposition 2 in [35]. \square

Proposition 3.1 shows a sequence of tightened sets for the nominal system state. By considering tube parameters $\{\alpha_{l|k}\}$ as extra decision variables of the MPC optimization problem, we can obtain the optimal tube cross-sections online.

According to the proposed parameter estimator, we can obtain the new estimation of the real system with non-increasing estimation error at each time instant. Hence, a time-varying nominal system is used to improve the accuracy of prediction. However, the system is considered to be invariant during the prediction. In order to improve the control performance, a time-varying terminal set is constructed based on the new estimation of uncertainty, which will be presented in the following.

3.4.2 Construction of terminal sets

Based on Proposition 3.1, we define the following dynamics of $z_{l|k}$ and $\alpha_{l|k}$ for $l \in \mathbb{N}_N^\infty$ at time k

$$\alpha_{l+1|k} = \max_{j \in \mathbb{N}_0^{n_c}} \{H_k^j \alpha_{l|k} + V \Delta \phi_{k+1}^j z_{l|k}\}, \quad (3.16a)$$

$$z_{l+1|k} = \phi_{k+1} z_{l|k}, \quad (3.16b)$$

where the maximization is taken for each element in the vector. Let \mathcal{Z}_k denote the polytopic RPI set for the system $x_{k+1} = (A(\theta) + B(\theta)K)x_k$ with respect to the uncertainty set Θ_{k+1} . Since $\hat{\theta}_{k+1} \in \Theta_{k+1}$, \mathcal{Z}_k is also RPI for the system (3.16b).

Define $\mathcal{Z}_{l+1|k}^j$ as $\mathcal{Z}_{l+1|k}^j = \phi_{k+1}^j \mathcal{Z}_{l|k}^j$ with $\mathcal{Z}_{0|k}^j = \mathcal{Z}_k$ for all $j \in \mathbb{N}_0^{n_c}$, then we have $\mathcal{Z}_{l+1|k}^j \subseteq \mathcal{Z}_{l|k}^j \subseteq \mathcal{Z}_k$ since ϕ_{k+1}^j is Schur stable for all $j \in \mathbb{N}_0^{n_c}$. Inspired by Proposition 3 in [35], the following proposition is given to construct the invariant set for the system (3.16a).

Proposition 3.2. *Define*

$$\begin{aligned} \bar{f}_{l|k}^j &= \max_{z \in \mathcal{Z}_{l|k}^j} \{(F + GK)z\}, \\ \bar{c}_{l|k}^j &= \max_{z \in \mathcal{Z}_{l|k}^j} \{V(\phi_{k+1}^j - \phi_{k+1})z\}, \\ \bar{g}_{l|k}^j &= \max_{z_1, z_2 \in \mathcal{Z}_{l|k}^j} \{V\phi_{k+1}^j(z_1 - z_2)\}. \end{aligned} \quad (3.17)$$

The set $\mathcal{A}_k = \{\alpha \mid \|\alpha\|_\infty \leq \gamma_k, \alpha \geq 0\}$ is invariant for the system (3.16a) while the constraint $H\alpha + (F + GK)z \leq \mathbf{1}$ is satisfied if the following condition holds

$$\bar{\gamma}_{l|k} \geq \gamma_k \geq \underline{\gamma}_{l|k} \quad (3.18)$$

where

$$\underline{\gamma}_{l|k} = \frac{\max_{j \in \mathbb{N}_0^{n_c}} \|\bar{c}_{l|k}^j\|_\infty + \|\bar{g}_{l|k}^j\|_\infty}{1 - \max_{j \in \mathbb{N}_0^{n_c}} \|H_{k+1}^j\|_\infty}, \quad \bar{\gamma}_{l|k} = \frac{1 - \max_{j \in \mathbb{N}_0^{n_c}} \|\bar{f}_{l|k}^j\|_\infty}{\|H\|_\infty}.$$

In addition, there exists a γ_k satisfying the condition (3.18) if l is sufficiently large.

Proof. This proposition can be proved by following the proof of Proposition 3 in [35]. \square

As shown in [35], the invariant set \mathcal{A}_k for the system (3.16a) is nonempty if $\|H_k^j\|_\infty < 1$ for all $k \geq 0$. This condition can be satisfied by choosing the appropriate V such that the set $\{x \mid Vx \leq \mathbf{1}\}$ is a λ -contractive set for the system $z_{k+1} = \phi(\theta)z_k, \forall \theta \in \Theta_0$. An example of computing the matrix V can be found in [205].

To find the terminal set for the nominal state $z_{N|k}$, we have the following assumption:

Assumption 3.1. Let \mathcal{Z}_k and \mathcal{Z}_{k+1} denote the MRPI sets with respect to the uncertainty set Θ_{k+1} and Θ_{k+2} , respectively. Then the following condition holds

$$\phi(\theta)x \in \mathcal{Z}_{k+1}, \forall (x, \theta) \in \mathcal{Z}_k \times \Theta_{k+2} \quad (3.19)$$

if $\Theta_{k+2} \subseteq \Theta_{k+1}$.

Remark 3.1. To compute the set \mathcal{Z}_{k+1} satisfying the condition (3.19), we can compute the RPI set $\tilde{\mathcal{Z}}_{k+1}$ by following Algorithm 1 in [210] without considering (3.19). Then starting with $\tilde{\mathcal{Z}}_{k+1}$, \mathcal{Z}_{k+1} can be computed by solving the linear programming problem with the additional constraint (3.19). In addition, given $\mathcal{Z}_k, \Theta_{k+1}$ and Θ_{k+2} with $\Theta_{k+2} \subseteq \Theta_{k+1}$, there always exists one \mathcal{Z}_{k+1} such that (3.19) holds. A simple example is to choose \mathcal{Z}_{k+1} as $\mathcal{Z}_{k+1} = \mathcal{Z}_k$ directly.

Assumption 3.2. Let $M_k, M_{k+1}, \mathcal{A}_k$ and \mathcal{A}_{k+1} are the horizons and invariant sets satisfying Proposition 3.2 with respect to uncertainty sets Θ_{k+1} and Θ_{k+2} , respectively. Given M_k and \mathcal{A}_k , if the condition $\Theta_{k+2} \subseteq \Theta_{k+1}$ holds, there exist M_{k+1} and \mathcal{A}_{k+1} such that $M_k \geq M_{k+1}$ and $\mathcal{A}_k \subseteq \mathcal{A}_{k+1}$.

According to Proposition 3.2, the feasible solution set of γ_k in (3.18) becomes larger when l increases. Therefore, the larger invariant set \mathcal{A}_k can be found by choosing the

larger horizon \mathcal{M}_k . In addition, it follows from (3.11) that $\Theta_{k+2} \subseteq \Theta_{k+1}$ for all $k \geq 0$. Let $\gamma_k = \bar{\gamma}_{M_k|k}$, $\gamma_{k+1} = \bar{\gamma}_{M_{k+1}|k+1}$ and $M_{k+1} = M_k$, then we have $\mathcal{A}_k \subseteq \mathcal{A}_{k+1}$ since $\gamma_{k+1} \geq \gamma_k$. Therefore, given M_k and \mathcal{A}_k , we can always find M_{k+1} and \mathcal{A}_{k+1} such that Assumption 3.2 holds. As a result, the computational complexity of the MPC optimization problem is still non-increasing under this assumption.

Suppose that the RPI set \mathcal{Z}_k has the polyhedral form $\mathcal{Z}_k = \{x | V_k x \leq \mathbf{1}\}$, then the terminal constraints for the systems in (3.16) are summarized as follows:

$$V_k z_{N|k} + D_k \alpha_{N|k} \leq \mathbf{1}, \quad (3.20a)$$

$$0 \leq \alpha_{N+M_k|k} \leq \gamma_k \mathbf{1}, \quad (3.20b)$$

where D_k is a non-negative matrix satisfying $D_k V = V_k$.

3.4.3 Construction of the cost function

Let $\mathbf{v}_k = \text{col}(v_{0|k}, v_{1|k}, v_{2|k}, \dots, v_{N-1|k})$. Define E and T as shift matrices such that $v_{0|k} = E \mathbf{v}_k$ and $\mathbf{v}_{k+1} = T \mathbf{v}_k$, then the prediction of $z_{l|k}$ can be written as $\xi_{l+1|k} = \Psi_{k+1} \xi_{l|k}$, where

$$\xi_{l|k} = \begin{bmatrix} z_{l|k} \\ \mathbf{v}_k \end{bmatrix}, \Psi_{k+1} = \begin{bmatrix} \phi_{k+1} & B_{k+1} E \\ 0 & T \end{bmatrix}.$$

Similarly, the real system state $x_{l|k}$ can be predicted by using the following dynamics $\bar{\xi}_{l+1|k} = \Psi^* \bar{\xi}_{l|k}$ with

$$\bar{\xi}_{l|k} = \begin{bmatrix} x_{l|k} \\ \mathbf{v}_k \end{bmatrix}, \Psi^* = \begin{bmatrix} \phi^* & B^* E \\ 0 & T \end{bmatrix}.$$

In this work, the objective is to minimize a cost function with a quadratic form $\bar{J}_k = \sum_{i=0}^{\infty} (x_{i|k}^T Q x_{i|k} + u_{i|k}^T R u_{i|k})$, where $Q > 0$ and $R > 0$ are penalty matrices for the state and input, respectively. Note that the cost function \bar{J}_k can be equivalently represented by $\bar{J}_k = \xi_{0|k}^T W^* \xi_{0|k}$, where W^* is the solution of a Lyapunov equation

$$(\Psi^*)^T W^* (\Psi^*) - W^* + \bar{Q} = 0, \bar{Q} = \begin{bmatrix} Q + K^T R K & K^T R E \\ E^T R K & E^T R E \end{bmatrix}. \quad (3.21)$$

Since ϕ^* is unknown, we cannot find the matrix W^* exactly. Alternatively, we consider an over approximation of \bar{J}_k based on the uncertainty set updated at each time instant.

Lemma 3.2. Define a new cost function J_k as $J_k = \xi_{0|k}^T W_{k+1} \xi_{0|k}$, where W_{k+1} is a positive

definite matrix, then $J_k \geq \bar{J}_k$ if the following condition

$$W_{k+1} \geq \begin{bmatrix} \phi(\theta) & B(\theta)E \\ 0 & T \end{bmatrix}^T W_{k+1} \begin{bmatrix} \phi(\theta) & B(\theta)E \\ 0 & T \end{bmatrix} + \bar{Q} \quad (3.22)$$

holds for all $\theta \in \Theta_{k+1}$.

Proof. From Lemma 3.1, we have $\theta^* \in \Theta_{k+1}$. Then following (3.22) yields $W_{k+1} \geq (\Psi^*)^T W_{k+1} (\Psi^*) + \bar{Q}$. By substituting $\bar{Q} = W^* - (\Psi^*)^T W (\Psi^*)$ into the above equation, we have $W_{k+1} - W^* \geq (\Psi^*)^T (W_{k+1} - W^*) (\Psi^*) \geq 0$. In addition, $J_k - \bar{J}_k = \xi_{0|k}^T W_{k+1} \xi_{0|k} - \bar{\xi}_{0|k}^T W^* \bar{\xi}_{0|k}$. Since $\bar{\xi}_{0|k} = \xi_{0|k}$ and $W_{k+1} - W^* \geq 0$, it can be concluded that $J_k \geq \bar{J}_k$ for all $\theta \in \Theta_{k+1}$. \square

Assumption 3.3. Let W_{k+1} denote the weighting matrix at time k , if $\Theta_{k+1} \subseteq \Theta_k$, then the following condition holds for all $k \geq 0$

$$\xi_{0|k}^T W_{k+1} \xi_{0|k} \leq \xi_{0|k}^T W_k \xi_{0|k}. \quad (3.23)$$

Remark 3.2. Following (3.4)-(3.11), it can be guaranteed that $\Theta_{k+1} \subseteq \Theta_k$ for all $k \geq 0$. Given W_k , by imposing (3.23) as an additional constraint for the *linear matrix inequality (LMI)* problem used for computing W_{k+1} , we can find a W_{k+1} satisfying the condition (3.23). An example of formulating the LMI problem can be found in [9] for details.

3.4.4 Adaptive MPC algorithm

According to the developed terminal sets and cost function, the adaptive MPC algorithm is based on the following MPC optimization problem:

$$\begin{aligned} \mathbb{P} : \min_{\mathbf{v}_k, \{\alpha_{l|k}\}} \quad & J_k = \xi_{0|k}^T W_{k+1} \xi_{0|k} \\ \text{s.t.} \quad & z_{0|k} = x_k \\ & (3.3), (3.13), (3.15a), (3.15b), (3.20a), (3.20b) \end{aligned}$$

At time instant k , we update the estimation of the unknown parameters and the uncertainty set based on new measurements, then reformulate the optimization problem \mathbb{P} . Note that the reformulation of \mathbb{P} with respect to the new estimation is not necessary if the estimation error is sufficiently small. To reduce redundant estimating actions, we introduce a

termination criterion for the proposed estimator. Let $\epsilon_x > 0$ and $\epsilon_r > 0$ denote the tolerances for the state estimation error and the error bound of parameter estimation, then the proposed adaptive MPC algorithm is summarized in Algorithm 3.1.

Algorithm 3.1 The Adaptive MPC algorithm

Input: Given initial conditions x_0, Θ_0 and weighting matrices Q, R , determine the prestabilizing feedback gain K and MRPI set \mathcal{Z}_0 . Compute the terminal set \mathcal{A}_0 and the horizon M_0 according to Proposition 3.2. Calculate the weighting matrix W_0 satisfying (3.22).

- 1: **for** each time instant $k = 0, 1, 2, \dots$ **do**
 - 2: **if** $\|\tilde{x}_k\| \geq \epsilon_x$ or $\mathcal{V}_k \geq \epsilon_r$ **then**
 - 3: Calculate $\hat{\theta}_{k+1}$ and Θ_{k+1} by using (3.4)-(3.11).
 - 4: Compute $M_k, \mathcal{A}_k, W_{k+1}$ and \mathcal{Z}_k with respect to Θ_{k+1} such that Assumptions 3.1, 3.2 and 3.3 hold.
 - 5: **else**
 - 6: Let $\hat{\theta}_{k+1} = \hat{\theta}_k, \Theta_{k+1} = \Theta_k, \mathcal{Z}_k = \mathcal{Z}_{k-1}, W_{k+1} = W_k, M_k = M_{k-1}$ and $\mathcal{A}_k = \mathcal{A}_{k-1}$.
 - 7: **end if**
 - 8: Reformulate and solve the optimization problem \mathbb{P} based on $\hat{\theta}_{k+1}$ and Θ_{k+1} to obtain \mathbf{v}_k^* ,
 - 9: Calculate the control input as $u_k = Kx_k + v_{0|k}^*$, and then implement u_k to the system.
 - 10: **end for**
-

Theorem 3.1. *Suppose that Assumptions 3.1, 3.2 and 3.3 hold, and there is a feasible solution to the optimal control problem \mathbb{P} when $k = 0$. Then \mathbb{P} is recursively feasible by following Algorithm 3.1.*

Proof. Suppose that \mathbb{P} is feasible at time k . Let \mathbf{v}_k^* and $\boldsymbol{\alpha}_k^* = \{\alpha_{l|k}^*\}_{l=0}^{N+M_k}$ denote the optimal solution of the MPC problem at time k . $\{z_{l|k}^*, \mathcal{S}_{l|k}^* = \{e_{l|k} | V_k e_{l|k} \leq \alpha_{l|k}^*\}, \mathcal{X}_{l|k}^* = z_{l|k}^* \oplus S_{l|k}^*\}_{l=0}^{N+M_k}$ are the corresponding nominal states, error tubes and state tubes, respectively. Define a candidate input sequence at time $k+1$ as $\bar{\mathbf{v}}_{k+1} = \{v_{1|k}^*, v_{2|k}^*, \dots, v_{N-1|k}^*, 0\}$.

Two cases are investigated to prove this theorem.

Case (1): Suppose that the estimation termination criterion in Algorithm 3.1 is not satisfied. Based on $z_{0|k+1}$ and $\bar{v}_{l|k+1}$, we firstly construct the following sequence $\bar{\boldsymbol{\alpha}}_{k+1} = \{\alpha_{l|k+1}\}_{l=0}^{N+M_{k+1}-1}$ such that $\mathcal{X}_{l|k+1} = \mathcal{X}_{l+1|k}^*$. Let

$$\alpha_{N+M_{k+1}|k+1} = \max_{j \in \mathbb{N}_0^{n_c}} \{H_{k+2}^j \alpha_{N+M_{k+1}-1|k+1} + V \Delta \phi_{k+2}^j z_{N+M_{k+1}-1|k+1}\},$$

we show that $\{\bar{\mathbf{v}}_{k+1}, \bar{\boldsymbol{\alpha}}_{k+1}\}$ is a feasible solution for \mathbb{P} in the following.

- For $l \in \mathbb{N}_0^{N+M_{k+1}-1}$, since $\mathcal{X}_{l|k+1} = \mathcal{X}_{l+1|k}^*$, we have $\{z_{l+1|k}^*, S_{l+1|k}^*\}$ satisfying the condition $z_{l+1|k}^* \oplus S_{l+1|k}^* = z_{l|k+1} \oplus S_{l|k+1}$, which verifies that the candidate sequence $\{z_{l|k+1}, \alpha_{l|k+1}, \bar{v}_{l|k+1}\}_{l=0}^{N+M_{k+1}-1}$ satisfies the constraints (3.15a) and (3.15b).
- When $l = N$, it follows from (3.20a) that $V_k z_{N|k}^* + D_k V e_{N|k} \leq \mathbf{1}$. By using $D_k V = V_k$, we have $V_k(z_{N|k}^* + e_{N|k}) = V_k x_{N|k} \leq \mathbf{1}$, implying that $\mathcal{X}_{N|k}^* \subseteq \mathcal{Z}_k$. As aforementioned, $\mathcal{X}_{N-1|k+1} = \mathcal{X}_{N|k}^*$, then $\mathcal{X}_{N-1|k+1} \subseteq \mathcal{Z}_k$. Since \mathcal{Z}_k is an RPI set, $\bar{v}_{N-1|k+1} = 0$ and $\Theta_{k+2} \subseteq \Theta_{k+1}$, it yields that $\mathcal{X}_{N|k+1} \subseteq \phi_{k+2} \mathcal{Z}_k \subseteq \mathcal{Z}_{k+1}$ by following Assumption 3.1. Hence, we have $z_{N|k+1} + e_{N|k+1} \in \mathcal{Z}_{k+1}$ for all admissible $e_{N|k+1}$. As a result, the constraint (3.20a) is satisfied.
- When $l = N + M_{k+1}$, taking the infinity norm of (3.16a), we have $\|\alpha_{l|k+1}\|_\infty \leq \max_{j \in \mathbb{N}_0^{n_c}} \{ \|H_{k+2}^j\|_\infty \|\alpha_{l-1|k+1}\|_\infty + \|\bar{c}_{l-1|k+1}^j\|_\infty \}$. Since $\mathcal{X}_{l-1|k+1} = \mathcal{X}_{l|k}^*$ and $\Theta_{k+2} \subseteq \Theta_{k+1}$, following Proposition 3.2 and Assumption 3.2, it is concluded that $\|\alpha_{l|k+1}\|_\infty \leq \gamma_k \leq \gamma_{k+1}$. Hence, the constraint (3.20b) is satisfied.

Case (2): Suppose that the estimation termination criterion in Algorithm 3.1 is satisfied. Then we have $\hat{\theta}_{k+2} = \hat{\theta}_{k+1}$, $\mathcal{Z}_{k+1} = \mathcal{Z}_k$, $W_{k+2} = W_{k+1}$, $\gamma_{k+1} = \gamma_k$ and $M_{k+1} = M_k$. The recursive feasibility can be proved by constructing the following candidate sequence $\bar{\mathbf{v}}_{k+1}, \{\alpha_{1|k}^*, \alpha_{2|k}^*, \dots, \alpha_{N+M_k|k}^*, \max_{j \in \mathbb{N}_0^{n_c}} \{H_{k+1}^j \alpha_{N+M_k|k} + V \Delta \phi_{k+1}^j z_{N+M_k|k}\}\}$.

In summary, there is a feasible solution for the optimal control problem \mathbb{P} at time $k+1$ if it is feasible at time k . Therefore \mathbb{P} is proved to be recursively feasible. \square

Theorem 3.2. *Suppose that Assumptions 3.1, 3.2 and 3.3 hold, then the system (3.1) in closed-loop is asymptotically stable by applying the adaptive MPC Algorithm 3.1.*

Proof. To prove this theorem, in the following, we show that the optimal cost J_k^* is a Lyapunov function for the system (3.1) in closed-loop with Algorithm 3.1.

Case (1): Suppose that the estimation termination criterion in Algorithm 3.1 is not satisfied. Let $z_{0|k+1} = x_{k+1}$, $\xi_{0|k+1} = \text{col}(z_{0|k+1}, \bar{\mathbf{v}}_{k+1})$, $\xi_{0|k} = \text{col}(z_{0|k}, \mathbf{v}_k^*)$ and $\bar{J}_{k+1} = \xi_{0|k+1}^\top W_{k+2} \xi_{0|k+1}$, based on Lemma 3.2, we have

$$\begin{aligned} \xi_{0|k+1}^\top W_{k+1} \xi_{0|k+1} - J_k^* &= \xi_{0|k}^\top (\Psi^*)^\top W_{k+1} \Psi^* \xi_{0|k} - \xi_{0|k}^\top W_{k+1} \xi_{0|k} \\ &\leq -\xi_{0|k}^\top \bar{Q} \xi_{0|k} = -z_{0|k}^\top Q z_{0|k} - u_{0|k}^\top R u_{0|k}. \end{aligned}$$

Since Q and R are positive definite and $z_{0|k} = x_k$, it can be derived that

$$\bar{\xi}_{0|k+1}^\top W_{k+1} \bar{\xi}_{0|k+1} - J_k^* \leq -x_k^\top Q x_k - u_{0|k}^\top R u_{0|k}.$$

In addition, from Assumption 3.1, we have

$$\bar{J}_{k+1} = \bar{\xi}_{0|k+1}^T W_{k+2} \bar{\xi}_{0|k+1} \leq \bar{\xi}_{0|k+1}^T W_{k+1} \bar{\xi}_{0|k+1},$$

which yields

$$J_{k+1}^* - J_k^* \leq \bar{J}_{k+1} - J_k^* \leq -x_k^T Q x_k - u_k^T R u_k \leq 0, \forall x_k \neq 0, u_k \neq 0.$$

Since W_k is positive definite, J_k^* is a Lyapunov function for the system (3.1).

Case (2): Suppose that the estimation termination criterion in Algorithm 1 is satisfied. Then we have $\hat{\theta}_{k+2} = \hat{\theta}_{k+1}$, $\mathcal{Z}_{k+1} = \mathcal{Z}_k$, $W_{k+2} = W_{k+1}$, $\gamma_{k+1} = \gamma_k$ and $M_{k+1} = M_k$. By repeating the above procedure, we can prove that J_k^* is a Lyapunov function.

In summary, the optimal cost function J_k^* is a Lyapunov function for the system (3.1) in closed-loop with Algorithm 3.1. Hence, based on Theorem 2.1, it can be concluded the closed-loop system is asymptotically stable. \square

Remark 3.3. Note that, unlike the robust method in [35], the propagation of homothetic tube $\mathcal{S}_{l|k}$ (3.15) in our proposed method depends on the estimation $\hat{\theta}_{k+1}$ and $\hat{\Theta}_{k+1}$. In addition, the nominal system (3.13), the terminal conditions in (3.20) and the weighting matrix W_{k+1} are also updated based on the estimation of uncertainty at each time instant. By following (3.4)-(3.11), the non-increasing properties on the proposed estimation scheme are guaranteed. Therefore, the resulting adaptive MPC scheme can reduce conservatism compared with the original robust MPC method. The numerical simulations will elaborate on this argument.

Remark 3.4. As shown in Algorithm 3.1, when updating the parameter estimate $\hat{\theta}_k$ and uncertainty set Θ_k , we need to re-compute M_k , \mathcal{Z}_{k+1} and W_{k+1} , which is relatively computationally expensive. For some problems which have strict requirements on the computational load, a solution to reduce the computational complexity is to choose the relatively large ϵ_x and ϵ_r . An alternative is to omit the update of terminal conditions and cost function by setting $M_k = M_0$, $\mathcal{Z}_k = \mathcal{Z}_0$ and $W_k = W_0$ for all $k \geq 0$. Due to the fact that $\Theta_{k+1} \subseteq \Theta_k \subseteq \Theta_0$, this strategy can significantly reduce the computational load with guaranteed closed-loop stability and recursive feasibility but results in relatively conservative control performance. Note that the recursive updates of the system model and uncertainty sets are considered in the tube propagation. Thus, this simplified method still has less conservative closed-loop performance compared with the robust MPC method. The numerical simulation will demonstrate this argument.

3.5 Simulation Results

In this section, a numerical example is presented to show the effectiveness of proposed adaptive MPC algorithms. The numerical test is conducted in Matlab, where the MPC optimization problem is formulated and solved by using Yalmip [211].

We consider the following example for testing:

$$A_0 = \begin{bmatrix} 0.42 & -0.28 \\ 0.02 & 0.6 \end{bmatrix}, A_1 = \begin{bmatrix} -0.12 & -0.08 \\ -0.12 & -0.17 \end{bmatrix}, A_2 = -A_1, \\ B_0 = \begin{bmatrix} 0.3 & -0.4 \end{bmatrix}^T, B_1 = \begin{bmatrix} 0.04 & -0.08 \end{bmatrix}^T, B_2 = -1.5B_1.$$

$\Theta_0 = \{\theta \in \mathbb{R}^2 \mid \|\theta\| \leq 1\}$, $\{x \mid \|x\|_\infty \leq 17\}$ and $\{u \mid \|u\|_\infty \leq 4\}$. The weighting matrices are chosen as $Q = I_2$ and $R = 1$. By following [9], the prestabilizing feedback gain is chosen as $K = [-0.4187 \ 1.1562]$. Set the prediction horizon $N = 10$, then the horizon and terminal region are derived as $M_0 = 3$ and $\gamma_0 = 0.4266$. The parameters used in Algorithm 3.1 are given in the following $\epsilon_r = 0.001$, $\epsilon_x = 0.001$, $\lambda = 0.5$ and $\Gamma_0 = 0.15I_2$.

The robust MPC method in [35] (RMPC1) and [42] (RMPC2) are introduced for the purpose of comparison. The initial point is set as $x_0 = [8, 8]^T$. The real system parameter $\theta^* = [-0.2, 0.5]^T$ is given to evaluate the proposed parameter estimator. Figures 3.1 and 3.2 show the trajectories of system state and control input obtained by applying different control methods. From these figures, it can be seen that the recursive feasibility can be guaranteed by using these methods while the proposed method can accelerate the convergence of system states. To further compare the control performances of different MPC formulations, we introduce the following index $\bar{J}_p = \sum_{k=0}^{T_{stp}} (x_k^T Q x_k + u_k^T R u_k) / T_{stp}$, where T_{stp} denotes the simulation time. The corresponding results are illustrated in Table 3.1, implying that the proposed method can achieve the less conservative performance. The polytopic approximation of uncertainty sets obtained at time $k = 0, 3, 7, 20$ are depicted in Figure 3.4. It can be seen that the estimate of the uncertainty set is non-increasing and finally converges to a fixed set, which verifies the proposed results.

	Algorithm 3.1	Remark 15	RMPC1	RMPC2
\bar{J}_p	9.2023	9.2524	9.2524	9.3747

Table 3.1: The comparison of system performance.

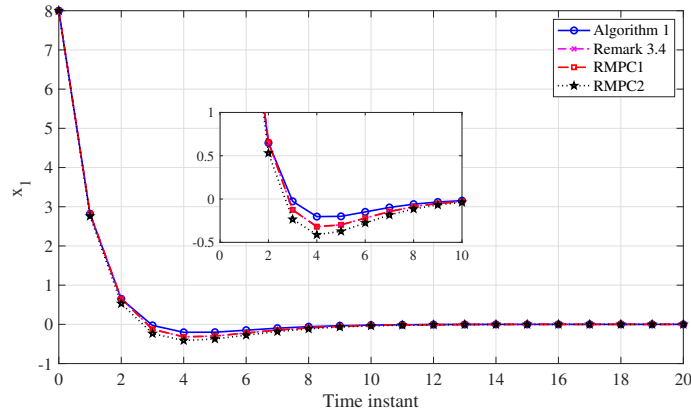


Figure 3.1: The time evolution of the system state x_1 .

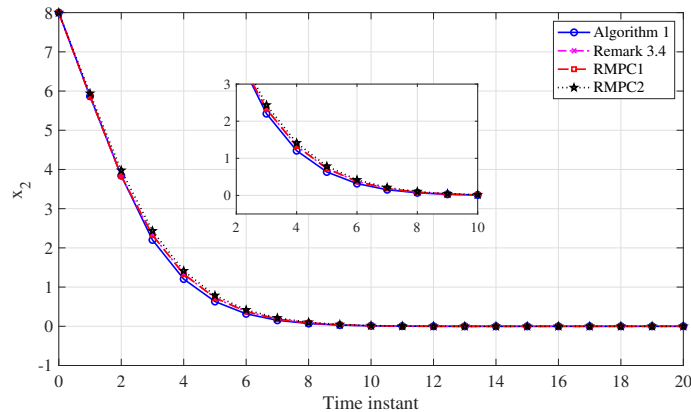


Figure 3.2: The time evolution of the system state x_2 .

3.6 Conclusion

In this chapter, we have investigated adaptive MPC for constrained linear systems subject to multiplicative uncertainties. An online parameter estimator has been designed based on the RLS technique for simultaneous parameter identification and uncertainty set estimation. By integrating the proposed estimator with homothetic prediction tubes, the resultant tube-based adaptive MPC scheme can efficiently handle the parametric uncertainties while enhancing performance compared with the robust tube MPC method. The simplified version of the proposed adaptive MPC method was also given to provide a trade-off between conservatism and computational complexity. We have proven that the closed-loop system is asymptotically stable, and the proposed adaptive MPC algorithm is recursively feasible under recursive model updates. Numerical simulations and comparison studies have been

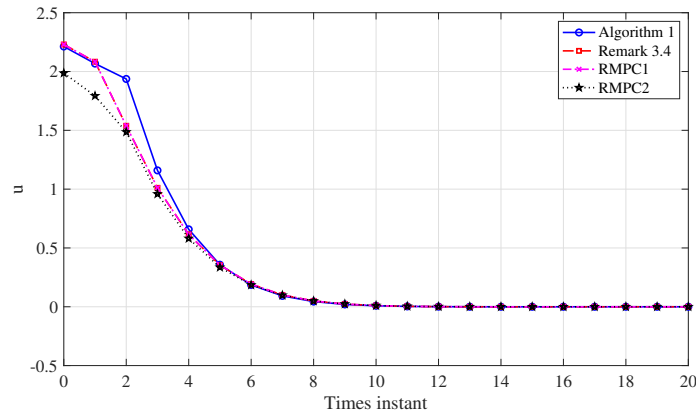


Figure 3.3: Trajectories of control input u .

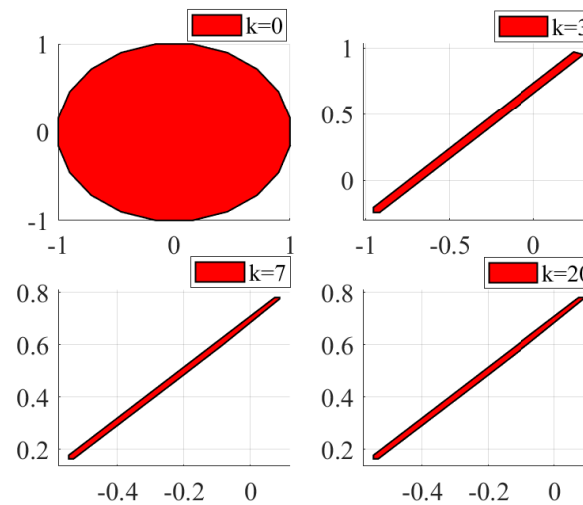


Figure 3.4: The estimated uncertainty set Θ obtained at $k = 0, 3, 7, 20$.

given to demonstrate the efficacy and advantages of the proposed adaptive MPC method.

On the other hand, the main limitation of the proposed adaptive MPC approach comes from the polytopic over-approximation of the uncertainty set employed in the construction of homothetic tubes, leading to an undesired increase in conservatism and computational complexity. Furthermore, this work considered the constant parametric uncertainties only, which potentially poses certain limitations to practical applications.

Chapter 4

Self-Triggered Adaptive Model Predictive Control of Constrained Nonlinear Systems: A Min-Max Approach

In Chapter 3, we investigate adaptive MPC for linear systems with periodic sampling. This chapter studies the event-based aperiodic execution of adaptive MPC for networked dynamic systems.

4.1 Introduction

Event-based aperiodic control has proved to be effective in achieving the trade-off between the closed-loop performance and the overall communication load [178]. In this chapter, we are interested in applying the event-based triggering mechanism to MPC. In particular, we focus on a class of constrained discrete-time nonlinear systems subject to parametric uncertainties and additive disturbances. A brief literature review on ST-RMPC is presented in 1.4. But these results deal with the uncertainties by considering its worst-case realization based on *a priori* knowledge of the uncertainty bound. Inherently, those methods become conservative when the uncertainty is over-estimated and time-varying. Hence, an intriguing question naturally arises: Is it possible to an online estimate of the uncertainty bound based on the input and state history in the ST-RMPC framework to improve the control performance and enlarge the average sampling period simultaneously? This question will

be answered in this work considering an adaptive MPC formulation.

For periodic control, adaptive MPC has proved to be a promising solution to relieve the conservativeness of robust MPC methods [42, 44, 102], where the main insight is to leverage the online estimation of uncertainty within a robust MPC framework. In order to supplement and enhance the results in [188], this chapter investigates ST-AMPC for discrete-time nonlinear systems subject to both parametric uncertainties and additive disturbances. Due to inherent differences between robust MPC and adaptive MPC, the proposed ST-AMPC scheme is significantly different from the robust method [188]. To allow the online uncertainty estimation in the ST-RMPC method [188], a sufficiently large uncertainty bound taking account of all admissible realization of uncertainties (or all possible uncertainty estimation) should be considered for designing the MPC optimization problem and the self-triggering mechanism. Indeed, this setup can guarantee constraint satisfaction and closed-loop stability, which, however, inevitably leads to conservative closed-loop performance. Therefore, a tailored design is required to accommodate the recursive updates of the prediction model and the estimation of uncertainty sets. On the other hand, in the self-triggered setting, the control inputs may be implemented in an open-loop fashion. As a result, most of the existing results on adaptive MPC, e.g., [42, 44, 102], cannot be incorporated into the self-triggering mechanism since the control input implementation depends on measurements of system states or outputs at every time instant. Another remarkable difficulty lies in the implementation of the uncertainty estimation with discontinuous state measurement of the system.

To solve these issues, we develop an ST-AMPC scheme based on the min-max MPC framework for uncertain nonlinear systems in the following. The **main contributions** of this work are three-fold:

- An adaptive MPC scheme with a zonotope-based set-membership parameter estimator is developed. We introduce a zonotope-based indirect polytopic set computation method to estimate the sets of unknown system states between two successive triggering time instants such that the proposed estimator can be used for the system with the aperiodic self-triggered sampling.
- Similar to the ST-RMPC method [188], we co-design the control inputs and sampling intervals by developing a self-triggering mechanism in our framework to maximize the average triggering interval based on the estimation of unknown parameters. Compared with [188], a weighting factor update strategy is introduced to our framework based on the estimated uncertainty set, leading to the further reduced average sam-

pling frequency.

- It is theoretically shown that the resulting ST-AMPC method is recursively feasible, and the closed-loop system is input-to-state practical stable (ISpS) at triggering time instants. A numerical example and comparison study are presented to illustrate the advantages of the proposed method.

4.2 Problem Formulation and Control objective

Consider a discrete-time nonlinear system subject to the parametric uncertainty and the additive disturbance

$$x_{t+1} = \mathcal{F}(x_t, u_t, v_t, d_t) \triangleq f(x_t, u_t) + g(x_t, u_t)v_t + d_t, \quad (4.1)$$

where $x_t \in \mathbb{R}^{n_x}$ and $u_t \in \mathbb{R}^{n_u}$, $v_t \in \mathcal{V} \subset \mathbb{R}^{n_v}$ and $d_t \in \mathcal{D} \subset \mathbb{R}^{n_x}$ are the system state, the control input, the parametric uncertainty, and the additive disturbance, respectively. Both v_t and d_t are unknown and time-varying, and \mathcal{V} and \mathcal{D} are known zonotopes. $f : \mathbb{R}^{n_x} \times \mathbb{R}^{n_u} \rightarrow \mathbb{R}^{n_x}$ and $g : \mathbb{R}^{n_x} \times \mathbb{R}^{n_u} \rightarrow \mathbb{R}^{n_x \times n_v}$ are nonlinear functions satisfying conditions $f(0, 0) = 0$ and $g(0, 0) = 0$. The system is subject to constraints $x_t \in \mathcal{X}$ and $u_t \in \mathcal{U}$ for all $t \in \mathbb{N}$, where \mathcal{X} and \mathcal{U} are compact sets containing the origin. It is assumed that x_t is always measurable. For the uncertainties d_t and v_t , we have the following assumption.

Assumption 4.1. *For all $d_t \in \mathcal{D}$ and $v_t, v_{t+1} \in \mathcal{V}$, there exist constants $\bar{d}, \bar{v}, \bar{\delta} \in \mathbb{R}_{>0}$ such that $\|d_t\| \leq \bar{d}$, $\|v_t\| \leq \bar{v}$, and $\|v_{t+1} - v_t\| \leq \bar{\delta}$.*

Assumption 4.1 indicates the boundedness of the additive disturbance d_t and the parametric uncertainty v_t , which is common in related literature on MPC. We also assume that v_t is slowly changing. This assumption is satisfied in a host of real-world applications. Similar assumptions can be found in [42, 212].

In this chapter, we aim to design a feedback control law, which can robustly stabilize the system (4.1) without violating state and input constraints for all admissible realization of uncertainties while reducing the frequency of updating the control input with the guaranteed closed-loop performance. To achieve this goal, we co-design the control inputs and sampling intervals in the adaptive MPC framework. Particularly, at the sampling time instant $t_k \in \mathbb{N}$, the next sampling time instant t_{k+1} and the control inputs between two sampling instants, i.e., $u_t, t \in \mathbb{N}_{[t_k, t_{k+1}-1]}$, will be determined by a self-triggered scheme

with the following form.

$$u_t = \tau(x_{t_k}, t - t_k), t \in \mathbb{N}_{[t_k, t_{k+1}-1]}, \quad (4.2a)$$

$$t_{k+1} = t_k + H_{\mathcal{V}_{t_k}}(x_{t_k}), \quad (4.2b)$$

where $k \in \mathbb{N}$ and $t_0 = 0$; $H_{\mathcal{V}_{t_k}} : \mathbb{R}^{n_x} \rightarrow \mathbb{N}_{>0}$ is the self-triggering scheduler related to the bounding set \mathcal{V}_{t_k} of the unknown parameter v_{t_k} , and $\tau : \mathbb{R}^{n_x} \times \mathbb{N} \rightarrow \mathbb{R}^{n_u}$ is a function to be designed. It can be seen from (4.2) that the state measurements and control inputs are only updated at sampling time instant t_k .

In this work, we expect to achieve a large sampling interval $H_{\mathcal{V}_{t_k}}(x_{t_k})$ with guaranteed closed-loop stability without violating the state and input constraints. This problem is addressed by designing functions $H_{\mathcal{V}_{t_k}}$ and τ based on the adaptive MPC technique. Benefiting from the model refinement in adaptive MPC framework, we can further reduce the sampling frequency by designing suitable $H_{\mathcal{V}_{t_k}}$ based on the parameter estimation \mathcal{V}_{t_k} . According to the min-max optimal control problem \mathcal{P}_0 in (2.14), the following section presents an ST-AMPC solution for the design of functions $H_{\mathcal{V}_{t_k}}$ and τ .

4.3 Self-Triggered Adaptive Min-Max MPC

In this section, we firstly present a zonotope-based set-membership parameter estimator capable of handling the aperiodic sampling induced by the self-triggering mechanism. Then a self-triggering scheduler accommodating the estimation of uncertainty is developed, followed by a summary of the proposed self-triggered adaptive min-max MPC algorithm. Finally, this section is concluded with an analysis of closed-loop stability and recursive feasibility.

4.3.1 Zonotope-based set-membership parameter estimator

Section 2.4.1 introduces the standard set-membership parameter estimator for the system (4.1) with the periodic sampling. However, under the self-triggering mechanism (4.2b), the state measurements are updated aperiodically. The resulting sampling interval between sampling time instants t_k and t_{k+1} may be greater than 1, i.e., $t_{k+1} - t_k > 1$. Consequently, the parameter set $\mathcal{L}_{t_{k+1}}$ cannot be computed by following (2.16), and hence the set-membership parameter estimator presented in Section 2.4.1 cannot be applied to the current problem with the aperiodic sampling. To solve this issue, a zonotope-based set-

membership parameter estimator is presented in the following.

Let the set $X_{t_{k+1}-1}$ denote the exact uncertain state set for the state $x_{t_{k+1}-1}$. By replacing the state $x_{t_{k+1}-1}$ in (2.16) with the set $X_{t_{k+1}-1}$ an over-approximation of the parameter set $\mathcal{L}_{t_{k+1}}$ is given by $\hat{\mathcal{L}}_{t_k}(X_{t_{k+1}-1})$ where

$$\hat{\mathcal{L}}_{t_k}(X_{t_{k+1}-1}) = \{v \in \mathbb{R}^{n_v} : x_{t_k} - f(x, u_{t_{k-1}-1}) - g(x, u_{t_{k-1}-1})v \in \mathcal{D}, x \in X\}. \quad (4.3)$$

With this, we definitely have $\mathcal{L}_{t_{k+1}} = \hat{\mathcal{L}}_{t_k}(X_{t_{k+1}-1})$ when $X_{t_{k+1}-1} = \{x_{t_{k+1}-1}\}$. It can be seen from (4.3) that the key ingredient of calculating $\hat{\mathcal{L}}_{t_k}(X_{t_{k+1}-1})$ is to find the set $X_{t_{k+1}-1}$. Since the state measurement x_{t_k} and inter-sampling control inputs $u_t, t \in \mathbb{N}_{[t_k, t_{k+1}-1]}$, are known at the sampling time instant t_{k+1} , it is possible to compute $X_{t_{k+1}-1}$ by using the zonotopic set computation method presented in Section 2.4.2. Therefore, by replacing the parameter set $\mathcal{L}_{t_{k+1}}$ in (2.17) as $\hat{\mathcal{L}}_{t_k}(X_{t_{k+1}-1})$, the bounding set $\mathcal{V}_{t_{k+1}}$ can be computed under the self-triggering mechanism.

According to (2.17) and (4.3), it can be seen that the conservatism of $\mathcal{V}_{t_{k+1}}$ is primarily determined by the exact uncertain state set $X_{t_{k+1}-1}$. Note that, in order to compute the outer bound of $X_{t_{k+1}-1}$ by using the method in Section 2.4.2, the sets $\mathcal{V}_{t_{k+1}-2}$ and \mathcal{D} are required to be zonotopic, which, however, cannot be guaranteed due to the intersection operation in (2.17). To solve this problem, a zonotopic bounding process has to be performed. But this strategy may result in unnecessary overestimation, leading to the conservative estimation performance for the set-membership parameter estimator. Alternatively, motivated by [213], a zonotope-based indirect set computation method is introduced in the following to reduce the conservatism in calculating the outer bound of $X_{t_{k+1}-1}$.

At the sampling time instant t_k , suppose that $t_{k+1} - t_k > 1$ and there is a group of zonotopes $\hat{\mathcal{V}}_{t_k, i}, i \in \mathbb{N}_{[1, n_{z_{t_k}}]}$, such that $\mathcal{V}_{t_k} = \bigcap_{i=0}^{n_{z_{t_k}}} \hat{\mathcal{V}}_{t_k, i}$. Using the set theory results in

$$\mathcal{G}_{\mathcal{F}}(\hat{X}_{t_k}, u_{t_k}, \mathcal{V}_{t_k}, \mathcal{D}) \subseteq \bigcap_{i=0}^{n_{z_{t_k}}} \mathcal{G}_{\mathcal{F}}(\hat{X}_{t_k}, u_{t_k}, \hat{\mathcal{V}}_{t_k, i}, \mathcal{D}).$$

Since the sets $\hat{X}_{t_k}, \hat{\mathcal{V}}_{t_k, i}, \mathcal{D}$ are zonotopic, we can compute $\mathcal{G}_{\mathcal{F}}(\hat{X}_{t_k}, u_{t_k}, \hat{\mathcal{V}}_{t_k, i}, \mathcal{D})$ by following the method in Section 2.4.2. Therefore, the zonotopic bounding process can be avoided even if \mathcal{V}_{t_k} is polytopic. With this, for $l \in \mathbb{N}_{[t_k, t_{k+1}-2]}$, we define the following recursion

$$\hat{X}_{l+1, i} = \mathcal{G}_{\mathcal{F}}(\hat{X}_{l, i}, u_l, \mathcal{V}_{l, i}, \mathcal{D}), i \in \mathbb{N}_{[0, n_{z_{t_k}}]}, \quad (4.4a)$$

$$\mathcal{V}_{l+1, i} = \begin{cases} \mathcal{V}_{l, i} \oplus \bar{\delta} \mathbb{B}^{n_v}, & \text{if } \mathcal{V}_{l, i} \oplus \bar{\delta} \mathbb{B}^{n_v} \subseteq \mathcal{V} \\ \mathcal{V}, & \text{otherwise} \end{cases} \quad (4.4b)$$

where $\hat{X}_{t_k,i} = \{x_{t_k}\}$. Then the outer bound of $X_{t_{k+1}-1}$ can be computed by $\hat{X}_{t_{k+1}-1} = \bigcap_{i=0}^{n_z t_k} \hat{X}_{t_{k+1}-1,i}$. Note that the set $\mathcal{V}_{l,i}$ can also be updated via the equation $\mathcal{V}_{l,i} = \mathcal{V}_{l,i} \oplus (\bar{\delta}\mathbb{B}^{n_v}) \cap \mathcal{V}$, which is less conservative compared with (4.4b). But this method requires the zonotopic bounding process since the intersection operator may render the set $\mathcal{V}_{l,i}$ polytopic. Therefore, $\mathcal{V}_{l,i}$ is updated via (4.4b) in this work. Based on (2.17), (4.3) and (4.4), the bounding set $\mathcal{V}_{t_{k+1}}$ can be computed by

$$\mathcal{V}_{t_{k+1}} = ((\mathcal{V}_{t_k} \cap \hat{\mathcal{L}}_{t_k}(\hat{X}_{t_{k+1}-1})) \oplus (t_{k+1} - t_k)\bar{\delta}\mathbb{B}^{n_v}) \cap \mathcal{V}. \quad (4.5)$$

The proposed zonotope-based set-membership parameter estimator for the system (4.1) with the aperiodic sampling is summarized in Algorithm 4.1.

Algorithm 4.1 Zonotope-based set-membership parameter estimation algorithm

Input: System states $x_{t_{k-1}}$ and x_{t_k} ; sampling time instants t_{k-1} and t_k ; the control input sequence $\{u_i\}$, $i \in \mathbb{N}_{[t_{k-1}, t_k-1]}$; the bounding set $\mathcal{V}_{t_{k-1}}$.

- 1: **if** $t_k - t_{k-1} = 1$ **then**
 - 2: Compute the parameter set \mathcal{L}_{t_k} via (2.16) and then calculate the bounding set \mathcal{V}_{t_k} according to (2.17).
 - 3: **else**
 - 4: Set $\hat{X}_{t_{k-1}} = \{x_{t_{k-1}}\}$ and find a sequence of zonotopes such that $\mathcal{V}_{t_{k-1}} = \bigcap_{i=0}^{n_z t_{k-1}} \hat{\mathcal{V}}_{t_{k-1},i}$.
 - 5: Calculate set $\hat{X}_{t_{k-1}} = \bigcap_{i=0}^{n_z t_{k-1}} \hat{X}_{t_{k-1},i}$ via (4.4).
 - 6: Compute $\hat{\mathcal{L}}_{t_k}(\hat{X}_{t_{k-1}})$ via (4.3) and then calculate the bounding set \mathcal{V}_{t_k} according to (4.5).
 - 7: **end if**
-

Remark 4.1. For each polytope \mathcal{X}_{t_k} , we can always find a group of zonotopes $\hat{\mathcal{X}}_{t_k,i}$ whose intersection is \mathcal{X}_{t_k} . Suppose that the polytope \mathcal{X}_{t_k} has m half-spaces. Then \mathcal{X}_{t_k} can be exactly represented by the intersection of at most m zonotopic sets. Assume that the i -th half-space $\mathcal{H}_{t_k,i}$ has the form $\mathcal{H}_{t_k,i} = \{v \in \mathbb{R}^{n_v} : a_{t_k,i}^\top v \leq b_{t_k,i}\}$ with $a_{t_k,i} \in \mathbb{R}^{n_v}$, $b_{t_k,i} \in \mathbb{R}$ and $i \in \mathbb{N}_{[1,m]}$. Under this definition, it is obvious that $\mathcal{X}_{t_k} = \bigcap_{i=0}^m \mathcal{H}_{t_k,i}$. In addition, for each \mathcal{X}_{t_k} , it is easy to find the box $\blacksquare(\mathcal{X}_{t_k})$ bounding the set \mathcal{X}_{t_k} . Then based on $\mathcal{H}_{t_k,i}$, we can find a vector $p_{t_k,i} \in \mathbb{R}^{n_v}$ and a scalar $h_{t_k,i} \in \mathbb{R}$ to establish a strip $\mathcal{S}_{t_k,i} = \{v \in \mathbb{R}^{n_v} : |a_{t_k,i}^\top (v - p_{t_k,i})| \leq h_{t_k,i}\}$ such that $\mathcal{X}_{t_k} \subseteq \mathcal{S}_{t_k,i}$, where $p_{t_k,i}$ and $h_{t_k,i}$ satisfy the condition $b_{t_k,i} = h_{t_k,i} + a_{t_k,i}^\top p_{t_k,i}$. Based on each $\mathcal{S}_{t_k,i}$, we can find a zonotope bounding the polytope \mathcal{X}_{t_k} . Therefore, at most m zonotopes are needed to construct the polytope \mathcal{X}_{t_k} . The calculation of zonotopes $\hat{\mathcal{X}}_{t_k,i}$ for a 2-dimensional case can be found in [213].

4.3.2 ST-AMPC algorithm

As shown in (4.2), the measurements of system states are only updated at sampling time instants in self-triggered control. Since the system states at inner-sampling time instants are unknown under the self-triggering mechanism, and the optimal solution depends on the system state, the adaptive min-max MPC scheme presented in Section 2.3.3 cannot be directly employed to design the ST-AMPC algorithm. To address this issue, similar to [188], we formulate a cost function combining both open-loop predictions and closed-loop predictions for the proposed ST-AMPC algorithm, resulting in the following min-max optimization problem \mathcal{P}_1 .

$$\mathcal{P}_1 : V_N^M(x_{t_k}, \beta_{t_k}) = \min_{\mathbf{u}_{t_k, N}} \left\{ \max_{v_{l|t_k} \in \mathcal{V}_{l|t_k}, d_{l|t_k} \in \mathcal{D}} \left\{ \sum_{l=0}^{M-1} \frac{1}{\beta_{t_k}} \ell(x_{l|t_k}, u_{l|t_k}) + V_{N-M}(x_{M|t_k}) \right\} \right. \\ \left. \text{such that } x_{M|t_k} \in \mathcal{X}_{N-M}, \forall v_{l|t_k} \in \mathcal{V}_{l|t_k}, d_{l|t_k} \in \mathcal{D} \right\} \quad (4.6a)$$

$$\text{s.t. } x_{l+1|t_k} = \mathcal{F}(x_{l|t_k}, u_{l|t_k}, v_{l|t_k}, d_{l|t_k}), \quad (4.6b)$$

$$x_{0|t_k} = x_{t_k}, x_{l|t_k} \in \mathcal{X}, u_{l|t_k} \in \mathcal{U}, \quad (4.6c)$$

where $l \in \mathbb{N}_{[0, M-1]}$; $\beta_{t_k} > 1$ is a scalar to be designed; $M \in \mathbb{N}_{[1, N-1]}$ is an integer; $V_{N-M}(x_{M|t_k})$ is the optimal cost function in $(N-M)$ -step defined by (2.15) with i replaced by $N-M$, and $\mathbf{u}_{t_k, N} = \{u_{l|t_k}\}_{l \in \mathbb{N}_{[0, N-1]}}$ is the control input sequence. Here $u_{l|t_k}, l \in \mathbb{N}_{[0, M-1]}$ is the control input and $u_{l|t_k} = \mu_{i|t_k}(x_{i|t_k}), l \in \mathbb{N}_{[M, N-1]}$ where $\mu_{i|t_k}(x_{i|t_k})$ is the control policy depending on the predicted state $x_{i|t_k}$. Note that the term $V_{N-M}(x_{M|t_k})$ is based on the close-loop min-max MPC formulation [202]. To inherit the properties of the close-loop min-max MPC method, we impose an additional condition that $x_{M|t_k} \in \mathcal{X}_{N-M}$ is satisfied for all admissible realizations of uncertainties $v_{l|t_k}$ and $d_{l|t_k}$ with $l \in \mathbb{N}_{[0, M-1]}$ when formulating the worse-case cost function. Therefore, the cost function (4.6a) implicitly ensures the satisfaction of the constraint $x_{M|t_k} \in \mathcal{X}_{N-M}$.

As shown in (4.6), the entire prediction horizon is divided into two parts: The first M steps (open-loop predictions) and the remainder (closed-loop predictions). This formulation allows for evaluating the effects of open-loop predictions on the control performance, thereby facilitating the co-design of control inputs and sampling time instants. Let $V_j^i(x_{t_k}, \beta_{t_k})$ be defined by (4.6) with M and N replaced by i and j , respectively, where $i \in \mathbb{N}_{[1, H_{\max}]}, j \in \mathbb{N}_{>0}$ and $i \leq j$. Here $H_{\max} \in \mathbb{N}_{[1, N-1]}$ denotes the maximum number of time instants allowed for the open-loop phase. Similar to self-triggered MPC methods

[184, 188, 190], the self-triggering scheduler in (4.2b) is designed as follows

$$H_{\mathcal{V}_{t_k}}(x_{t_k}) \triangleq \max \{ H \in \mathbb{N}_{[1, H_{\max}]} : V_N^H(x_{t_k}, \beta_{t_k}) \leq V_N^1(x_{t_k}, \beta_{t_k}) \}. \quad (4.7)$$

It can be seen from (4.7) that the sum of stage costs related to the open-loop prediction is weighted by the scalar β_{t_k} . Using a larger β_{t_k} will result in a larger sampling interval $H_{\mathcal{V}_{t_k}}(x_{t_k})$, but will deteriorate the regulation performance [188]. Furthermore, the sampling interval is also affected by the bound of uncertainties: A larger bound of uncertainties renders a shorter sampling interval by following (4.7). Then based on the proposed zonotope-based set-membership parameter estimator, we develop the following adaptive mechanism associated with \mathcal{V}_{t_k} to further reduce the average sampling frequency,

$$\beta_{t_k} = \bar{\beta} \cdot e^{(\bar{\xi} - \xi_{t_k})}, \quad (4.8)$$

where $\bar{\beta} > 1$ is a tuning factor; $\bar{\xi} = \sup_{v_1, v_2 \in \mathcal{V}} \|v_1 - v_2\|$ is the upper bound of the estimation error and $\xi_{t_k} = \sup_{v_1, v_2 \in \mathcal{V}_{t_k}} \|v_1 - v_2\|$. According to (2.17), one has $\mathcal{V}_{t_k} \subseteq \mathcal{V}$ for all $t_k \geq 0$, which implies $0 \leq \xi_{t_k} \leq \bar{\xi}$. Therefore, the range of β_{t_k} is given by $\bar{\beta} \leq \beta_{t_k} \leq \bar{\beta} e^{\bar{\xi}}$.

According to the developed set-membership parameter estimator, the proposed ST-AMPC scheme is summarized in Algorithm 4.2. Let $\mathbf{u}_{t_k, N}^* = \{u_{l|t_k}^*\}_{l \in \mathbb{N}_{[0, N-1]}}$ denote the optimal solution to the optimization problem (4.6) with $M = H_{\mathcal{V}_{t_k}}(x_{t_k})$. Then the feedback control law (4.2a) and the sampling instant are given by

$$\begin{aligned} \tau(x_{t_k}, t - t_k) &= u_{t-t_k|t_k}^*, t \in \mathbb{N}_{[t_k, t_{k+1}-1]}, \\ t_{k+1} &= t_k + H_{\mathcal{V}_{t_k}}(x_{t_k}), \end{aligned}$$

which results in the following closed-loop system

$$x_{t+1} = \mathcal{F}(x_t, \tau(x_{t_k}, t - t_k), v_t, d_t). \quad (4.9)$$

Remark 4.2. Compared with the ST-RMPC method [188] using the constant tuning factor $\bar{\beta}$, we consider the time-varying factor β_{t_k} which is updated with respect to the bounding set \mathcal{V}_{t_k} in the proposed method. Under this mechanism, when a more accurate \mathcal{V}_{t_k} is obtained, ξ_{t_k} becomes smaller and β_{t_k} becomes larger, thereby leading to a larger sampling interval. On the other hand, we can choose the update strategy such that the value of β_{t_k} is inversely proportional to the size of \mathcal{V}_{t_k} , resulting in the control performance improvement. Therefore, a trade-off between the communication load and closed-loop performance can

be achieved by designing the appropriate updating mechanism for β_{t_k} .

Algorithm 4.2 Self-triggered adaptive MPC algorithm

Input: The initial system state x_0 ; the prediction horizon N ; tuning parameters $\bar{\beta}, \bar{\xi}$ and H_{\max} .

- 1: Set $t = 0$ and $t_0 = t$.
- 2: **for** $k = 0, 1, 2, \dots$ **do**
- 3: Measure the system state x_{t_k} .
- 4: **if** $t_k > 0$ **then**
- 5: Compute \mathcal{V}_{t_k} by following **Algorithm 4.1**.
- 6: **end if**
- 7: Solve the optimization problems in (4.6) and (4.7) to obtain the optimal control input sequence $\mathbf{u}_{t_k, N}^*$ and the sampling interval $H_{\mathcal{V}_{t_k}}(x_{t_k})$.
- 8: **for** $t = t_k, t_k + 1, \dots, t_k + H_{\mathcal{V}_{t_k}}(x_{t_k}) - 1$ **do**
- 9: Implement the control input $u_t = u_{t-t_k|t_k}^*$ to the system (4.1).
- 10: **end for**
- 11: Set $t = t + 1$ and $t_{k+1} = t$.
- 12: **end for**

4.3.3 Recursive feasibility and closed-loop stability

The feasibility result is shown in the following theorem.

Theorem 4.1. *For the nonlinear system (4.1), suppose that Assumption 2.1 holds, then the proposed ST-AMPC scheme in Algorithm 4.2 is recursively feasible for all $x_0 \in \mathcal{X}_N$.*

Proof. At the triggering time t_k , suppose that $x_{t_k} \in \mathcal{X}_N$, and the next sampling time instant is $t_{k+1} = t_k + H_{\mathcal{V}_{t_k}}(x_{t_k})$. For simplicity, we use the notation $H_{t_k}^*$ to denote $H_{\mathcal{V}_{t_k}}(x_{t_k})$ in the following. Let the sequence $\mathbf{u}_{t_k, N}^* = \{u_{l|t_k}^*\}_{l=0}^{N-1}$, $\mathbf{w}_{t_k, N}^* = \{d_{l|t_k}^*, v_{l|t_k}^*\}_{l=0}^{N-1}$ denote the optimal solution of the optimization problem (4.6), and $x_{l|t_k}^*$ is the predicted optimal state trajectory for the system (4.1) under $u_{l|t_k}^*$, $d_{l|t_k}^*$ and $v_{l|t_k}^*$. Then we construct the following candidate input sequence at next sampling time instant

$$\bar{\mathbf{u}}_{t_{k+1}, N} = \{\bar{u}_{l|t_{k+1}}\}_{l=0}^{N-1}, \bar{u}_{l|t_k} = \begin{cases} u_{H_{t_k}^*+l|t_k}^*, & l \in \mathbb{N}_{[0, N-H_{t_k}^*-1]} \\ \kappa_f(x_{l|t_{k+1}}), & l \in \mathbb{N}_{[N+H_{t_k}^*, N-1]} \end{cases}$$

where $\{x_{l|t_{k+1}}\}$ is the corresponding state trajectory under $\bar{\mathbf{u}}_{t_{k+1}, N}$ and $\mathbf{w}_{t_k, N}^*$. Since $v_{t_k+l} \in \mathcal{V}_{l|t_k} \subseteq \mathcal{V}$ and $d_{t_k+l} \in \mathcal{D}$ for all $l \in \mathbb{N}_{[0, H_{t_k}^*-1]}$, by the optimization problem (4.6) we have

$x_{t_{k+1}} \in \mathcal{X}_{N-H_{t_k}^*}$. Therefore, it can be concluded from (2.15) and Assumption 2.1 that \mathcal{X}_N is a robust invariant set for the system (4.1) under the proposed ST-AMPC algorithm. \square

Remark 4.3. As shown in Theorem 4.1, we investigate the recursive feasibility of the proposed method at triggering time instants. Although the control inputs are executed in an open-loop configuration between two triggering time instants, it still can be guaranteed that $x_t \in \mathcal{X}$ and $u_t \in \mathcal{U}$ for all $t \geq 0$ and $x_0 \in \mathcal{X}_N$ by considering the worst-case realization of uncertainties in the MPC optimization problem.

Theorem 4.2. For the nonlinear system (4.1), suppose that Assumption 2.1 holds and $x_0 \in \mathcal{X}_N$. If the triggering time instants t_k are determined by (4.7), under the proposed ST-AMPC method presented in Algorithm 4.2, the closed-loop system (4.9) is ISpS at the triggering time instants.

Proof. To prove ISpS of the closed-loop system, we need to show that the optimal cost function $V_N^{H_{t_k}^*}(x_{t_k}, \beta_{t_k})$ is an ISpS Lyapunov function satisfying conditions (2.8a) and (2.8b). We start the proof by finding the function $\alpha_1(\|x_{t_k}\|)$. Recalling the optimization problem (4.6), the lower bound of $V_N^{H_{t_k}^*}(x_{t_k}, \beta_{t_k})$ can be derived as follows

$$V_N^{H_{t_k}^*}(x_{t_k}, \beta_{t_k}) = J_N^H(x_{t_k}, \mathbf{u}_{t_k, N}^*, \mathbf{w}_{t_k, N}^*, \beta_{t_k}) \geq \min_{\mathbf{u}_{t_k}} J_N^H(x_{t_k}, \mathbf{u}_{t_k, N}, \mathbf{0}, \beta_{t_k}) \geq \frac{\sigma_1(\|x_{t_k}\|)}{\bar{\beta}e^{\bar{\xi}}}.$$

Hence the function $\alpha_1(\|x_{t_k}\|)$ can be chosen as $\alpha_1(\|x_{t_k}\|) = \sigma_1(\|x_{t_k}\|)/\bar{\beta}e^{\bar{\xi}}$.

The next step is to find the function $\alpha_2(\|x_{t_k}\|)$. We firstly consider the case $x_{t_k} \in \mathcal{X}_f$. Let $\tilde{\mathbf{u}}_{t_k, N}$ denote the optimal solution associated with $V_N^1(x_{t_k}, \beta_{t_k})$, and define a control sequence $\tilde{\mathbf{u}}_{t_k, N+1}$ as $\tilde{\mathbf{u}}_{t_k, N+1} = \{\tilde{\mathbf{u}}_{t_k, N}, \kappa_f(x_{N|t_k})\}$. We define the following cost function

$$J_j^i(x_{t_k}, \mathbf{u}_{t_k, N}, \mathbf{w}_{t_k, N}, \beta_{t_k}) \triangleq \ell_f(x_{j|t_k}) + \sum_{l=0}^{i-1} \frac{1}{\beta_{t_k}} \ell(x_{l|t_k}, u_{l|t_k}) + \sum_{l=i}^{j-1} \ell(x_{l|t_k}, u_{l|t_k}), \quad (4.10)$$

where $i \in \mathbb{N}_{[1, H_{\max}]}$, $j \in \mathbb{N}_{>0}$ and $i \leq j$. Then we have

$$\begin{aligned} J_{N+1}^1(x_{t_k}, \tilde{\mathbf{u}}_{t_k, N+1}, \mathbf{w}_{t_k, N+1}, \beta_{t_k}) &= J_N^1(x_{t_k}, \tilde{\mathbf{u}}_{t_k, N}, \mathbf{v}_{t_k, N}, \mathbf{d}_{t_k, N}, \beta_{t_k}) - \ell_f(x_{N|t_k}) \\ &\quad + \ell_f(x_{N+1|t_k}) + \ell(x_{N|t_k}, \kappa_f(x_{N|t_k})). \end{aligned}$$

for all $x_{t_k} \in \mathcal{X}_f$. Since the sequence $\tilde{\mathbf{u}}_{t_k, N+1}$ is a suboptimal solution, the relation between

$V_N^1(x_{t_k}, \beta_{t_k})$ and $V_{N+1}^1(x_{t_k}, \beta_{t_k})$ can be derived as follows

$$\begin{aligned}
V_{N+1}^1(x_{t_k}, \beta_{t_k}) &\leq \max_{\mathbf{w}_{t_k, N+1}} J_{N+1}^1(x_{t_k}, \tilde{\mathbf{u}}_{t_k, N+1}, \mathbf{w}_{t_k, N+1}, \beta_{t_k}) \\
&\leq \max_{\mathbf{w}_{t_k, N}} J_N^1(x_{t_k}, \check{\mathbf{u}}_{t_k, N}, \mathbf{w}_{t_k, N}, \beta_{t_k}) + \alpha(\bar{d}) \\
&\leq V_N^1(x_{t_k}, \beta_{t_k}) + \alpha(\bar{d}), \tag{4.11}
\end{aligned}$$

where the third inequality in (4.11) is obtained from Assumption 2.1. Therefore, by iteratively using the above inequality, for all $x_{t_k} \in \mathcal{X}_f$, we have $V_N^1(x_{t_k}, \beta_{t_k}) \leq V_1^1(x_{t_k}, \beta_{t_k}) + (N-1)\alpha(\bar{d})$. In addition, from (4.6) one has

$$V_N^1(x_{t_k}, \beta_{t_k}) \leq V_N(x_{t_k}) + \frac{1 - \beta_{t_k}}{\beta_{t_k}} \ell(x_{l|t_k}^*, u_{t_k}^*),$$

leading to the following upper bound of $V_N^1(x_{t_k}, \beta_{t_k})$

$$\begin{aligned}
V_N^1(x_{t_k}, \beta_{t_k}) &\leq V_1(x_{t_k}) + \frac{1 - \beta_{t_k}}{\beta_{t_k}} \ell(x_{t_k}, \kappa_f(x_{t_k})) + (N-1)\alpha(\bar{d}) \\
&\leq \ell_f(x_{t_k}) + \frac{1 - \beta_{t_k}}{\beta_{t_k}} \ell(x_{t_k}, \kappa_f(x_{t_k})) + N\alpha(\bar{d}) \\
&\leq \sigma_3(\|x_{t_k}\|) + N\alpha(\bar{d}).
\end{aligned}$$

Hence, by (4.7) it is concluded that

$$V_N^{H_{t_k}^*}(x_{t_k}, \beta_{t_k}) \leq \sigma_3(\|x_{t_k}\|) + N\alpha(\bar{d}).$$

For $x_{t_k} \in \mathcal{X}_N$ but $x_{t_k} \notin \mathcal{X}_f$, the upper bound can be found by following Lemma 1 in [202]. Let $\mathcal{B}_r = \{x \in \mathbb{R}^{n_x} \mid \|x\| \leq r\}$. Since $\mathcal{X}, \mathcal{U}, \mathcal{V}$ and \mathcal{D} are compact sets, there exists a finite constant $\bar{V}_N \in \mathbb{R}_{\geq 0}$ such that $V_N^{H_{t_k}^*}(x_{t_k}, \beta_{t_k}) \leq \bar{V}_N$ for all $x_{t_k} \in \mathcal{X}_N$. For $x_{t_k} \in \mathcal{X}_N$ but $x_{t_k} \notin \mathcal{B}_r$, we have $\|x_{t_k}\| \geq r$ and $V_N^{H_{t_k}^*}(x_{t_k}, \beta_{t_k}) \leq \bar{V}_N$, which in turn leads to $V_N^{H_{t_k}^*}(x_{t_k}, \beta_{t_k}) \leq \frac{\bar{V}_N}{r} \|x_{t_k}\|$. Consequently, we have $V_N^{H_{t_k}^*}(x_{t_k}, \beta_{t_k}) \leq \alpha_2(\|x_{t_k}\|) + N\alpha(\bar{d})$ for all $x_{t_k} \in \mathcal{X}_N$, where $\alpha_2(\|x_{t_k}\|) = \max(\sigma_3(\|x_{t_k}\|), \frac{\bar{V}_N}{r} \|x_{t_k}\|)$.

The remainder of this proof is to find the function α_3 . Let $H_{t_{k+1}}^*$ denote the sampling interval computed at time instant t_{k+1} . Note that $v_{t_k+l} \in \mathcal{V}_{l|t_k}$ and $d_{t_k+l} \in \mathcal{D}$ for all $l \in \mathbb{N}_{[0, H_{t_k}^* - 1]}$. Taking into account the triggering condition (4.7), for all $x_{t_k} \in \mathcal{X}_N$, we evaluate the discrepancy between the optimal cost functions at two triggering time instants in the following

$$V_N^{H_{t_{k+1}}^*}(x_{k+1}, \beta_{t_{k+1}}) - V_N^{H_{t_k}^*}(x_{t_k}, \beta_{t_k})$$

$$\begin{aligned} &\leq V_N^1(x_{k+1}, \beta_{t_{k+1}}) - \max_{v_{l|t_k} \in \mathcal{V}_{l|t_k}, d_{l|t_k} \in \mathcal{D}} \left\{ \sum_{l=0}^{H_{t_k}^* - 1} \frac{1}{\beta_{t_k}} \ell(x_{l|t_k}, u_{l|t_k}^*) + V_{N-H_{t_k}^*}(x_{H_{t_k}^*|t_k}) \right\} \\ &\leq V_N^1(x_{k+1}, \beta_{t_{k+1}}) - V_{N-H_{t_k}^*}(x_{t_{k+1}}) - \sum_{l=0}^{H_{t_k}^* - 1} \frac{1}{\beta_{t_k}} \ell(x_{t_k+l}, u_{l|t_k}^*). \end{aligned}$$

It is similar to (4.11) that $V_{N+1}(x_{t_{k+1}}) - V_N(x_{t_{k+1}}) \leq \alpha(\bar{d})$, which yields $V_N^1(x_{k+1}, \beta_{t_{k+1}}) \leq V_N(x_{t_{k+1}}) \leq V_{N-H_{t_k}^*}(x_{t_{k+1}}) + H_{t_k}^* \alpha(\bar{d})$ for $x_{t_{k+1}} \in \mathcal{X}_{N-H_{t_k}^*}$. By choosing $\alpha_3(\|x_{t_k}\|) = \sigma_2(\|x_{t_k}\|)/\bar{\beta}e^{\bar{\xi}}$ and $\rho(\bar{d}) = H_{t_k}^* \alpha(\bar{d})$, one has $V_N^{H_{t_k}^*+1}(x_{k+1}, \beta_{t_{k+1}}) - V_N^{H_{t_k}^*}(x_{t_k}, \beta_{t_k}) \leq -\alpha_3(\|x_{t_k}\|) + \rho(\bar{d})$. Therefore, the optimal value function $V_N^{H_{t_k}^*}(x_{t_k}, \beta_{t_k})$ is an ISpS Lyapunov function at triggering time instants. Then according to Theorem 2.3, it is proved that the closed-loop system (4.9) is ISpS under the proposed ST-AMPC algorithms for all $x_0 \in \mathcal{X}_N$ at triggering time instants. \square

Remark 4.4. *In Theorem 4.2, it is rigorously proved that the closed-loop system is ISpS at triggering time instants under the proposed ST-AMPC algorithm. Compared with the periodic adaptive min-max MPC method, the proposed ST-AMPC scheme can significantly reduce the communication load since the state measurements are only updated at the sampling time instants. The simulation results will demonstrate this argument. On the other hand, this work only investigates the stability of the closed-loop system at sampling time instants. The proposed ST-AMPC method would suffer increased conservatism compared with the periodic method since the closed-loop stability at all time instants is investigated in the periodic method. How to guarantee the closed-loop stability at inter-sampling time instants will be considered in our further research.*

4.4 Illustrative Example

In this section, a numerical example is presented to validate our theoretical results. We consider the following discrete-time nonlinear system which is the modification of the example in [40]

$$\begin{aligned} x_{t+1}(1) &= x_t(1) + \frac{S}{2}(1 + x_t(1))u_t - x_t(2)v_t(1) + d_t(1), \\ x_{t+1}(2) &= x_t(2) + \frac{S}{2}(1 - 4x_t(2))u_t + x_t(1)v_t(2) + d_t(2). \end{aligned}$$

where $x_t = [x_t(1), x_t(2)]^T$ and u_t are the system state and input subject to the constraints $|u_t| \leq 1.5$ and $\|x_t\|_\infty \leq 5$. The parameter $S = 0.4$ is the sampling period of the system. The parametric uncertainty $v_t = [v_t(1), v_t(2)]^T$ and additive disturbance $d_t =$

$[d_t(1), d_t(2)]^T$ are limited by $0.1 \leq \|v_t\|_\infty \leq 0.35$, $\|d_t\|_\infty \leq 0.01$ and $\|v_{t+1} - v_t\| \leq 0.004$, respectively. The sequences of uncertainties used in the simulation are illustrated in Fig. 4.1.

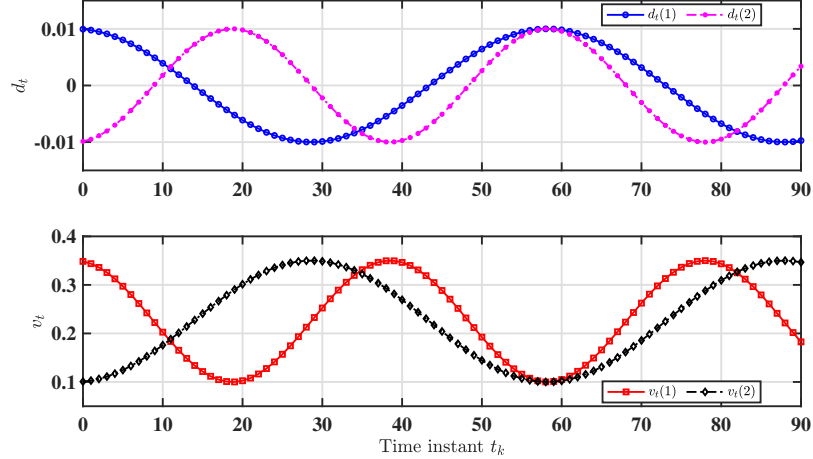


Figure 4.1: Trajectories of uncertainties.

For the proposed ST-AMPC scheme, we set the prediction horizon $N = 6$. The stage cost function is chosen as $\ell(x, u) = x^T Q x + u^T R u$ with $Q = \text{diag}(10, 10)$ and $R = 5$. We set

$$\begin{aligned} \mathcal{X}_f &= \{x : x^T P x \leq 2.171\}, P = [63.7335, -60.1802; -60.1802, 275.2859], \\ \ell_f(x) &= x^T P x, \kappa_f(x) = [-0.4707, -4.7538]x. \end{aligned}$$

The feedback policy in (2.15) is set as $\mu(x) = \kappa_f(x) + x^T x + c$ where $c \in \mathbb{R}$ is the decision variable for the optimization problem in (2.15). For the self-triggering scheduler, we set $H_{\max} = 5$ and $\beta_0 = 1.07$. At time instant t_k , the optimal sampling interval is obtained based on (4.7). More specifically, we firstly solve the optimization problem \mathcal{P}_1 with $M = 1$ to obtain the value of optimal cost $V_N^1(x_{t_k}, \beta_{t_k})$. Then we repeatedly solve \mathcal{P} by choosing different M from a decreasing sequence $\{H_{\max}, H_{\max} - 1, \dots, 2\}$ until $V_N^M(x_{t_k}, \beta_{t_k}) \leq V_N^1(x_{t_k}, \beta_{t_k})$. To demonstrate the effectiveness of the proposed methods, the ST-RMPC [188] the periodic robust MPC (P-RMPC) method in [14, 202] and the periodic adaptive MPC (P-AMPC) method in Section 2.3.3 are also implemented with the same parameters for the purpose of comparison.

In the simulation, we employ the Julia Toolbox *JuMP* [214] to formulate the MPC optimization problem, where the nonlinear programming solver *KNITRO* [215] is used to solve the optimization problem efficiently. Since it is almost impossible to exactly solve

the min-max MPC optimization problem \mathcal{P}_1 , we approximately solve \mathcal{P}_1 by considering the different realization of uncertainties. More specially, we sample N_a regularly distributed points in the uncertainty sets \mathcal{V}_{t_k} and \mathcal{D} , i.e., $\mathcal{V}_{t_k} = \{v_{l,t_k}\}$ and $\mathcal{D} = \{d_l\}$ with $l \in \mathbb{N}_{[0,N_a]}$. This can be achieved by using the Julia toolbox *GeoStats.jl* [216] in the simulation. Starting from the initial condition $x_0 = [4, 4]^T$ and $N_a = 5$, the time evolution of the system states and control inputs under different methods is shown in Figs. 4.2-4.3. The triggering time instants are reported in the bottom of Fig. 4.2. From these figures, it can be seen that the proposed ST-AMPC scheme can stabilize the system state within a small region around the origin while the state and input constraints are satisfied. Fig. 4.4 demonstrates the comparison of estimated bounding sets \mathcal{V}_{t_k} obtained by using the proposed ST-AMPC method (blue square) and P-AMPC method (green square) at the different triggering time instants, in which the black star indicates the real value of v_{t_k} and the gray square indicates the initial set \mathcal{V} . It is worthwhile to observe that the set-valued description of v_{t_k} can be refined by using the proposed set-membership parameter estimator under the self-triggering mechanism.

Let $J_p = \sum_{t=0} x_t^T Q x_t + u_t^T R u_t$ denote the system cost. We define $T_\Delta = T_{\text{total}}/N_s$ as the average time of computing the optimal triggering interval, where T_{total} is the total computing time and N_s is the times of solving the min-max optimization problem. In the simulation, we repeat the test 20 times to further compare the closed-loop performance and the computing time. The comparison of performance index J_p , average sampling interval H_s , average computing time T_Δ , and the total computing time T_{total} are shown in Table 4.1. We observe that, by using the proposed ST-AMPC method, the average sampling interval increases 12.44%, while the total cost increases 3.49% compared with the ST-RMPC method. In addition, the average computing time for these methods is less than the sampling time S . Although using the proposed ST-AMPC method leads to slightly increased average computing time T_Δ , the total computing time T_{total} can be reduced. In summary, the presented numerical example demonstrates that the proposed ST-AMPC method can significantly reduce the average sampling frequency compared with the ST-RMPC method and the periodic methods while preserving comparable closed-loop performance.

4.5 Conclusion

In this work, we have developed an ST-AMPC approach for constrained discrete-time nonlinear systems subject to parametric uncertainties and additive disturbances. A zonotope-based set-membership parameter estimator has been developed to refine a set-valued de-

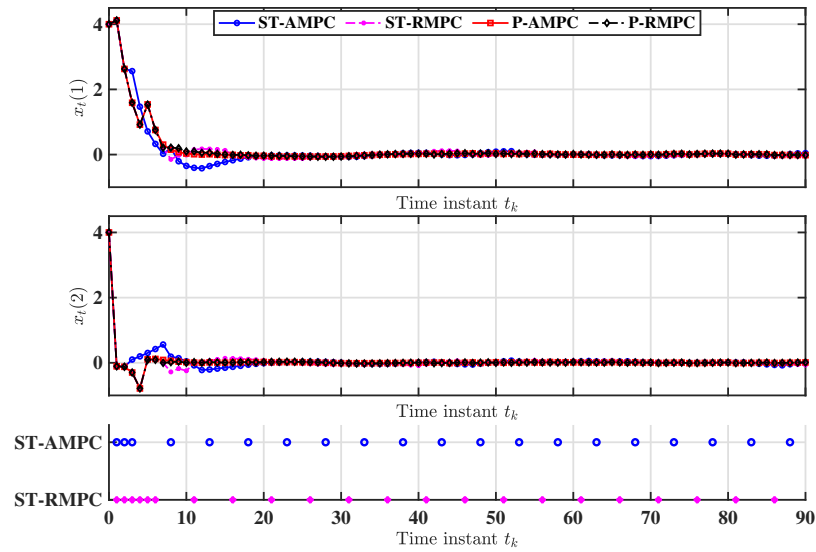


Figure 4.2: Trajectories of system state x_t and triggering time instant t_k .

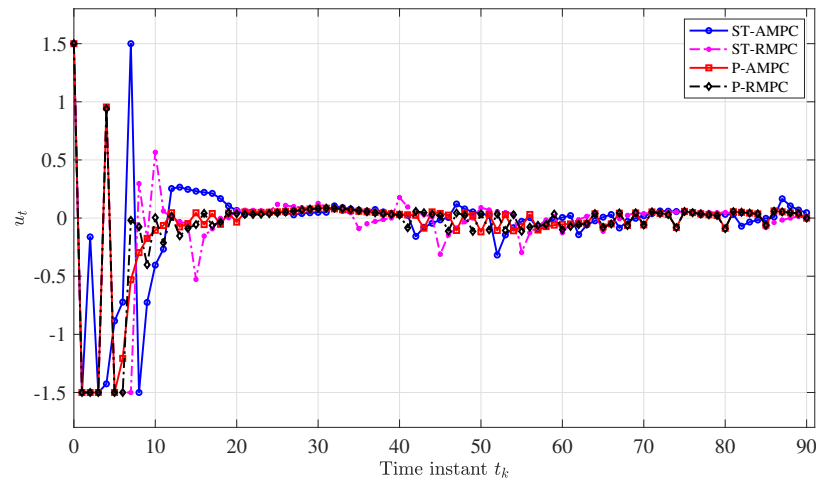


Figure 4.3: Control input u_t .

	J_p	H_s	N_s	T_Δ	T_{total}
ST-AMPC	751.70	4.6	20	0.3568 s	7.1353 s
ST-RMPC	726.38	4.09	22	0.3466 s	7.6262 s
P-AMPC	702.75	1	90	0.1265 s	11.3825 s
P-RMPC	705.73	1	90	0.13 s	11.6981 s

Table 4.1: Closed-loop performance comparison.

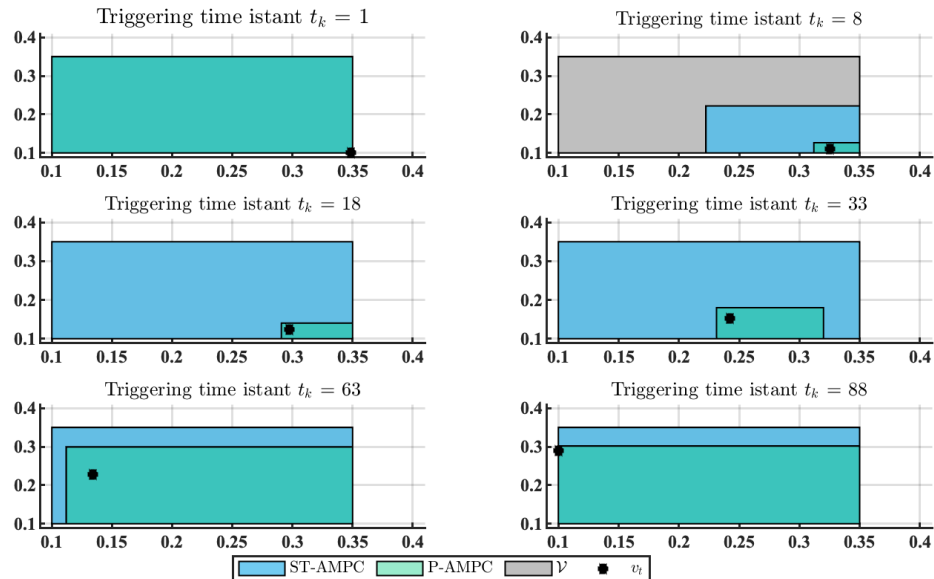


Figure 4.4: Comparison of uncertainty estimation at triggering time instants $t_k = 1, 5, 7, 36, 66, 79$.

scription of the time-varying parametric uncertainty. The proposed estimator does not rely on the continuous measurement of the system state. Hence the estimation performance is guaranteed under the aperiodic sampling induced by the self-triggering mechanism. The estimated uncertainty set has been incorporated to facilitate the co-design of control inputs and sampling intervals to reduce the conservatism further and enlarge the average sampling interval compared with the ST-RMPC method. We have proved that the proposed ST-AMPC approach is recursively feasible, and the closed-loop system is ISpS at triggering time instants. Numerical results have illustrated the efficacy and advantages of the proposed method.

Chapter 5

Robust Nonlinear Model Predictive Control Based Visual Servoing of Quadrotor UAVs

The previous chapters study robust and adaptive MPC for general linear and nonlinear systems. This chapter focuses on applying the robust MPC scheme to the quadrotor UAVs.

5.1 Introduction

In recent decades, quadrotors have received considerable attention in many fields, such as agriculture, industry, and transportation, due to their high maneuverability, agile mobility, and VTOL capability [217]. Tremendous results have been published in this field [193–196]. The navigation of quadrotors usually relies on the position information measured by the GPS or other positioning systems. However, the position information may be unavailable in some indoor or cluttered urban areas. For the quadrotor equipped with a camera, visual servoing provides an alternative solution to this problem, where the image data are employed as the feedback to regulate the quadrotor's pose with respect to a predefined visual target, allowing the navigation of quadrotors in GPS-denied environments [218].

In the existing literature, visual servoing techniques are mainly classified into two categories: IBVS and position-based visual servoing (PBVS). Compared with PBVS using 3-D features defined in the Cartesian space, IBVS does not require additional geometrical information to reconstruct the camera pose. Hence it is relatively easy to be implemented and insensitive to camera calibration errors [218]. However, taking image features as the

system state may destroy the cascaded structure of the original quadrotor system. Therefore, the appropriate design of image moments is desired for the IBVS of quadrotors, which has been intensively studied in the literature. In this chapter, we only focus on the IBVS based on the virtual camera technique and refer readers to a recent thesis by Xie [219] for an overview of existing IBVS techniques.

The main insight of the virtual camera based method is to introduce a virtual camera frame by defining a virtual camera. This virtual camera frame has the same origin and the yaw angle as the real camera frame but zero pitch and roll angles, facilitating the estimation of depth information. By choosing suitable image moments in the virtual camera plane, we can derive the image kinematics independent of the quadrotor's roll and pitch motion, thereby simplifying the controller design. But the IBVS approaches generally require that the visual target should stay in the FOV of the camera during the visual servoing process, which cannot be guaranteed in practical applications. If the quadrotor loses sight of the visual target, its visual servoing process may fail due to the loss of image data. Therefore, keeping the visual target within the FOV of the camera, i.e., ensuring the satisfaction of the visibility constraint, should be primarily addressed during the servoing process.

Due to the inherent characteristics, it is promising to fulfill the visibility constraint in the visual servoing by using MPC. In [220], an NMPC approach is designed for the camera projection model to handle the input and visibility constraints. In [221], a stabilizing NMPC based IBVS approach is designed for the setpoint tracking of underwater vehicles. Sheng *et al.* proposed an output feedback NMPC strategy in [222] for the IBVS of quadrotors, where a high-gain observer is developed to estimate the linear velocity. Note that the aforementioned methods assume the absence of external disturbances, which is unrealistic in practical control problems. Therefore, robust MPC has attracted increasing attention in the existing literature on IBVS. The authors in [223] established a linear parameter-varying model for the IBVS of the manipulator with an eye-in-hand camera structure, where the worst-case cost with respect to the parametric uncertainty is considered in the MPC optimization problem to handle uncertainties. In [224] a robust NMPC strategy is proposed for the image kinematics defined in the virtual camera plane, in which a tightened state constraint is constructed to handle external disturbances.

In this chapter, we investigate the MPC-based IBVS of quadrotors subject to external disturbances. Similar to our previous work [222], the IBVS system model is derived by integrating the image kinematics and quadrotor dynamics. Then a robust MPC scheme is developed for the IBVS of quadrotors, in which the external disturbances are handled based on the constraint tightening strategy presented in [225]. Different from the existing IBVS

method [224], the MPC objective function used in the proposed method is not required to be Lipschitz continuous, thereby reducing the conservatism.

The **main contributions** are two-folded

- Inspired by [225], a sequence of tightened state constraints is designed based on the Lipschitz condition such that the constraint satisfaction can be guaranteed for all admissible realization of uncertainties. In addition, due to the offline construction of the tightened constraints, the computational complexity of the proposed method is almost equivalent to the standard NMPC scheme, making it applicable to real quadrotor platforms while ensuring robust constraint satisfaction.
- A robust MPC scheme is developed for the IBVS of quadrotors to fulfill the visibility constraints. Compared with our previous work [222] where the rigorous analysis of the closed-loop prosperities is not provided, the sufficient conditions on guaranteeing the recursive feasibility of the proposed robust NMPC algorithm are established in this work. It is also theoretically shown that the tracking error will converge to a small set around the origin in finite time under the proposed conditions. Numerical simulation and experimental validation are provided to illustrate the efficacy of the proposed method.

5.2 System Modeling

In this section, different coordinates used for describing the motion of a quadrotor are firstly presented, followed by the modeling of a quadrotor system. Then image features are introduced to derive the decoupled image kinematics. Finally, we establish the dynamics of the quadrotors expressed in the virtual camera frame.

5.2.1 Quadrotor dynamics

As shown in Figure 5.1, the inertia frame $\mathcal{N} = \{O_n, n_1, n_2, n_3\}$ and the body-fixed frame $\mathcal{B} = \{O_b, b_1, b_2, b_3\}$ are introduced to describe the motion of the quadrotor. It is assumed that the origin of the frame \mathcal{B} is located at the center of gravity (COG) of the quadrotor. The orientation relationship between two coordinate frames is characterized by a rotation matrix. The third frame is the camera frame $\mathcal{C} = \{O_c, c_1, c_2, c_3\}$, where O_c is located at the optical center of the camera. Since the camera is attached underneath the geometric center of the quadrotor, it is assumed that \mathcal{B} and \mathcal{C} are aligned by neglecting the displacement

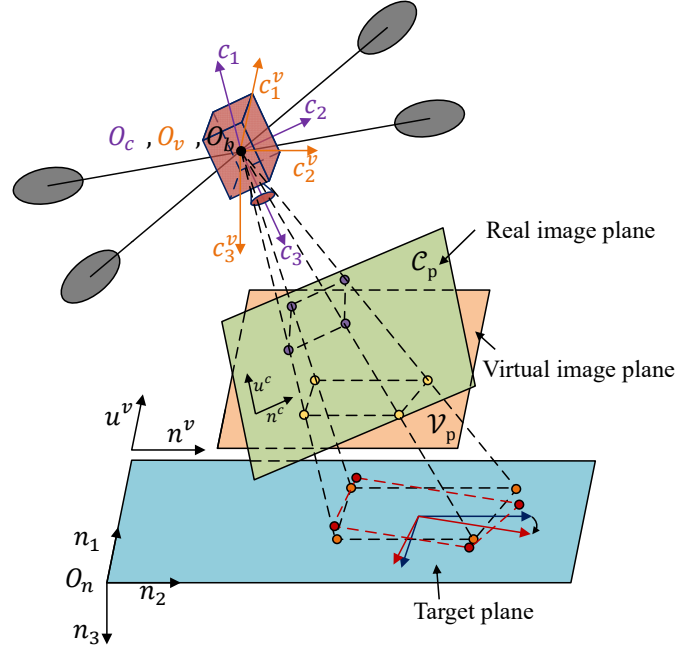


Figure 5.1: Reference coordinate frames.

between O_b and O_c . Hence, only \mathcal{C} is considered in the following for the convenience of presentation. The last one is the virtual camera frame $\mathcal{V} = \{O_v, c_1^v, c_2^v, c_3^v\}$, where the origin O_v coincides with O_c and c_3^v is parallel to n_3 . Let $\boldsymbol{\eta} = [\phi, \theta, \psi]^T$ denote the attitude vector of the quadrotor represented in \mathcal{B} , where ϕ, θ and ψ are roll, pitch, and yaw angles, respectively. Then the quadrotor orientation from \mathcal{C} to \mathcal{N} can be described by the following rotation matrix

$$\mathbf{R}_{\mathcal{C}}^{\mathcal{N}} = \begin{bmatrix} c_{\theta}c_{\psi} & s_{\theta}s_{\phi}c_{\psi} - s_{\psi}c_{\phi} & s_{\theta}c_{\phi}c_{\psi} + s_{\psi}s_{\phi} \\ c_{\theta}s_{\psi} & s_{\theta}s_{\phi}s_{\psi} + c_{\psi}c_{\phi} & s_{\theta}c_{\phi}s_{\psi} - s_{\phi}c_{\psi} \\ -s_{\theta} & c_{\theta}s_{\phi} & c_{\theta}c_{\phi} \end{bmatrix}$$

where $s. = \sin(\cdot)$ and $c. = \cos(\cdot)$. Similarly, $\mathbf{R}_{\mathcal{V}}^{\mathcal{N}}$ and $\mathbf{R}_{\mathcal{C}}^{\mathcal{V}}$ are rotation matrices from \mathcal{V} to \mathcal{N} and from \mathcal{C} to \mathcal{V} , respectively.

Let $\boldsymbol{\zeta}^n = [x^n, y^n, z^n]^T$ and $\mathbf{v}^n = [v_x^n, v_y^n, v_z^n]^T$ denote the position and linear velocity of the quadrotor expressed in \mathcal{N} , and $\boldsymbol{\Omega}^c = [\Omega_1^c, \Omega_2^c, \Omega_3^c]^T$ is the angular velocity expressed in \mathcal{C} . Without considering uncertainties, the motion of the quadrotor in \mathcal{N} is described by following equations [226]

$$\dot{\boldsymbol{\zeta}}^n = \mathbf{v}^n \quad (5.1a)$$

$$\dot{\mathbf{v}}^n = -\mathbf{R}_{\mathcal{C}}^{\mathcal{N}} \mathbf{E}_3 F/m + g \mathbf{E}_3 \quad (5.1b)$$

$$\dot{\mathbf{R}}_{\mathcal{C}}^{\mathcal{N}} = \mathbf{R}_{\mathcal{C}}^{\mathcal{N}} [\boldsymbol{\Omega}^c]_{\times} \quad (5.1c)$$

$$\dot{\boldsymbol{\Omega}}^c = -\mathbf{I}^{-1} [\boldsymbol{\Omega}^c]_{\times} \mathbf{I} \boldsymbol{\Omega}^c + \mathbf{I}^{-1} \boldsymbol{\tau} \quad (5.1d)$$

where m is the mass of the quadrotor; g is the gravitational constant; \mathbf{I} is the moment of inertia of the quadrotor; F is the magnitude of the thrust generated by all propellers; $\boldsymbol{\tau}$ is the resultant torque generated by the propellers; $\mathbf{E}_3 = [0, 0, 1]^T$ and $[\boldsymbol{\Omega}^c]_{\times}$ denotes the operation spanning the vector $\boldsymbol{\Omega}^c$ into a skew-symmetric matrix [227].

5.2.2 Image feature and IBVS dynamics

Similar to [227, 228], a pinhole camera model is considered in this work. The ground target considered here is a 2-D polytope consisting of multiple points. The positions of these points are extracted from captured images. Here it is assumed that the ground target consists of more than one point. As shown in Figure 5.1, we firstly introduce a 2-D image plane \mathcal{C}_p whose basis $\{u^c, n^c\}$ is parallel to $\{c_1, c_2\}$. Analogously, \mathcal{V}_p is a 2-D plane with its basis $\{u^v, n^v\}$ parallel to $\{c_1^v, c_2^v\}$. Given a point $\boldsymbol{\zeta}^c = [x^c, y^c, z^c]^T$ expressed in \mathcal{C} , its projection in \mathcal{C}_p can be calculated by using the perspective projection equation as follows [229]

$$\boldsymbol{\zeta}_p^c = \begin{bmatrix} u_p^c \\ n_p^c \end{bmatrix} = \frac{\lambda}{z^c} \begin{bmatrix} x^c \\ y^c \end{bmatrix}, \quad (5.2)$$

where λ is the camera focal length. Similarly, for a point $\boldsymbol{\zeta}^v = [x^v, y^v, z^v]^T$ expressed in \mathcal{V} , its projection in the plane \mathcal{V}_p can be calculated by using (5.2). Then recalling the image features defined in [229], the image moments are given as follows

$$s_1 = s_3 \frac{u_g^v}{\lambda}, s_2 = s_3 \frac{n_g^v}{\lambda}, s_3 = \sqrt{\frac{a^*}{a}}, s_4 = \frac{1}{2} \arctan \left(\frac{2\mu_{11}}{\mu_{20} - \mu_{02}} \right), \quad (5.3)$$

where $\mathbf{s} = [s_1, s_2, s_3, s_4]^T$ is image moment; $u_g^v = \frac{1}{N} \sum_{k=1}^N u_{k,p}^v$; $n_g^v = \frac{1}{N} \sum_{k=1}^N n_{k,p}^v$; $(u_{k,p}^v, n_{k,p}^v), k \in \mathbb{N}_{[1,N]}$, is the position of the k th point in the virtual image plane; N is the number of points contained in the target object; $\mu_{ij} = \sum_{k=1}^N (u_{k,p}^v - u_g^v)^i (n_{k,p}^v - n_g^v)^j$, $a = \mu_{20} + \mu_{02}$, and a^* is the value of a when the quadrotor is at the desired pose. As derived

in [219], the kinematics of image moments is given by

$$\dot{\mathbf{s}} = f_s(\mathbf{s}, \mathbf{v}^v, \dot{\psi}) = \begin{bmatrix} -\frac{1}{\bar{z}^c} v_x^v + s_2 \dot{\psi} \\ -\frac{1}{\bar{z}^c} v_y^v - s_1 \dot{\psi} \\ -\frac{1}{\bar{z}^c} v_z^v \\ -\dot{\psi} \end{bmatrix} \quad (5.4)$$

where $\mathbf{v}^v = [v_x^v, v_y^v, v_z^v]^T$ denotes the linear velocity of the quadrotor expressed in \mathcal{V} and \bar{z}^c is the desired height of the quadrotor expressed in \mathcal{C} . Since s_1, s_2 and s_3 are image features for the horizontal and vertical motion of the quadrotor, the quadrotor's workspace can be restricted by imposing an additional constraint on the image moment \mathbf{s} . Therefore, the visibility constraint $\mathcal{S} = \{\mathbf{s} \in \mathbb{R}^4 : -\mathbf{s}_{\max} \leq \mathbf{s} \leq \mathbf{s}_{\max}\}$ is incorporated to maintain the target of interest within the FOV of the camera, where $\mathbf{s}_{\max} \in \mathbb{R}^4$ is a known constant vector. In addition, by substituting $\mathbf{v}^n = \mathbf{R}_{\mathcal{V}}^{\mathcal{N}} \mathbf{v}^v$ into (5.1b), the translational motion of the quadrotor in virtual camera frame \mathcal{V} can be obtained, i.e., $\dot{\mathbf{v}}^v = -[\dot{\psi} \mathbf{E}_3]_{\times} \mathbf{v}^v - \mathbf{R}_{\mathcal{C}}^{\mathcal{V}} \mathbf{E}_3 T/m + g \mathbf{E}_3$, which can be rewritten as

$$\dot{\mathbf{v}}^v = f_v(\mathbf{v}^v, \mathbf{h}, \dot{\psi}) = -[\dot{\psi} \mathbf{E}_3]_{\times} \mathbf{v}^v + \mathbf{h}. \quad (5.5)$$

where $\mathbf{h} = [h_1, h_2, h_3]^T = g \mathbf{E}_3 - \mathbf{R}_{\mathcal{C}}^{\mathcal{V}} \mathbf{E}_3 T/m$. Since the velocity and acceleration of a real quadrotor system are limited, the following physical constraints are considered: $\mathcal{V} = \{\mathbf{v} \in \mathbb{R}^3 : -\mathbf{v}_{\max} \leq \mathbf{v} \leq \mathbf{v}_{\max}\}$, $\mathcal{U} = \{(\mathbf{h}, \dot{\psi}) \in \mathbb{R}^4, -\mathbf{h}_{\max} \leq \mathbf{h} \leq \mathbf{h}_{\max}, |\dot{\psi}| \leq \Omega_{\max}\}$, where $\mathbf{v}_{\max} \in \mathbb{R}^3$, $\mathbf{h}_{\max} \in \mathbb{R}^3$ and $\Omega_{\max} \in \mathbb{R}$ are constant and known. Let $\mathbf{x} = \text{col}(\mathbf{s}, \mathbf{v}^v)$ and $\mathbf{u} = \text{col}(\mathbf{h}, \dot{\psi})$, based on (5.4) and (5.5), the quadrotor IBVS model is derived as follows

$$\dot{\mathbf{x}} = f(\mathbf{x}, \mathbf{u}) := \begin{bmatrix} f_s(\mathbf{s}, \mathbf{v}^v, \dot{\psi}) \\ f_v(\mathbf{v}^v, \mathbf{h}, \dot{\psi}) \end{bmatrix}. \quad (5.6)$$

5.2.3 Control objective

In this work, the control objective is to regulate the relative position and yaw angle of the quadrotor to a prescribed visual target based on captured images and measured velocities. Instead of generating the actuator level commands directly, we adopt a dual-loop control structure shown in Figure 5.2, where the outer-loop IBVS controller receives the extracted image features to output desired attitude and velocity signals for the inner-loop, while the inner-loop tracking controller drives the quadrotor to the desired position. Since a class of commercial quadrotors, e.g., DJI Phantom 4 and Parrot Bebop 2, with the embedded

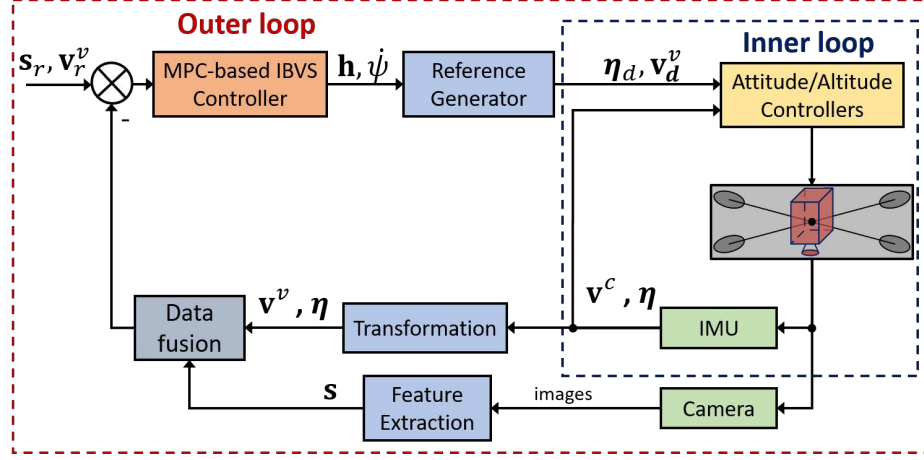


Figure 5.2: The dual-loop control structure.

autopilot function, is considered here, we only focus on designing the outer-loop IBVS controller in this work.

Let $\mathbf{h}_d(t) = [h_{1,d}(t), h_{2,d}(t), h_{3,d}(t)]^T$ and $\dot{\psi}_d(t)$ denote the output from the IBVS controller at time t , then the desired attitudes and velocity are given as follows:

$$\begin{aligned}\phi_d(t + \delta) &= \arcsin \left(\frac{h_{2,d}(t)}{\sqrt{h_{1,d}(t)^2 + h_{2,d}(t)^2 + (h_{3,d}(t) - g)^2}} \right), \\ \theta_d(t + \delta) &= \arctan \left(\frac{h_{1,d}(t)}{h_{3,d}(t) - g} \right), \\ \psi_d(t + \delta) &= \dot{\psi}_d(t)\delta + \psi(t), \\ \mathbf{v}_d^v(t + \delta) &= f_v(\mathbf{v}^v(t), \mathbf{h}_d(t), \dot{\psi}_d(t))\delta + \mathbf{v}^v(t),\end{aligned}$$

where $\boldsymbol{\eta}_d(t) = [\phi_d(t), \theta_d(t), \psi_d(t)]^T$ and $\mathbf{v}_d^v(t)$ are the desired attitude vector and velocity vector for the inner-loop controller, respectively. δ is the sampling interval. Our objective of this study is to design a robust NMPC based IBVS controller to robustly stabilize the quadrotor to the desired pose based on the image and velocity information while satisfying the visibility constraint \mathcal{S} and the physical constraints \mathcal{V} and \mathcal{U} .

5.3 Controller Design

In this section, a robust NMPC scheme is developed for the IBVS of the quadrotor system subject to unknown disturbances. A state constraint tightening strategy is introduced to handle external disturbances. Then a summary of the proposed MPC algorithm is presented. Finally, this section concludes with sufficient conditions for ensuring recursive

feasibility and closed-loop stability.

5.3.1 Robust NMPC scheme

In this subsection, we consider the quadrotor IBVS model in (5.6) with the presence of external disturbances $\boldsymbol{\omega}(t) \in \mathbb{R}^7$

$$\dot{\mathbf{x}}(t) = f(\mathbf{x}(t), \mathbf{u}(t)) + \boldsymbol{\omega}(t). \quad (5.7)$$

It is assumed that $\mathbf{x}(t) \in \mathcal{X}$ and $\mathbf{u}(t) \in \mathcal{U}$, where \mathcal{X} can be obtained from the constraints \mathcal{V} and \mathcal{S} . We further assume that $\boldsymbol{\omega}(t)$ belongs to a bounded set \mathcal{W} . The variable $\bar{\mathbf{x}}(t)$ is defined as the state of the following nominal system

$$\dot{\bar{\mathbf{x}}}(t) = f(\bar{\mathbf{x}}(t), \mathbf{u}(t)). \quad (5.8)$$

Our control objective is to regulate the system state to its desired value $\mathbf{x}_r = \text{col}(\mathbf{s}_r, \mathbf{v}_r^v) \in \mathbb{R}^7$, where $\mathbf{s}_r \in \mathbb{R}^4$, $\mathbf{v}_r^v \in \mathbb{R}^3$ are constant vectors, and $(\mathbf{x}_r, 0)$ is an equilibrium point of the system (5.6). Then for the nominal system (5.8) we have the following assumption, which is common in robust MPC, e.g., [180, 188]

Assumption 5.1. 1) The function $f(\mathbf{x}(t), \mathbf{u}(t))$ is locally Lipschitz continuous in $\mathbf{x}(t) \in \mathcal{X}$ with a Lipschitz constant L , and 2) there exists a feedback gain \mathbf{K} such that $\mathbf{A} + \mathbf{BK}$ is Hurwitz, where $\mathbf{A} = \left. \frac{\partial f(\mathbf{x}(t), \mathbf{u}(t))}{\partial \mathbf{x}} \right|_{(\mathbf{x}_r, 0)}$ and $\mathbf{B} = \left. \frac{\partial f(\mathbf{x}(t), \mathbf{u}(t))}{\partial \mathbf{u}} \right|_{(\mathbf{x}_r, 0)}$.

MPC optimization problem

Let $\bar{\mathbf{x}}(l|t)$, $l \in [t, t+T]$ denote the trajectory of the nominal system state, which is predicted at the time t by using the nominal system model in (5.8) with the control input trajectory $\mathbf{u}(l|t)$. Here, T is the prediction horizon. Let $\hat{\mathbf{x}}(t) = \mathbf{x}(t) - \mathbf{x}_r$ and $\hat{\mathbf{x}}(l|t) = \bar{\mathbf{x}}(l|t) - \mathbf{x}_r$ with $l \in [t, t+T]$. Define the cost function as

$$J_T(\hat{\mathbf{x}}(l|t), \mathbf{u}(l|t)) = \int_t^{t+T} \ell(\hat{\mathbf{x}}(\tau|t), \mathbf{u}(\tau|t)) d\tau + \ell_f(\hat{\mathbf{x}}(t+T|t)),$$

where $\ell(\hat{\mathbf{x}}(l|t), \mathbf{u}(l|t)) : \mathbb{R}^7 \times \mathbb{R}^4 \rightarrow \mathbb{R}_{\geq 0}$ and $\ell_f(\hat{\mathbf{x}}(t+T|t)) : \mathbb{R}^7 \rightarrow \mathbb{R}_{\geq 0}$ are the stage cost function and the terminal cost function to be designed, respectively. Then the MPC

Algorithm 5.1 Robust NMPC algorithm

Input: Initial system state \mathbf{x}_0 ; prediction horizon T ; sampling interval δ ; terminal constraint $\Omega(\epsilon)$

- 1: Set $t = 0$.
 - 2: Measure the system state $\mathbf{x}(t)$ and calculate the tracking error $\hat{\mathbf{x}}(t) = \mathbf{x}(t) - \mathbf{x}_r$.
 - 3: **while** $\hat{\mathbf{x}}(t) \notin \Omega(\epsilon)$ **do**
 - 4: Solve the optimization problem \mathcal{P} in (5.9) to obtain the optimal control input trajectory $\mathbf{u}^*(l|t)$.
 - 5: Apply the control input $\mathbf{u}(\tau) = \mathbf{u}^*(\tau|t)$, $\tau \in [t, t + \delta)$ to the system (5.7).
 - 6: **end while**
 - 7: Apply the input $\mathbf{u}(t) = \mathbf{K}\hat{\mathbf{x}}(t)$ to the system (5.7).
-

optimization problem is formulated as follows:

$$\mathcal{P} : V_T(\hat{\mathbf{x}}(t)) = \min_{\mathbf{u}(l|t)} J_T(\hat{\mathbf{x}}(l|t), \mathbf{u}(l|t)) \quad (5.9a)$$

$$\text{s.t. } \bar{\mathbf{x}}(t|t) = \hat{\mathbf{x}}(t) + \mathbf{x}_r, \quad (5.9b)$$

$$\dot{\bar{\mathbf{x}}}(l|t) = f(\bar{\mathbf{x}}(l|t), \mathbf{u}(l|t)), \quad (5.9c)$$

$$\bar{\mathbf{x}}(l|t) \in \mathcal{X}_{l-t}, \mathbf{u}(l|t) \in \mathcal{U}, \quad (5.9d)$$

$$\hat{\mathbf{x}}(t + T|t) \in \Omega(\epsilon), \quad (5.9e)$$

where \mathcal{X}_{l-t} is the tightened state constraint and $\Omega(\epsilon)$ is the terminal constraint, which will be introduced later.

In this work, we consider a dual-mode MPC framework proposed in [230]. Specifically, when the tracking error $\hat{\mathbf{x}}(t) \notin \Omega(\epsilon)$, an optimal control trajectory $\mathbf{u}^*(l|t)$ is obtained by solving the optimization problem in (5.9). Then the control input to be implemented is given by $\mathbf{u}(\tau) = \mathbf{u}^*(\tau|t)$, $\tau \in [t, t + \delta]$. When $\hat{\mathbf{x}}(t) \in \Omega(\epsilon)$, the locally stabilizing control law $\mathbf{u}(t) = \mathbf{K}\hat{\mathbf{x}}(t)$ is applied. Algorithm 5.1 summarizes the proposed robust NMPC approach.

Tightened state constraint

Given the optimal control input trajectory $\mathbf{u}^*(l|t)$, $l \in [t, t + T]$, we use $\mathbf{x}(l|t)$ and $\bar{\mathbf{x}}^*(l|t)$ to denote the trajectories of real system state and optimal nominal system state obtained by using the system models in (5.7) and (5.8), respectively. In order to guarantee the satisfaction of state and input constraints for all admissible realization of uncertainties, we need to ensure that $\mathbf{x}(l|t) \in \mathcal{X}$ for all admissible realizations of the uncertainty. Suppose

that \mathbf{P} is a positive definite matrix. By using the Lipschitz condition in Assumption (5.1), the deviation between two states $\mathbf{x}(l|t)$ and $\bar{\mathbf{x}}^*(l|t)$ is derived as follows

$$\|\bar{\mathbf{x}}^*(l|t) - \mathbf{x}(l|t)\|_{\mathbf{P}} \leq \int_t^l (L(\|\bar{\mathbf{x}}^*(\tau|t) - \mathbf{x}(\tau|t)\|_{\mathbf{P}}) + \bar{\omega}_P) d\tau,$$

where $\bar{\omega}_P = \bar{\omega}\bar{\lambda}(\sqrt{\mathbf{P}})$ and $\bar{\omega} = \sup_{\omega(t) \in \mathcal{W}} \|\omega(t)\|$. Then the Gronwall–Bellman inequality implies that

$$\|\bar{\mathbf{x}}^*(l|t) - \mathbf{x}(l|t)\|_{\mathbf{P}} \leq \frac{\bar{\omega}_P}{L}(e^{L(l-t)} - 1), \quad (5.10)$$

which describes the upper bound of the error between the optimal predicted nominal state $\bar{\mathbf{x}}^*(l|t)$ and the real state $\mathbf{x}(l|t)$. Motivated by [225], we design the tightened constraint \mathcal{X}_{l-t} as follows:

$$\begin{aligned} \mathcal{X}_{l-t} &= \mathcal{X} \ominus \mathcal{E}_{l-t} \\ \mathcal{E}_{l-t} &:= \{\mathbf{x} \in \mathbb{R}^7 : \|\mathbf{x}\|_{\mathbf{P}} \leq \frac{\bar{\omega}_P}{L}(e^{L(l-t)} - 1)\}. \end{aligned} \quad (5.11)$$

Consequently, we can ensure that $\mathbf{x}(l|t) \in \mathcal{X}$ if $\bar{\mathbf{x}}(l|t) \in \mathcal{X}_{l-t}$. Therefore, the robust satisfaction of state constraints is guaranteed.

Objective function and terminal constraint

In this work, we consider the stage and terminal cost functions with a quadratic form:

$$\ell(\hat{\mathbf{x}}(t), \mathbf{u}(t)) = \|\hat{\mathbf{x}}(t)\|_{\mathbf{Q}}^2 + \|\mathbf{u}(t)\|_{\mathbf{R}}^2, \ell_f(\hat{\mathbf{x}}(t)) = \|\hat{\mathbf{x}}(t)\|_{\mathbf{P}}^2,$$

where matrices \mathbf{Q} , \mathbf{R} and \mathbf{P} are positive definite. In addition, we consider an ellipsoidal terminal constraint $\Omega(\epsilon) = \{\mathbf{x} \in \mathbb{R}^7 : \ell_f(\mathbf{x}) \leq \epsilon^2\}$. For the objective function and terminal constraint, we have the following assumption.

Assumption 5.2. *For the system (5.8), there exist a feedback gain \mathbf{K} and matrices \mathbf{Q} , \mathbf{R} and \mathbf{P} such that the following conditions hold for all $\hat{\mathbf{x}}(t) \in \Omega(\epsilon)$: 1) $\mathbf{K}\hat{\mathbf{x}}(t) \in \mathcal{U}$, 2) $\Omega(\epsilon)$ is a control invariant set for the system (5.8) under the control law $\mathbf{u}(t) = \mathbf{K}\hat{\mathbf{x}}(t)$, and 3) $\dot{\ell}_f(\hat{\mathbf{x}}(t)) \leq -\ell(\hat{\mathbf{x}}(t), \mathbf{K}\hat{\mathbf{x}}(t))$.*

Remark 5.1. *Assumption 5.2 is common in MPC, e.g.[180, 225, 231]. As shown in [231], given \mathbf{Q} , \mathbf{R} and \mathbf{K} , if there exists a unique positive definite solution \mathbf{P} for the following Lyapunov equation $(\mathbf{A}_K + \kappa\mathbf{I})^T \mathbf{P} (\mathbf{A}_K + \kappa\mathbf{I}) = -\bar{\mathbf{Q}}$ with $\bar{\mathbf{Q}} = \mathbf{Q} + \mathbf{K}^T \mathbf{R} \mathbf{K}$, $\mathbf{A}_K = \mathbf{A} + \mathbf{B} \mathbf{K}$ and $\kappa < -\bar{\lambda}(\mathbf{A}_K)$, the inequalities in Assumption 5.2 hold. In addition, the suitable matrices \mathbf{P} and \mathbf{K} satisfying conditions in Assumption 5.2 can be found by solving a linear*

matrix inequality problem.

5.3.2 Feasibility and stability analysis

In this subsection, the main theoretical results of this work are presented. We firstly investigate the sufficient conditions that guarantee the recursive feasibility of the proposed robust NMPC scheme. Then we illustrate the stability result for the closed-loop system.

Theorem 5.1. *Suppose that Assumptions 5.1 and 5.2 hold, and there exists a feasible solution for the optimization problem \mathcal{P} at the time instant $t = 0$. The proposed robust NMPC scheme, summarized in Algorithm 5.1, is recursively feasible if the following conditions hold*

$$L \leq \bar{\lambda}(\sqrt{\mathbf{P}})(e^{L\delta} - 1), \quad (5.12a)$$

$$\mathbf{x}_r \oplus \Omega(\epsilon) \subseteq \mathcal{X}_{T+\delta}, \quad (5.12b)$$

$$\epsilon(e^{-\delta\lambda(\bar{\mathbf{Q}})/(2\bar{\lambda}(\mathbf{P}))} - 1) + \bar{\omega}e^{LT} \leq 0. \quad (5.12c)$$

Proof. To prove the recursive feasibility, we need to show that the optimization problem \mathcal{P} admits a feasible solution at time $t + \delta$ if it is feasible at time t . We construct the following candidate solution

$$\tilde{\mathbf{u}}(l|t + \delta) = \begin{cases} \mathbf{u}^*(l|t), & l \in [t + \delta, t + T) \\ \mathbf{K}\bar{\mathbf{x}}^*(l|t), & l \in [t + T, t + T + \delta] \end{cases} \quad (5.13)$$

Here, we suppose that the state trajectory $\bar{\mathbf{x}}^*(l|t), l \in [t + T, t + T + \delta]$ is obtained under the input trajectory $\mathbf{u}^*(l|t) = \mathbf{K}\bar{\mathbf{x}}^*(l|t)$. Let $\tilde{\mathbf{x}}(l|t + \delta)$ denote the nominal state trajectory predicted by using the input trajectory $\tilde{\mathbf{u}}(l|t + \delta)$ and the system model in (5.8) with $\tilde{\mathbf{x}}(t + \delta|t + \delta) = \mathbf{x}(t + \delta)$. Define $\hat{\mathbf{x}}^*(l|t) = \bar{\mathbf{x}}^*(l|t) - \mathbf{x}_r$ and $\hat{\mathbf{x}}(l|t + \delta) = \tilde{\mathbf{x}}(l|t + \delta) - \mathbf{x}_r$. We show that $\tilde{\mathbf{u}}(l|t + \delta)$ is a feasible solution at time $t + \delta$ in the following.

Case 1: $l \in [t + \delta, t + T)$. As mentioned in Assumption 5.1, the nominal system (5.8) is locally Lipschitz continuous. Then by the Gronwall–Bellman inequality, we can derive the upper bound of the derivation between the states $\tilde{\mathbf{x}}(l|t + \delta)$ and $\bar{\mathbf{x}}^*(l|t)$

$$\|\tilde{\mathbf{x}}(l|t + \delta) - \bar{\mathbf{x}}^*(l|t)\|_{\mathbf{P}} \leq \bar{\omega}e^{L(l-t-\delta)} \quad (5.14)$$

Furthermore, it follows from (5.11) and (5.12a) that

$$\frac{\bar{\omega}_P}{L}(e^{L(l-t)} - 1) - \frac{\bar{\omega}_P}{L}(e^{L(l-t-\delta)} - 1) \geq \bar{\omega}e^{L(l-t-\delta)},$$

which implies

$$(\tilde{\mathbf{x}}(l|t + \delta) - \bar{\mathbf{x}}^*(l|t)) \in \mathcal{X}_{l-t} \cap \mathcal{X}_{l-t-\delta}.$$

Since $\bar{\mathbf{x}}^*(l|t) \in \mathcal{X}_{l-t}$, we have $\tilde{\mathbf{x}}(l|t + \delta) \in \mathcal{X}_{l-t-\delta}$, indicating that the constraint (5.9d) is satisfied for $l \in [t + \delta, t + T)$.

Case 2: $l \in [t + T, t + T + \delta)$. According to Assumption 5.2, we have

$$\hat{\mathbf{x}}^*(l|t) \in \Omega(\epsilon), \mathbf{K}\bar{\mathbf{x}}^*(l|t) \in \mathcal{U}, \forall l \in [t + T, t + T + \delta).$$

In addition, it follows from (5.12b) that

$$\bar{\mathbf{x}}^*(l|t) \in \mathbf{x}_r \oplus \Omega(\epsilon), \forall l \in [t + T, t + T + \delta).$$

Then by repeating the above procedure, we can prove that constraint (5.9d) holds for $l \in [t + T, t + T + \delta)$.

Case 3: $l = t + T + \delta$. Since $\hat{\mathbf{x}}^*(l|t) \in \Omega(\epsilon)$, according to Assumption 5.2, it can be derived that

$$\dot{\ell}_f(\hat{\mathbf{x}}^*(l|t)) \leq -\ell(\hat{\mathbf{x}}^*(l|t), \mathbf{K}\hat{\mathbf{x}}^*(l|t)) \leq -\frac{\lambda(\bar{\mathbf{Q}})}{\lambda(\bar{\mathbf{P}})} \ell_f(\hat{\mathbf{x}}^*(l|t)).$$

Applying the comparison principle [232] yields

$$\ell_f(\hat{\mathbf{x}}^*(t + T + \delta|t)) \leq \ell_f(\hat{\mathbf{x}}^*(t + T|t))e^{-\frac{\lambda(\bar{\mathbf{Q}})}{\lambda(\bar{\mathbf{P}})}\delta} \leq \epsilon^2 e^{-\frac{\lambda(\bar{\mathbf{Q}})}{\lambda(\bar{\mathbf{P}})}\delta}.$$

Similarly, we have $\|\tilde{\mathbf{x}}(l|t + \delta) - \bar{\mathbf{x}}^*(l|t)\|_{\mathbf{P}} \leq \bar{\omega}e^{LT}$, implying that

$$\|\tilde{\mathbf{x}}(l|t + \delta) - \mathbf{x}_r\|_{\mathbf{P}} \leq \epsilon e^{-\frac{\delta\lambda(\bar{\mathbf{Q}})}{2\lambda(\bar{\mathbf{P}})}} + \bar{\omega}e^{LT} \leq \epsilon.$$

Therefore, the constraint (5.9e) is satisfied. In summary, $\tilde{\mathbf{u}}(l|t + \delta)$ is a feasible solution for the optimization problem \mathcal{P} , which proves this theorem. \square

Theorem 5.1 presents our feasibility result of the proposed robust NMPC scheme. In the following, we investigate the stability of the closed-loop system.

Theorem 5.2. *Suppose that Assumptions 5.1 and 5.2 hold, and conditions presented in Theorem 5.1 are satisfied. If the following condition*

$$\frac{2\bar{\omega}\bar{\lambda}(\mathbf{Q})}{L^2\underline{\lambda}(\mathbf{P})}((L\epsilon + \xi)e^{LT} - L\epsilon - LT\xi - \xi) + 2\epsilon\bar{\omega}e^{LT} < \frac{\bar{\lambda}(\mathbf{Q})}{\underline{\lambda}(\mathbf{P})}\delta\epsilon^2 \quad (5.15)$$

holds, where $\xi = \sup_{\mathbf{x}(t) \in \mathcal{X}, \mathbf{u}(t) \in \mathcal{U}} \|f(\mathbf{x}(t), \mathbf{u}(t))\|_{\mathbf{P}}$, then the tracking error $\hat{\mathbf{x}}(t)$ will converge to the set $\Omega(\bar{\epsilon})$ in finite time with $\bar{\epsilon} = \sqrt{2\frac{\bar{\lambda}(\mathbf{P})\|\sqrt{\bar{\mathbf{P}}}\|}{\underline{\lambda}(\mathbf{Q})}\epsilon\bar{\omega}}$.

Proof. In this proof, we consider the following two cases: $\hat{\mathbf{x}}(t) \notin \Omega(\epsilon)$ and $\hat{\mathbf{x}}(t) \in \Omega(\epsilon)$. To prove this theorem, we firstly show that the proposed robust NMPC scheme will steer the tracking error $\hat{\mathbf{x}}(t)$ into the terminal set $\Omega(\epsilon)$.

When $\hat{\mathbf{x}}(t) \notin \Omega(\epsilon)$, it holds that

$$\begin{aligned} V_T(\hat{\mathbf{x}}(t + \delta)) - V_T(\hat{\mathbf{x}}(t)) &\leq J_T(\hat{\mathbf{x}}(l|t + \delta), \tilde{\mathbf{u}}(l|t + \delta)) - V_T(\hat{\mathbf{x}}(t)) \leq \Delta_1 + \Delta_2 + \Delta_3 \\ \Delta_1 &= \int_{t+\delta}^{t+T+\delta} \ell(\hat{\mathbf{x}}(\tau|t + \delta), \tilde{\mathbf{u}}(\tau|t + \delta)) - \ell(\hat{\mathbf{x}}^*(\tau|t), \mathbf{u}^*(\tau|t)) d\tau, \\ \Delta_2 &= - \int_t^{t+\delta} \ell(\hat{\mathbf{x}}^*(\tau|t), \mathbf{u}^*(\tau|t)) d\tau, \\ \Delta_3 &= \ell_f(\hat{\mathbf{x}}(t + T + \delta|t + \delta)) - \ell_f(\hat{\mathbf{x}}^*(t + T + \delta|t)). \end{aligned}$$

In the following, the upper bounds of the Δ_1 , Δ_2 and Δ_3 will be derived.

According to triangle inequality, it can be derived that

$$\begin{aligned} \Delta_1 &\leq \int_{t+\delta}^{t+T+\delta} \|\hat{\mathbf{x}}(\tau|t + \delta)\|_{\mathbf{Q}}^2 - \|\hat{\mathbf{x}}^*(\tau|t)\|_{\mathbf{Q}}^2 d\tau \\ &\leq \frac{\bar{\lambda}(\mathbf{Q})}{\underline{\lambda}(\mathbf{P})} \int_{t+\delta}^{t+T+\delta} (\|\hat{\mathbf{x}}(\tau|t + \delta) - \hat{\mathbf{x}}^*(\tau|t)\|_{\mathbf{P}})(\|\hat{\mathbf{x}}(\tau|t + \delta)\|_{\mathbf{P}} + \|\hat{\mathbf{x}}^*(\tau|t)\|_{\mathbf{P}}) d\tau. \end{aligned}$$

In order to find the upper bound of Δ_1 , we need to quantify the term $\|\hat{\mathbf{x}}(\tau|t + \delta)\|_{\mathbf{P}} + \|\hat{\mathbf{x}}^*(\tau|t)\|_{\mathbf{P}}$. Since $\bar{\mathbf{x}}^*(t + T|t) = \bar{\mathbf{x}}^*(l|t) + \int_l^{t+T} f(\bar{\mathbf{x}}^*(\tau|t), \mathbf{u}(\tau|t)) d\tau$, recalling the triangle inequality implies that

$$\|\hat{\mathbf{x}}^*(l|t)\|_{\mathbf{P}} \leq \|\hat{\mathbf{x}}^*(t + T|t)\|_{\mathbf{P}} + (t + T - l)\xi$$

Analogously,

$$\|\hat{\mathbf{x}}^*(l|t + \delta)\|_{\mathbf{P}} \leq \|\hat{\mathbf{x}}^*(t + T + \delta|t + \delta)\|_{\mathbf{P}} + (t + \delta + T - l)\xi.$$

Then based on (5.14), the upper bound of Δ_1 is derived as follows:

$$\begin{aligned}\Delta_1 &\leq \frac{\bar{\lambda}(\mathbf{Q})}{\underline{\lambda}(\mathbf{P})} \int_{t+\delta}^{t+T+\delta} \bar{\omega} e^{L(\tau-t-\delta)} (2\epsilon + 2(t+\delta+T-\tau)\xi) d\tau \\ &\leq \frac{\bar{\lambda}(\mathbf{Q})}{\underline{\lambda}(\mathbf{P})} \int_0^T \bar{\omega} e^{L\tau} (2\epsilon + 2(T-\tau)\xi) d\tau \\ &\leq \frac{2\bar{\omega}\bar{\lambda}(\mathbf{Q})}{L^2\underline{\lambda}(\mathbf{P})} ((L\epsilon + \xi)e^{LT} - L\epsilon - LT\xi - \xi).\end{aligned}$$

Similarly, using the triangle inequality yields

$$\Delta_3 \leq \|\hat{\mathbf{x}}(t+\delta+T|t+\delta) - \hat{\mathbf{x}}^*(t+\delta+T|t)\|_{\mathbf{P}} \cdot (\|\hat{\mathbf{x}}(t+\delta+T|t+\delta)\| + \|\hat{\mathbf{x}}^*(t+\delta+T|t)\|) \leq 2\epsilon\bar{\omega}e^{LT}.$$

Furthermore, we have $\|\hat{\mathbf{x}}(t)\|_{\mathbf{P}} \geq \epsilon$ for $\hat{\mathbf{x}}(t) \notin \Omega(\epsilon)$. Therefore, it holds that

$$\Delta_2 \leq -\frac{\bar{\lambda}(\mathbf{Q})}{\underline{\lambda}(\mathbf{P})} \int_t^{t+\delta} \|\hat{\mathbf{x}}^*(\tau|t+\delta)\|_{\mathbf{P}}^2 d\tau \leq -\frac{\bar{\lambda}(\mathbf{Q})}{\underline{\lambda}(\mathbf{P})} \delta\epsilon^2.$$

Recalling the stability condition (5.15), we have

$$V_T(\hat{\mathbf{x}}(t+\delta)) - V_T(\hat{\mathbf{x}}(t)) \leq \Delta_1 + \Delta_2 + \Delta_3 < 0.$$

Therefore, based on [230, Theorem 2], it can be concluded that the error state $\hat{\mathbf{x}}(t)$ will finally converge to the terminal set $\Omega(\epsilon)$.

Next, we will show that the set $\Omega(\bar{\epsilon})$ is a positively robust invariant set for the closed-loop system under the control law $\mathbf{u}(t) = \mathbf{K}\hat{\mathbf{x}}(t)$. Suppose that $\hat{\mathbf{x}}(t_0) \in \Omega(\epsilon)$ and consider a Lyapunov function $V(\hat{\mathbf{x}}(t)) = \ell_f(\hat{\mathbf{x}}(t))$. Following [180, Lemma 1] yields that

$$\dot{V}(\hat{\mathbf{x}}(t)) \leq \frac{\bar{\lambda}(\bar{\mathbf{Q}})}{\underline{\lambda}(\mathbf{P})} (-\|\hat{\mathbf{x}}(t)\|_{\mathbf{P}}^2 + \bar{\epsilon}^2), \forall t \geq t_0.$$

As presented in the proof of Theorem 9 in [180], $\Omega(\bar{\epsilon})$ is a positively robust invariant set. Therefore, $\hat{\mathbf{x}}(t) \in \Omega(\bar{\epsilon}), \forall t \geq t_0$, which completes the proof. \square

Remark 5.2. *Theorems 5.1 and 5.2 demonstrate that, by using the proposed method, the tracking error $\hat{\mathbf{x}}(t)$ will be steered in a region whose size is decided by the uncertainty bound $\bar{\omega}$. From conditions (5.12) and (5.15), it can be seen that, although choosing a large T can provide a potential improvement of control performance, a small prediction horizon T is required to ensure the stability and feasibility if the uncertainty bound $\bar{\omega}$ is*

large, especially when the Lipschitz constant L is large. Therefore, a trade-off is desired to design the prediction horizon T .

5.4 Simulation and Experiment

In this section, the numerical simulation and the experimental test are presented to illustrate the efficacy of the proposed robust NMPC based IBVS technique.

5.4.1 Numerical simulation

In the simulation, we consider a quadrotor with the same parameters from [222]: $m = 1.2$ kg, $g = 9.8$ m/s² and $\mathbf{I} = \text{diag}([0.013, 0.013, 0.023])$. The camera focal length is $\lambda = 2.8 \times 10^{-3}$ m. The pixel of camera is assumed to be square with the side length 1.4×10^{-6} m. The target of interest are four coplanar points in the inertial frame:

$$[0.25, 0.2, 0]^T, [-0.25, 0.2, 0]^T, [0.25, -0.2, 0]^T, [-0.25, -0.2, 0]^T.$$

So the desired image features are $\mathbf{s}_r = [0, 0, 1, 0]^T$ and $a^* = 3.572 \times 10^{-7}$. The corresponding desired position and attitudes are $[0, 0, -1]^T$ and $[0, 0, 0]^T$, respectively. The objective is to steer the quadrotor from its initial position $\zeta^n(0) = [1, -0.6, -3]^T$ and $\eta(0) = [0, 0, -0.17]^T$ to the desired position. Therefore, the initial image moment is $\mathbf{s}(0) = [0.881, 0.764, 3, 0.174]^T$. When $t = 0$, it is assumed that the quadrotor hovers at its initial position with zero linear and angular velocities.

For the proposed robust NMPC scheme, the sampling interval is $\delta = 0.1$ s, and the prediction horizon is set to $T = 0.4$ s. The weighting matrices are chosen as follows: $\mathbf{Q} = \text{diag}([100, 100, 100, 100, 100, 100, 100])$ and $\mathbf{R} = \text{diag}([50, 50, 50, 50])$. To fulfill the visibility constraint, the state and input constraints are given by $\{\mathbf{x} \in \mathbb{R}^7 : -\mathbf{x}_{\max} \leq \mathbf{x} \leq \mathbf{x}_{\max}\}$ and $\{\mathbf{u} \in \mathbb{R}^4 : -\mathbf{u}_{\max} \leq \mathbf{u} \leq \mathbf{u}_{\max}\}$, where $\mathbf{x}_{\max} = [1, 1, 4, 3.14, 0.5, 0.5, 0.5]^T$ and $\mathbf{u}_{\max} = [0.3, 2, 2, 2]^T$. According to Remark 5.1, the terminal weighting matrix \mathbf{P} and the feedback gain \mathbf{K} can be computed with $\epsilon = 1.4702$. Based on [232], the Lipschitz constant is chosen as $L = 1.06$. The upper bound of the external disturbance is $\bar{\omega} = 0.015$. Moreover, we employ a nonlinear output-tracking controller from [233] with the sampling period 0.1δ to solve the inner-loop attitude tracking problem.

The simulation results are shown in Figures 5.3 and 5.4. It can be seen that the state and input constraints are satisfied by using the proposed robust NMPC method. The tra-

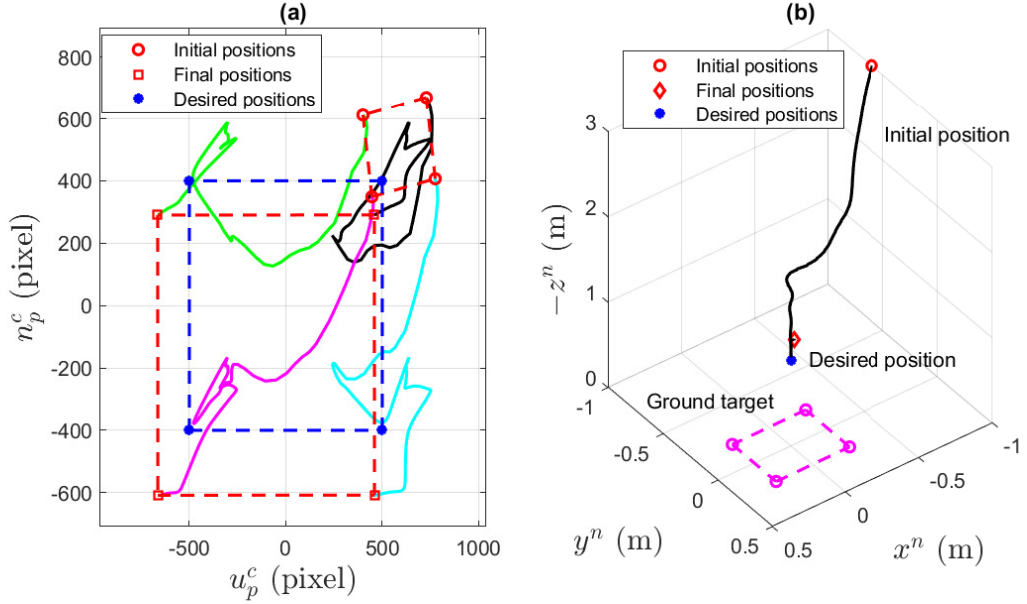


Figure 5.3: The trajectories of (a) ground target points in the real image plane and (b) the quadrotor in the inertia frame.

jectories of ground target points in the camera plane are presented in Figure 5.3(a), where the red circles, red squares, and blue stars denote the initial, final, and desired positions, respectively. The motion of the quadrotor in the inertial frame is described in Figure 5.3(b). From Figures 5.3 and 5.4, it can be observed that the quadrotor can be stabilized within a small region around the desired position by using the proposed robust NMPC based IBVS method, which verifies our theoretical results.

5.4.2 Experimental test

The schematic diagram of the experimental setup is shown in Figure 5.5. We consider a Parrot Bebop 2 quadrotor platform equipped with a wide-angle fisheye lens camera and an inertial measurement unit (IMU). The camera is mounted on the front of the quadrotor with the focal length $\lambda = 1.8 \times 10^{-6}$ m. Our proposed robust NMPC algorithm is implemented on the ground station. The image processing algorithm is developed based on OpenCV [234] to extract the image moments and is implemented on the same laptop. The MPC optimization problem is formulated and solved by using an open-source tool CasADi [235] in Python. When receiving the image features extracted from the captured image, the control command is generated by solving the optimization problem and then sent back to the quadrotor.

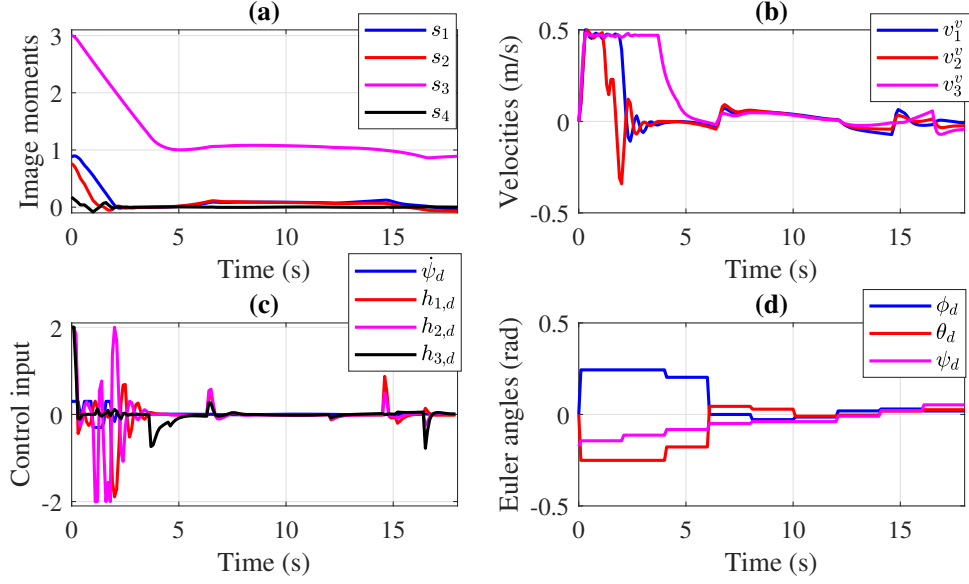


Figure 5.4: Time evolutions of (a) image moments s , (b) linear velocities in the virtual camera frame \mathbf{v}^v , (c) control inputs \mathbf{u} and (d) desired attitudes $\boldsymbol{\eta}_d$.

The control objective is to regulate the quadrotor to 1.35 m above the barycenter of the ground target with its yaw aligned with the principal axis of the target. Since O_v and O_c are different in the experiments, we manually drive the quadrotor to the desired position to calculate a^* before the experimental test. Hence $a^* = 5.5 \times 10^{-8}$ in the experiments. For the proposed robust NMPC algorithm, the state and input weighting matrices are chosen as $Q = \text{diag}([200, 200, 200, 2, 10, 10, 10])$ and $R = \text{diag}([1, 1, 1, 1])$. In addition, $\mathbf{x}_{\max} = [2, 2, 5, 3.14, 0.5, 0.5, 0.5]^T$, $\mathbf{u}_{\max} = [0.06, 2, 2, 2]^T$, $\delta = 0.1$ s and $T = 0.4$ s. In order to guarantee the practical implementation, the terminal constraint (5.9e) is not considered in the experiments. As ignoring the terminal constraint may degrade the performance, the dual-MPC framework is not employed in the experiments to improve the performance such that all control inputs are calculated by solving the optimization problem \mathcal{P} .

Experiment results are illustrated in Figures 5.6 - 5.7. Note that we consider the time instant when the first group of image features is successfully extracted as the initial time instant in the experiments. The time evolutions of the image moments and linear velocities are shown in Figures 5.6(a) and Figure 5.6(b), respectively. The control inputs are presented in Figures 5.6(c), and the corresponding desired attitudes for the inner-loop flight controller are illustrated in Figure 5.6(d). Figure 5.7 shows the processing of images captured by the camera, where the target points are recognized and marked as red, at time $t = 0$ s, 8.6 s, 17.1 s, and 23.1 s. From experiment results, it shows that, although the terminal

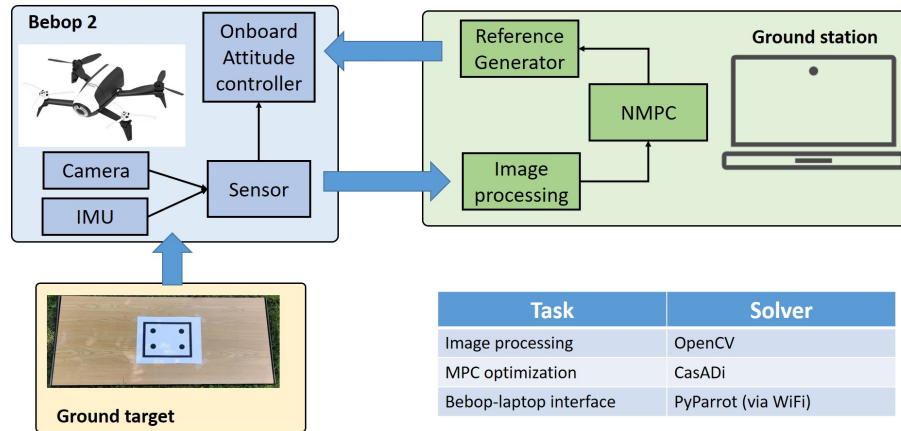


Figure 5.5: The schematic diagram of the experimental setup.

constraint is not considered, the proposed robust NMPC based IBVS method can steer the quadrotor to the neighborhood of the desired position while guaranteeing the physical and visibility constraints. Compared with the simulation results, the quadrotor finally arrived at a relatively larger region around the desired position since the actual value of uncertainty bound ω is unknown in the experiment. Another reason is that the inputs generated proposed method are not the direct control commands for the quadrotor propeller, which leads to additional disturbances. Therefore, the quadrotor finally arrived at the neighborhood of the desired position in the experiment. The experiment video can be found via <https://www.youtube.com/watch?v=b3dAPMjo920>.

5.5 Conclusion

In this chapter, we developed a robust NMPC scheme for the IBVS of quadrotors subject to external disturbances. By defining suitable image features in the virtual camera plane, the integration of the decoupled image kinematics and quadrotor dynamics was derived. Then the robust NMPC scheme was developed to guarantee the satisfaction of physical and visibility constraints, where the tightened state constraints were developed to handle external disturbances. In addition, sufficient conditions on guaranteeing recursive feasibility of the proposed robust NMPC-based IBVS scheme have been proposed. We have further proven that the quadrotor can be regulated to a small region around the desired position by using the proposed method. Simulation studies and experiment results have demonstrated the efficacy of the proposed robust NMPC based IBVS method.

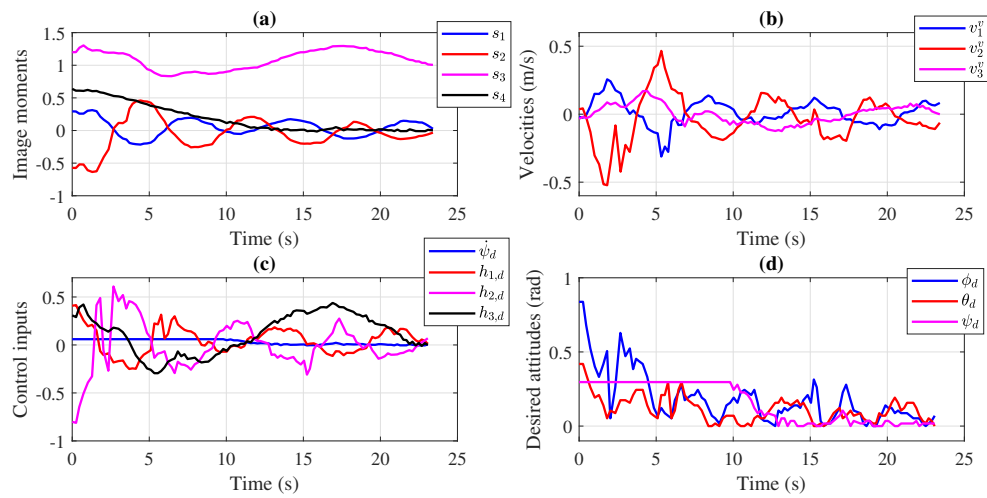


Figure 5.6: The experimental trajectories of (a) image moments s , (b) linear velocities in the virtual camera frame v^v , (c) control inputs u and (d) desired Euler angles η_d for the inner loop.

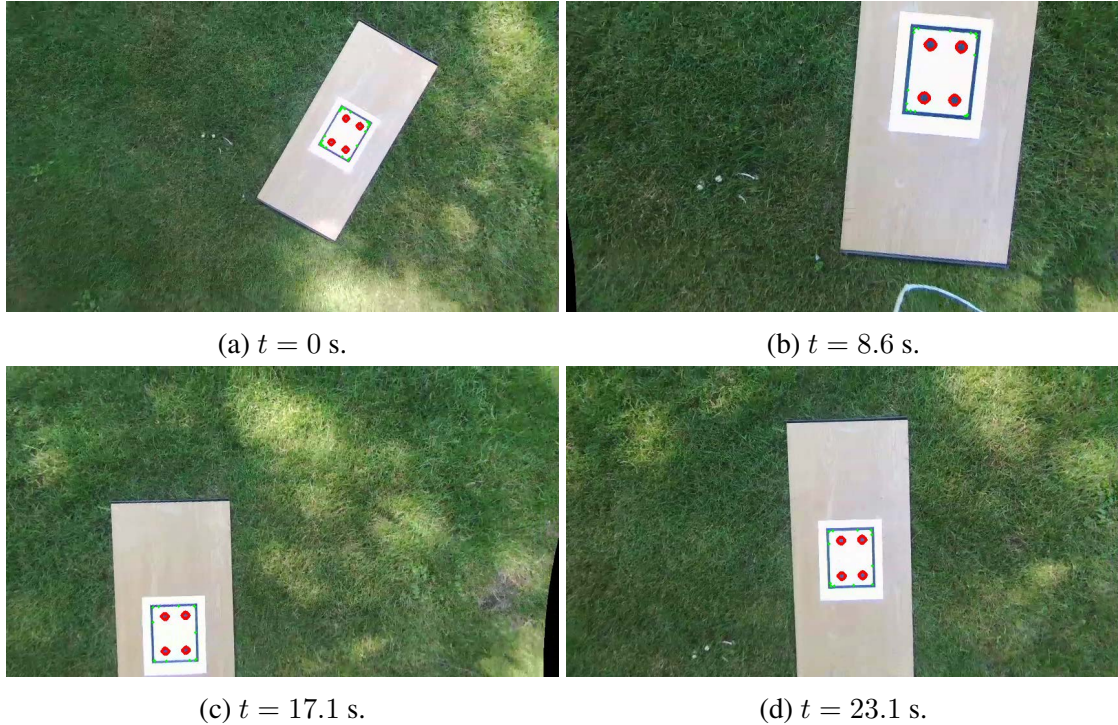


Figure 5.7: The processing of images captured by the onboard camera at different time instants.

Chapter 6

Trajectory Tracking Control of Autonomous Ground Vehicles Using Adaptive Learning MPC

Chapter 4 studies the application of robust MPC to quadrotors. In this chapter, we focus on the application of adaptive MPC to autonomous ground vehicles (AGVs).

6.1 Introduction

Over the past decades, AGVs have received considerable attention in modern military and civilian areas due to the high maneuverability, agile mobility and, low cost of AGVs [236]. Among related studies, trajectory tracking control is one of the fundamental control problems for AGVs. Many control schemes have been developed for the trajectory tracking of AGVs (e.g., [197–199]). In practical AGV applications, an important issue is that the presence of uncertainties, such as measurement noises and model mismatch, is inevitable. Accordingly, robust control methods have been employed in the AGV trajectory tracking problems, such as sliding mode control [237] and adaptive control [238]. The main focus of the aforementioned works is to explore feedback control laws that regulate tracking errors. But the physical constraints such as the speed limit and workspace restriction are ignored in these works. To address this issue, MPC stands out as a promising solution.

In this work, we develop an adaptive MPC scheme for the AGV trajectory tracking problem with input constraints. Similar to [239, 240], the dynamics of the tracking error represented in the local frame is firstly derived. Different from previous works consid-

ering the presence of external disturbances in the AGV trajectory tracking problem, this chapter considers an AGV system subject to both parametric uncertainties and external disturbances. A set-membership based parameter estimator is developed based on the RLS technique to identify the unknown system parameter with non-increasing estimation error, which provides a less conservative bounding set to describe the unknown parameter. The nominal system model used in MPC is recursively updated based on the estimated system parameter, leading to improved prediction accuracy. Note that the existing adaptive MPC methods [42–44, 102, 109] cannot be directly extended to solve the current problem since the established error dynamics is nonlinear and time-varying.

The **main contributions** of this chapter are two-fold:

- A novel adaptive MPC based trajectory tracking scheme is developed based on the robustness constraint method. We extend the robust MPC framework in [241] to the AGV tracking error dynamic system subject to additive and parametric uncertainties. Similar to the robust MPC method [241], the shape of the designed robustness constraint is computed offline based on the invariant set, but a dynamic shrinkage rate is designed and updated online associated with the estimated bounding set, thereby giving rise to further enhanced performance with slightly increased computational complexity compared with the original robust MPC method.
- Sufficient conditions on ensuring the recursive feasibility of the proposed adaptive MPC method are developed. We further prove that the closed-loop tracking system is input-to-state stable (ISS) under recursive updates of the system model. A numerical example and comparison study are provided to show the efficacy of the proposed method.

6.2 Problem Formulation

In this section, the kinematic model of the AGV is firstly introduced. Then the formulation of the tracking problem is described. Finally, the control objective is presented.

6.2.1 AGV kinematics

Consider a general AGV with two differential driving wheels, as shown in Figure 6.1. Each wheel is independently driven by an actuator. The points $\mathbf{p}_o = (x_o, y_o)$ and $\mathbf{p}_h = (x, y)$ are the midpoint between two wheels and the head position of the AGV, respectively. The head

point \mathbf{p}_h locates at the perpendicular bisector of the wheel axis, and the distance between \mathbf{p}_o and \mathbf{p}_h is r . Let $\theta(t)$ denote the AGV heading angle, then the kinematic model of the AGV is given by

$$\dot{\boldsymbol{\eta}}_o(t) = f_o(\boldsymbol{\eta}_o(t), \mathbf{u}(t)) = \begin{bmatrix} \cos \theta(t) & 0 \\ \sin \theta(t) & 0 \\ 0 & 1 \end{bmatrix} \mathbf{u}(t), \quad (6.1)$$

where $\boldsymbol{\eta}_o(t) = [x_o(t), y_o(t), \theta(t)]^T$; $\mathbf{u}(t) = [v(t), \omega(t)]^T$ is the control input, and $v(t)$ and $\omega(t)$ are linear and angular velocities, respectively. Then according to (6.1), the kinematics of the AGV's head position \mathbf{p}_h is described as follows:

$$\dot{\boldsymbol{\eta}}(t) = f_h(\boldsymbol{\eta}(t), \mathbf{u}(t), r) = \begin{bmatrix} \cos \theta(t) & -r \sin \theta(t) \\ \sin \theta(t) & r \cos \theta(t) \\ 0 & 1 \end{bmatrix} \mathbf{u}(t), \quad (6.2)$$

where $\boldsymbol{\eta}(t) = [x(t), y(t), \theta(t)]^T$ is the AGV system state. It can be seen from (6.1) and (6.2) that the position of head point \mathbf{p}_h is derived from the point \mathbf{p}_o . The vast majority of literature on the AGV trajectory tracking problem assumes that the point \mathbf{p}_o is the center of mass of the AGV. However, it is difficult to precisely measure the distance r between the points \mathbf{p}_o and \mathbf{p}_h since the position information of \mathbf{p}_o is usually inaccurate in practical control problems. Therefore, we assume that r is constant but unknown, whose true value is denoted by r^* . In addition, we consider the bounded linear and angular velocities of the AGV given by $|v(t)| \leq \check{v}$, $|\omega(t)| \leq \check{\omega}$, where $\check{v}, \check{\omega} > 0$ are known constants. Then the input constraint can be derived as $\mathcal{U} = \{\mathbf{u} \in \mathbb{R}^2 : \mathbf{H}\mathbf{u} \leq \mathbf{h}\}$, in which $\mathbf{H} = [\mathbf{I}_2, -\mathbf{I}_2]^T$ and $\mathbf{h} = [\check{v}, \check{\omega}, \check{v}, \check{\omega}]^T$.

In this work, the main control design objective is to track a time-parameterized reference trajectory $\boldsymbol{\eta}_s(t) = [x_s(t), y_s(t), \theta_s(t)]^T$. In order to avoid the singularity problem, we suppose that the reference trajectory satisfies the AGV kinematic model in (6.1) with a reference control input signal $\mathbf{u}_s(t) = [v_s(t), \omega_s(t)]^T$, i.e.,

$$\dot{\boldsymbol{\eta}}_s(t) = f_o(\boldsymbol{\eta}_s(t), \mathbf{u}_s(t)). \quad (6.3)$$

Similar to [198, 239], we define the tracking error state $\boldsymbol{\eta}_e(t) = [x_e(t), y_e(t), \theta_e(t)]^T$ in the

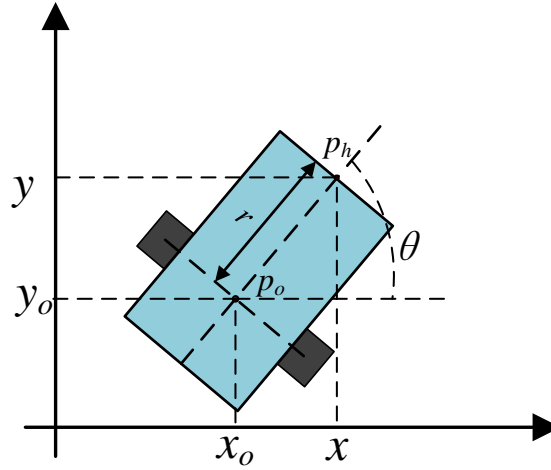


Figure 6.1: The structure of an AGV system.

local frame, which is given as follows:

$$\boldsymbol{\eta}_e(t) = \begin{bmatrix} \cos \theta(t) & \sin \theta(t) & 0 \\ -\sin \theta(t) & \cos \theta(t) & 0 \\ 0 & 0 & 1 \end{bmatrix} \begin{bmatrix} x_s(t) - x(t) \\ y_s(t) - y(t) \\ \theta_s(t) - \theta(t) \end{bmatrix}. \quad (6.4)$$

Then based on (6.2) and (6.3), the following error dynamics can be derived

$$\dot{\boldsymbol{\eta}}_e(t) = \begin{bmatrix} \omega(t)y_e(t) + v_s(t) \cos \theta_e(t) - v(t) \\ -\omega(t)x_e(t) + v_s(t) \sin \theta_e(t) - r\omega(t) \\ \omega_s(t) - \omega(t) \end{bmatrix}. \quad (6.5)$$

6.2.2 Tracking problem formulation

Since the designed tracking controller needs to be executed in the digital platform, we consider the discrete-time version of the system model in (6.2) by using the Euler forward approximation in the following. In addition, the presence of external disturbances caused by the wheel slipping is taken into account in this work, resulting in the following perturbed kinematics

$$\boldsymbol{\eta}(k+1) = f(\boldsymbol{\eta}(k), \mathbf{u}(k), r) + \mathbf{d}(k) = \delta f_h(\boldsymbol{\eta}(k), \mathbf{u}(k), r) + \boldsymbol{\eta}(k) + \mathbf{d}(k), \quad (6.6)$$

where $\mathbf{d}(k) = [d_x(k), d_y(k), d_\theta(k)]^T$ is the external disturbance and $\delta > 0$ is the sampling period. In this chapter, we only consider the disturbance of position measurement, i.e.,

$d_\theta(k)$ for all $k \geq 0$. Its corresponding nominal system model is given by

$$\boldsymbol{\eta}(k+1) = f(\boldsymbol{\eta}(k), \mathbf{u}(k), r). \quad (6.7)$$

Then we have the following general assumptions for the above systems.

Assumption 6.1. *The external disturbance $\mathbf{d}(k)$ and unknown parameter r belong to convex and compact sets \mathcal{D} and \mathcal{R}_0 , and bounded by constants $\check{d} \geq \|\mathbf{d}(k)\|, \forall \mathbf{d}(k) \in \mathcal{D}$ and $\check{r} \geq |r|, \forall r \in \mathcal{R}_0$, where \check{d} and \check{r} are positive and known.*

Assumption 6.2. *The reference system state $\boldsymbol{\eta}_s(k)$ and control input $\mathbf{u}_s(k)$ are bounded for all $k \geq 0$.*

Assumptions 6.1 and 6.2 indicate the bounded uncertainties and reference signals. Due to the limit of physical systems, Assumption 6.1 is commonly used in the literature on the AGV trajectory tracking problem. In addition, Assumption 6.2 can be satisfied by designing a suitable reference trajectory. Therefore, these assumptions are reasonable.

Define the AGV's head position $\mathbf{p}_h(k)$, the reference position $\mathbf{p}_s(k)$, the position error $\mathbf{p}_e(k)$ and the control input $\mathbf{u}(k)$ as $\mathbf{p}_h(k) = [x(k), y(k)]^T$, $\mathbf{p}_s(k) = [x_s(k), y_s(k)]^T$, $\mathbf{p}_e(k) = [x_e(k), y_e(k)]^T$ and $\mathbf{u}(k) = [v(k), \omega(k)]^T$, respectively. According to the definition of error state in (6.4), $\mathbf{p}_e(k)$ can be calculated by

$$\mathbf{p}_e(k) = f_p(\boldsymbol{\eta}(k), \boldsymbol{\eta}_s(k)) = \Psi(\theta(k))(\mathbf{p}_h(k) - \mathbf{p}_s(k)), \Psi(\theta(k)) = \begin{bmatrix} \cos \theta(k) & \sin \theta(k) \\ -\sin \theta(k) & \cos \theta(k) \end{bmatrix}.$$

Without considering the external disturbance, the discrete-time version of the error dynamics in (6.5) is given as follows:

$$\mathbf{p}_e(k+1) = f_e(\mathbf{p}_e(k), \mathbf{u}(k), r) = \mathbf{A}(\omega(k))\mathbf{p}_e(k) + \delta\mathbf{u}_e(k), \quad (6.8)$$

where

$$\mathbf{u}_e(k) = \begin{bmatrix} v_s(k) \cos \theta_e(k) - v(k) \\ v_s(k) \sin \theta_e(k) - r\omega(k) \end{bmatrix}, \mathbf{A}(\omega(k)) = \begin{bmatrix} 1 & \delta\omega(k) \\ -\delta\omega(k) & 1 \end{bmatrix}.$$

6.2.3 Control objective

In this work, the control objective is to design a stabilizing trajectory tracking controller for the system (6.6) based on the adaptive MPC method to be developed, where the robust

satisfaction of constraint \mathcal{U} is guaranteed and the unknown parameter r is identified online. Given the prediction horizon T and the parameter estimate $\hat{r}(k)$, we use $\bar{\boldsymbol{\eta}}(l|k)$, $l \in \mathbb{N}_{[0,T]}$, and $\bar{\mathbf{p}}_e(l|k)$ to denote the trajectories of predicted nominal state and error state under the control input $\mathbf{u}(l|k)$ with the nominal system model in (6.7) and the error dynamic model in (6.8), respectively. To achieve the desired objective, we propose a computationally tractable integration of the robustness constraint based MPC scheme and online set-membership system identification. More specifically, the estimate $\hat{r}(k)$ and the bounding set $\mathcal{R}(k)$ for the unknown parameter are updated consistently with *a priori* knowledge, i.e., the uncertainty sets \mathcal{D} and \mathcal{R}_0 , and the input and state trajectories. Both $\hat{r}(k)$ and $\mathcal{R}(k)$ are employed to construct the robustness constraint $\mathcal{X}(l|k)$, $l \in \mathbb{N}_{[0,T-1]}$, on the nominal error state $\bar{\mathbf{p}}_e(l|k)$. Consequently, the control input is determined by the following finite horizon optimal control problem

$$\min_{\mathbf{u}_T(k)} J_T(\mathbf{p}_e(k), \mathbf{u}_T(k)) = \sum_{l=0}^{T-1} \ell(\bar{\mathbf{p}}_e(l|k), \mathbf{u}(l|k)) + \ell_f(\bar{\mathbf{p}}_e(T|k)) \quad (6.9a)$$

$$\text{s.t. } \bar{\boldsymbol{\eta}}(0|k) = \boldsymbol{\eta}(k), \mathbf{p}_e(k) = f_p(\boldsymbol{\eta}(k), \boldsymbol{\eta}_s(k)) \quad (6.9b)$$

$$\bar{\boldsymbol{\eta}}(l+1|k) = f(\bar{\boldsymbol{\eta}}(l|k), \mathbf{u}(l|k), \hat{r}(k)), l \in \mathbb{N}_{[0,T-1]} \quad (6.9c)$$

$$\bar{\mathbf{p}}_e(l|k) \in \mathcal{X}(l|k), l \in \mathbb{N}_{[0,T-1]} \quad (6.9d)$$

$$\mathbf{u}(l|k) \in \mathcal{U}, l \in \mathbb{N}_{[0,T-1]} \quad (6.9e)$$

$$\bar{\mathbf{p}}_e(T|k) \in \Omega, \quad (6.9f)$$

where $\mathbf{u}_T(k) = \text{col}(\mathbf{u}(0|k), \mathbf{u}(1|k), \dots, \mathbf{u}(T-1|k))$ is the control input sequence; Ω is the terminal constraint; $\ell : \mathbb{R}^2 \times \mathbb{R}^2 \rightarrow \mathbb{R}_{\geq 0}$ and $\ell_f : \mathbb{R}^2 \rightarrow \mathbb{R}_{\geq 0}$ are the state and terminal cost functions to be designed, respectively. For the MPC optimization problem in (6.9), we have the following general assumption.

Assumption 6.3. *For the error dynamics in (6.8), there exist a terminal cost function $\ell_f : \mathbb{R}^2 \rightarrow \mathbb{R}_{\geq 0}$, a terminal control law $\tau_f : \mathbb{R}^2 \times \mathbb{R} \rightarrow \mathbb{R}^2$ and an invariant set Ω such that the following conditions hold*

$$\tau_f(\mathbf{p}_e(k), \hat{r}(k)) \in \mathcal{U}, \quad (6.10a)$$

$$f_e(\mathbf{p}_e(k), \tau_f(\mathbf{p}_e(k), \hat{r}(k))) \in \Omega, \quad (6.10b)$$

$$\ell_f(f_e(\mathbf{p}_e(k), \tau_f(\mathbf{p}_e(k), \hat{r}(k)))) - \ell_f(\mathbf{p}_e(k)) + \ell(\mathbf{p}_e(k), \mathbf{u}_e(k)) \leq 0, \quad (6.10c)$$

for all $(\mathbf{p}_e(k), \hat{r}(k)) \in \Omega \times \mathcal{R}_0$.

Assumption 6.3 describes the conditions on the terminal cost $\ell_f(\mathbf{p}_e(k))$, the terminal control law $\tau_f(\mathbf{p}_e(k), \hat{r}(k))$ and the invariant set Ω . Compared with the standard conditions used in robust MPC methods, e.g., [41, 180, 241], the main difference is that the terminal control law $\tau_f(\mathbf{p}_e(k), \hat{r}(k))$ in our work depends on the parameter estimate $\hat{r}(k)$. Therefore, the methods presented in [41, 180, 241] cannot be applied to the current problem where the model parameter is recursively updated. To solve this problem, the detailed discussion on parameter selection for the satisfaction of Assumption 6.3 is presented in Section 6.4.

6.3 Adaptive Learning MPC Algorithm

In this section, we present an adaptive MPC scheme for this trajectory tracking problem. We firstly introduce a parameter estimator for the simultaneous estimation of the unknown parameter and the uncertainty set. Then the formulation of the MPC optimization problem is presented. Finally, this section concludes with a summary of the proposed adaptive MPC algorithm.

6.3.1 Parameter estimation

In the following, we use $\hat{r}(k)$ and $\tilde{r}(k) = r^* - \hat{r}(k)$ to denote the estimate of the unknown system parameter r^* and the corresponding estimation error at time k , respectively. Let

$$h(k) = y(k) - y(k-1) - \delta v(k-1) \sin \theta(k-1), \quad g(k) = \delta \omega(k) \cos \theta(k).$$

Then the regression model for the unknown parameter derived from (6.6) is given as follows

$$h(k+1) = g(k)r^* + d_y(k).$$

It is assumed that the uncertainty set \mathcal{R}_0 has a form $\mathcal{R}_0 = \{r \in \mathbb{R}_{>0}, |r - \bar{r}_0| \leq \bar{\sigma}\}$, where constants $\bar{r}_0, \bar{\sigma}$ are positive.

At time instant k , assume that the true parameter r^* belongs to a set $\mathcal{R}(k) = \{r \in \mathbb{R} : (r - \hat{r}(k))^2 / \psi(k) \leq \hat{\sigma}^2(k)\}$ where $\psi(k), \hat{\sigma}(k)$ are variables to be designed later. In addition, Assumption 6.1 implies $|d_y(k)| = |(h(k+1) - g(k)r^*)| \leq \check{d}$. Then we can find a set $\mathcal{S}(k+1) = \{r \in \mathbb{R} : (h(k+1) - g(k)r)^2 \leq \check{d}^2\}$ such that $r^* \in \mathcal{S}(k+1)$. Therefore, r^* is consistent with both sets $\mathcal{S}(k+1)$ and $\mathcal{R}(k)$.

Our purpose is to design the uncertainty set estimation $\mathcal{R}(k+1)$ such that $\mathcal{S}(k+1) \cap \mathcal{R}(k) \subseteq \mathcal{R}(k+1)$. Recall the set-membership identification algorithm in [242], the

unknown parameter can be estimated as follows:

$$\psi^{-1}(k+1) = \psi^{-1}(k) + \lambda_f(k+1)g^2(k), \quad (6.11a)$$

$$\hat{r}(k+1) = \hat{r}(k) + \lambda_f(k+1)\psi(k+1)g(k)\tilde{h}(k+1), \quad (6.11b)$$

$$\tilde{h}(k+1) = h(k+1) - g(k)\hat{r}(k), \quad (6.11c)$$

$$G(k) = g^2(k)\psi(k), \quad (6.11d)$$

$$\lambda_f(k+1) = \begin{cases} 0, & \text{if } \tilde{h}^2(k+1) \leq \check{d}^2 \\ \frac{1}{\check{d}G(k)}(|\tilde{h}(k+1)| - \check{d}), & \text{otherwise} \end{cases} \quad (6.11e)$$

$$\hat{\sigma}^2(k+1) = \hat{\sigma}^2(k) + \lambda_f(k+1)\check{d}^2 - \frac{\lambda_f(k+1)\tilde{h}^2(k+1)}{1 + \lambda_f(k+1)G(k)}, \quad (6.11f)$$

where $\psi(0) = 1$ and $\hat{\sigma}(0) = \check{\sigma}$.

The following lemma shows the performance of parameter estimation.

Lemma 6.1. [242] *Suppose that Assumption 6.1 holds. For the bounded $g(k)$, the proposed parameter estimation scheme summarized in (6.11a) - (6.11f) has the following properties for all $k > 0$: 1) $r^* \in \mathcal{R}(k)$ if $r^* \in \mathcal{R}(0)$, and 2) $|\tilde{r}(k)|$ is bounded and non-increasing.*

Proof. Consider a candidate of Lyapunov function $\mathcal{V}(\tilde{r}(k)) = \tilde{r}^2(k)\psi^{-1}(k)$. We show the satisfaction of each statement in the following.

1): Suppose that $r^* \in \mathcal{R}(k-1)$. Following the analysis in [208, 242] yields

$$\begin{aligned} \mathcal{V}(\tilde{r}(k)) &= \mathcal{V}(\tilde{r}(k-1)) + \lambda_f(k) \left(d_y^2(k) - \frac{\tilde{h}^2(k)}{1 + \lambda_f(k)G(k-1)} \right) \\ &\leq \mathcal{V}(\tilde{r}(k-1)) + \lambda_f(k) \left(\check{d}^2 - \frac{\tilde{h}^2(k)}{1 + \lambda_f(k)G(k-1)} \right) \end{aligned}$$

Then it can be derived from (6.11f) that

$$\mathcal{V}(\tilde{r}(k)) \leq \mathcal{V}(\tilde{r}(k-1)) + \hat{\sigma}^2(k) - \hat{\sigma}^2(k-1).$$

In addition, due to the fact $r^* \in \mathcal{R}(k-1)$, we have $\mathcal{V}(\tilde{r}(k-1)) \leq \hat{\sigma}^2(k-1)$, implying $\mathcal{V}(\tilde{r}(k)) \leq \hat{\sigma}^2(k)$. Therefore, $r^* \in \mathcal{R}(k)$. Since $r^* \in \mathcal{R}(0)$, it can be concluded that $r^* \in \mathcal{R}(k), \forall k \geq 0$.

2): According to (6.11e) and (6.11f), it can be derived that

$$\hat{\sigma}^2(k) - \hat{\sigma}^2(k-1) = \lambda_f(k) \left(\check{d}^2 - \frac{\tilde{h}^2(k)}{1 + \lambda_f(k)G(k-1)} \right) \leq 0,$$

leading to $\mathcal{V}(\tilde{r}(k)) \leq \mathcal{V}(\tilde{r}(k-1))$. By (6.11a) one gets $\psi^{-1}(k) \geq \psi^{-1}(k-1)$. Therefore, it is easy to verify that $|\tilde{r}(k)|^2 \leq |\tilde{r}(k-1)|^2$. Since $|\tilde{r}(0)|$ is bounded, it can be concluded that $|\tilde{r}(k)|$ is bounded and non-increasing. \square

Remark 6.1. From Lemma 6.1, it can be seen that the proposed parameter estimation scheme presented in (6.11a) - (6.11f) ensures the estimation error to be bounded and non-increasing. This property is sufficient for guaranteeing closed-loop properties of the proposed adaptive MPC algorithm. Note that, as shown in [242, Theorem 3], if there exist two positive constants C_1 and C_2 such that the PE condition $0 < C_1 \leq \sum_{i=k}^{k+N} g^2(i) \leq C_2$ holds for the integer N and all $k \geq 0$, the developed estimator can theoretically provide better performance of convergence, i.e., $\lim_{k \rightarrow \infty} |\tilde{r}(k)| \leq 4Nd\check{d}^2/C_1$. As mentioned in Section 6.1, this can be achieved by imposing the PE condition as an extra constraint to the MPC optimization problem (6.9). However, this strategy may degrade the control performance because of the undesired system excitation arising from the excitation constraint. Therefore, the approach of introducing the PE condition is not considered in this work.

6.3.2 Adaptive MPC algorithm

In this chapter, we consider a standard stage cost function $\ell(\mathbf{p}_e(k), \mathbf{u}_e(k))$ and a terminal cost function $\ell_f(\mathbf{p}_e(k))$ with a quadratic form

$$\ell(\mathbf{p}_e(k), \mathbf{u}_e(k)) = \|\mathbf{p}_e(k)\|_{\mathbf{Q}}^2 + \|\mathbf{u}_e(k)\|_{\mathbf{R}}^2, \ell_f(\mathbf{p}_e(k)) = \|\mathbf{p}_e(k)\|_{\mathbf{P}}^2. \quad (6.12)$$

where \mathbf{P} , \mathbf{Q} and \mathbf{R} are positive definite matrices with appropriate dimensions. The terminal control law $\tau_f(\mathbf{p}_e(k), r(k))$ and invariant set Ω are designed as follows:

$$\tau_f(\mathbf{p}_e(k), r(k)) = \mathbf{D}_r(k)(\mathbf{K}\mathbf{p}_e(k) + \mathbf{D}_v(k)), \Omega = \{\mathbf{p}_e \in \mathbb{R}^2 : \|\mathbf{p}_e\|_{\mathbf{P}} \leq \varepsilon\}, \quad (6.13)$$

where $\mathbf{K} \in \mathbb{R}^{2 \times 2}$ and $\varepsilon > 0$ are the feedback gain matrix and constant, respectively; $\mathbf{D}_r(k) = \text{diag}(1, 1/r(k))$ and $\mathbf{D}_v(k) = [v_s(k) \cos \theta_e(k), v_s(k) \sin \theta_e(k)]^T$. The designable parameters should be chosen to satisfy the conditions in Assumption 6.3 as stated in Section 6.4. In the following, we demonstrate the parameterization of robustness constraint with

respect to the estimated upper bound of the estimation error.

According to the definition of the bounding set $\mathcal{R}(k)$, the estimation error $\tilde{r}(k)$ is bounded by $|\tilde{r}(k)| \leq \sigma(k)$ for all $r^* \in \mathcal{R}_0$, where $\sigma(k) = \sqrt{\psi(k)}\hat{\sigma}(k)$ is a scalar. From the proof of Lemma 6.1, we have $0 \leq \hat{\sigma}(k) \leq \hat{\sigma}(k-1)$ and $\psi^{-1}(k) \geq \psi^{-1}(k-1) > 0$. As a result, $\sigma(k) \leq \sigma(k-1) \leq \check{\sigma}$ for all $k \geq 1$. Define the following dynamic shrinkage rate $\alpha(k)$ associated with the upper bound of the estimation error $\sigma(k)$

$$\alpha(k) = \frac{e^{\xi_e \cdot (\check{\sigma} - \sigma(k))}}{\xi_\alpha}, \quad (6.14)$$

where $\xi_\alpha, \xi_e > 0$ are tuning factors. Motivated by [41, 180, 241], we design the robustness constraint as follows

$$\mathcal{X}(l|k) = \left\{ \mathbf{p}_e \in \mathbb{R}^2 : \|\mathbf{p}_e\| \leq \alpha(k)\varepsilon \frac{(T-l)\xi_x + l}{T} \right\}, l \in \mathbb{N}_{[0,T]} \quad (6.15)$$

where $\xi_x > 1$ is a constant. For the robust constraint (6.15), we have the following assumption.

Assumption 6.4. *Given the invariant set Ω , the robustness constraint satisfies the condition $\mathcal{X}(T|k) \subseteq \Omega$ for all $k \geq 0$.*

Assumption 6.4 indicates $\mathcal{X}(k+T|k) \subseteq \Omega$ for all $k \geq 0$, which can be satisfied by choosing suitable parameters ξ_α, ξ_e . Therefore, the terminal constraint Ω in the optimization problem (6.9) can be omitted. Consequently, the proposed adaptive MPC scheme is based on the following new optimization problem:

$$V_T(\mathbf{p}_e(k)) = \min_{\mathbf{u}_T(k)} J_T(\mathbf{p}_e(k), \mathbf{u}_T(k)) \quad (6.16a)$$

$$\text{s.t. } \bar{\boldsymbol{\eta}}(0|k) = \boldsymbol{\eta}(k), \bar{\mathbf{p}}_e(0|k) = \mathbf{p}_e(k) \quad (6.16a)$$

$$\bar{\boldsymbol{\eta}}(l+1|k) = f(\bar{\boldsymbol{\eta}}(l|k), \mathbf{u}(l|k), \hat{r}(k)), \quad (6.16b)$$

$$\bar{\mathbf{p}}_e(l|k) = f_p(\bar{\boldsymbol{\eta}}(l|k), \boldsymbol{\eta}_s(l+k)) \quad (6.16c)$$

$$\bar{\mathbf{p}}_e(l|k) \in \mathcal{X}(l|k), l \in \mathbb{N}_{[0,T]} \quad (6.16d)$$

$$\mathbf{u}(l|k) \in \mathcal{U}, l \in \mathbb{N}_{[0,T-1]}, \quad (6.16e)$$

where $\mathbf{p}_e(k) = f_p(\boldsymbol{\eta}(k), \boldsymbol{\eta}_s(k))$. By solving this optimization problem, the sequence of optimal control inputs $\mathbf{u}_T^*(k)$ are obtained. Then the control input to be implemented at

Algorithm 6.1 Proposed adaptive MPC algorithm

Input: Initial system state $\boldsymbol{\eta}(0)$; prediction horizon T ; sampling interval δ ; weighting matrices \mathbf{P} , \mathbf{Q} and \mathbf{R} ; robustness constraint parameters ε , ξ_α , ξ_e and ξ_x .

- 1: **for** $k = 0, 1, 2, 3, \dots$ **do**
 - 2: Measure the state $\boldsymbol{\eta}(k)$.
 - 3: **if** $k > 0$ **then**
 - 4: Update the estimation of the unknown parameter $\hat{r}(k)$ and the uncertainty set $\mathcal{R}(k)$ by using (6.11a)- (6.11f).
 - 5: **end if**
 - 6: Solve the optimization problem in (6.16) to obtain the optimal control input sequence $\mathbf{u}_T^*(k)$.
 - 7: Apply the control input $\mathbf{u}(k) = \mathbf{u}^*(k|k)$ to the system (6.6).
 - 8: **end for**
-

time instant k is $\mathbf{u}(k) = \mathbf{u}^*(k|k)$, leading to the following closed-loop system

$$\mathbf{p}_e(k+1) = f_e(\mathbf{p}_e(k), \mathbf{u}^*(k|k), r^*) - \Psi(\theta(k))\mathbf{d}_p(k), \quad (6.17)$$

where $\mathbf{d}_p(k) = [d_x(k), d_y(k)]^T$. The proposed adaptive MPC scheme is summarized in Algorithm 6.1.

Remark 6.2. *The robustness constraint approach is firstly proposed in [41], and is extended for the event-triggered robust MPC problem in [180]. This strategy has been applied in [239] to solve the AGV trajectory tracking problem. The authors in [241] improved the original robustness constraint to provide an enlarged initial feasible region. Inspired by these works, we develop a new robustness constraint which is parameterized by the estimated upper bound of the estimation error $\sigma(k)$. Compared with existing methods [41, 180, 239, 241] where a constant shrinkage rate $\bar{\alpha} = 1/\xi_\alpha$ is employed, the dynamic shrinkage rate (6.14) is employed in this work. According to Lemma 6.1 it can be ensured that $\alpha(k) \geq \bar{\alpha}$ for all $k \geq 0$. As a result, the size of $\mathcal{X}(l|k)$ is enlarged by introducing the dynamic shrinkage rate. Therefore the proposed robustness constraint (6.15) is less conservative compared with the existing methods [41, 180, 239, 241].*

6.4 Theoretical Analysis

Section 6.3 has described the proposed adaptive MPC scheme for the trajectory tracking problem presented in Section 6.2. In this section, the main theoretical results of this work are developed. We firstly provide the guideline for parameter selection such that Assump-

tion 6.3 holds. Then sufficient conditions on ensuring the recursive feasibility are presented in Theorem 6.1, and the stability results are summarized in Theorem 6.2.

6.4.1 Parameter selection

The following lemma provides some guidelines on how to design parameters \mathbf{P} , \mathbf{K} and ε such that Assumption 6.3 holds.

Lemma 6.2. *Suppose that Assumption 6.2 holds. Let $\mathbf{h}_f = [\xi_u \check{v} - \check{v}_s, \xi_u \underline{r} \check{\omega} - \check{v}_s, \xi_u \check{v} - \check{v}_s, \xi_u \underline{r} \check{\omega} - \check{v}_s]^\top$ where $\xi_u \in (0, 1]$, $\underline{r} = \min_{r \in \mathcal{R}} |r|$ and $\check{v}_s = \max_{k \geq 0} |v_s(k)|$. For the error dynamics in (6.8), if the following conditions hold*

$$\Omega \subseteq \mathcal{X}_U = \{\mathbf{p}_e \in \mathbb{R}^2 : \mathbf{H}\mathbf{K}\mathbf{p}_e \leq \mathbf{h}_f\}, \quad (6.18a)$$

$$(\mathbf{A}(\omega(k)) + \delta\mathbf{K})^\top \mathbf{P} (\mathbf{A}(\omega(k)) + \delta\mathbf{K}) - \mathbf{P} \prec -\bar{\mathbf{Q}}, \quad (6.18b)$$

for all $|\omega(k)| \leq \xi_u \check{\omega}$ and $\hat{r}(k) \in \mathcal{R}$ with $\bar{\mathbf{Q}} = \mathbf{Q} + \mathbf{K}^\top \mathbf{R} \mathbf{K}$, the terminal cost $\ell_f(\mathbf{p}_e(k))$, terminal controller $\tau_f(\mathbf{p}_e(k), \hat{r}(k))$ and invariant set Ω presented in (6.12) and (6.13) satisfy the conditions in Assumption 6.3.

Proof. To prove this lemma, we show the satisfaction of conditions (6.10a)-(6.10c) in the following.

Since $\mathbf{p}_e(k) \in \Omega \subseteq \mathcal{X}_U$, we have

$$\begin{aligned} |k_{11}x_e(k) + k_{12}y_e(k)| &\leq \xi_u \check{v} - \check{v}_s, \\ |k_{21}x_e(k) + k_{22}y_e(k)| &\leq \xi_u \underline{r} \check{\omega} - \check{v}_s. \end{aligned}$$

where k_{ij} denotes the (i, j) -th entry of the matrix \mathbf{K} . Then it can be derived from $|\hat{r}(k)| \geq \underline{r}$ and $|v_s(k)| \leq \check{v}_s$ that

$$\begin{aligned} &|k_{11}x_e(k) + k_{12}y_e(k) + v_s(k) \cos \theta_e(k)| \\ &\leq |k_{11}x_e(k) + k_{12}y_e(k)| + |v_s(k) \cos \theta_e(k)| \\ &\leq \xi_u \check{v} - \check{v}_s + |v_s(k)| \leq \xi_u \check{v} \leq \check{v} \end{aligned}$$

and

$$\begin{aligned} &|\frac{1}{\hat{r}(k)}(k_{21}x_e(k) + k_{22}y_e(k) + v_s(k) \sin \theta_e(k))| \\ &\leq |\frac{1}{\hat{r}(k)}||k_{11}x_e(k) + k_{12}y_e(k)| + |\frac{1}{\hat{r}(k)}||v_s(k) \sin \theta_e(k)| \\ &\leq |\frac{1}{\hat{r}(k)}|(\xi_u \underline{r} \check{\omega} - \check{v}_s) + |\frac{1}{\hat{r}(k)}||v_s(k) \sin \theta_e(k)| \\ &\leq \xi_u \check{\omega} \leq \check{\omega}. \end{aligned}$$

Therefore, it can be concluded that $\tau_f(\mathbf{p}_e(k), \hat{r}(k)) \in \mathcal{U}$ for all $\hat{r}(k) \in \mathcal{R}$.

In addition, substituting $\tau_f(\mathbf{p}_e(k), \hat{r}(k))$ into (6.8) yields

$$\mathbf{p}_e(k+1) = (\mathbf{A}(\omega(k)) + \delta\mathbf{K})\mathbf{p}_e(k).$$

where $\omega(k) = \frac{1}{\hat{r}(k)}(k_{21}x_e(k) + k_{22}y_e(k) + v_s(k) \sin \theta_e(k))$. Based on (6.18a), it can be derived that $\tau_f(\mathbf{p}_e(k), \hat{r}(k)) \in \xi_u \mathcal{U}$, implying $|\omega(k)| \leq \xi_u \tilde{\omega}$. Since \mathbf{P} , \mathbf{Q} and \mathbf{R} are positive definite, according to (6.18), one gets

$$\|\mathbf{p}_e(k+1)\|_{\mathbf{P}}^2 = \mathbf{p}_e^T(k)(\mathbf{A}(\omega(k)) + \delta\mathbf{K})^T \mathbf{P}(\mathbf{A}(\omega(k)) + \delta\mathbf{K})\mathbf{p}_e(k) \leq \|\mathbf{p}_e(k)\|_{\mathbf{P}}^2 \leq \varepsilon,$$

leading to $\mathbf{p}_e(k+1) \in \Omega$. Therefore, the condition in (6.10c) is satisfied.

Consider the terminal cost function $\ell_f(\mathbf{p}_e(k))$ and input $\mathbf{u}_e(k) = \tau_f(\mathbf{p}_e(k), \hat{r}(k))$, we have

$$\begin{aligned} & \ell_f(\mathbf{p}_e(k+1)) - \ell_f(\mathbf{p}_e(k)) + \ell(\mathbf{p}_e(k), \mathbf{u}_e(k)) \\ &= \|\mathbf{p}_e(k+1)\|_{\mathbf{P}}^2 - \|\mathbf{p}_e(k)\|_{\mathbf{P}}^2 + \|\mathbf{p}_e(k)\|_{\mathbf{Q}}^2 + \|\mathbf{u}_e(k)\|_{\mathbf{R}}^2 \\ &= \mathbf{p}_e(k)^T(\mathbf{A}(\omega(k)) + \delta\mathbf{K})^T \mathbf{P}(\mathbf{A}(\omega(k)) + \delta\mathbf{K}) - \mathbf{P})\mathbf{p}_e(k) + \mathbf{p}_e(k)^T(\mathbf{Q} + \mathbf{K}^T \mathbf{R} \mathbf{K})\mathbf{p}_e(k). \end{aligned}$$

Then recalling (6.18b) yields

$$\ell_f(\mathbf{p}_e(k+1)) - \ell_f(\mathbf{p}_e(k)) + \ell(\mathbf{p}_e(k), \tau_f(\mathbf{p}_e(k), \hat{r}(k))) \leq 0,$$

which completes the proof. \square

6.4.2 Recursive feasibility

Given two position $\boldsymbol{\eta}_1, \boldsymbol{\eta}_2$ and $\mathbf{u} \in \mathcal{U}$, by recalling the AGV kinematics in (6.2), it can be derived that

$$\begin{aligned} & \|f_h(\boldsymbol{\eta}_1, \mathbf{u}, r_1) - f_h(\boldsymbol{\eta}_2, \mathbf{u}, r_2)\| \\ &= \|f_h(\boldsymbol{\eta}_1, \mathbf{u}, r_1) - f_h(\boldsymbol{\eta}_2, \mathbf{u}, r_1) + f_h(\boldsymbol{\eta}_2, \mathbf{u}, r_1) - f_h(\boldsymbol{\eta}_2, \mathbf{u}, r_2)\| \\ &\leq \left\| \begin{bmatrix} v(\cos \theta_1 - \cos \theta_2) - \omega r_1 (\sin \theta_1 - \sin \theta_2) \\ v(\sin \theta_1 - \sin \theta_2) - \omega r_1 (\cos \theta_1 - \cos \theta_2) \\ 0 \end{bmatrix} \right\| + \left\| \begin{bmatrix} \omega \sin \theta_2 (r_2 - r_1) \\ \omega \cos \theta_2 (r_2 - r_1) \\ 0 \end{bmatrix} \right\| \\ &= \sqrt{(4v^2 + 4\omega^2 r_1^2) \sin^2\left(\frac{\theta_1 - \theta_2}{2}\right) + |\omega(r_2 - r_1)|} \end{aligned}$$

$$\begin{aligned}
&\leq \sqrt{(v^2 + \omega^2 r_1^2)(\theta_1 - \theta_2)^2 + |\omega(r_2 - r_1)|} \\
&\leq \sqrt{\check{v}^2 + \check{\omega}^2 r_1^2} \|\boldsymbol{\eta}_1 - \boldsymbol{\eta}_2\| + \check{\omega} |r_2 - r_1|.
\end{aligned}$$

In addition,

$$\begin{aligned}
\bar{\boldsymbol{\eta}}^*(l+1|k) &= \delta f_h(\bar{\boldsymbol{\eta}}^*(l|k), \mathbf{u}^*(l|k), \hat{r}(k)) + \bar{\boldsymbol{\eta}}^*(l|k) \\
&= \sum_{i=k}^l \delta f_h(\bar{\boldsymbol{\eta}}^*(i|k), \mathbf{u}^*(i|k), \hat{r}(k)) + \bar{\boldsymbol{\eta}}^*(k|k).
\end{aligned}$$

Then for $l \in \mathbb{N}_{[k+1, k+T-1]}$, the deviation between two predicted states, being predicted at two successive time instants, is evaluated in the following:

$$\begin{aligned}
&\|\bar{\boldsymbol{\eta}}(l+1|k+1) - \bar{\boldsymbol{\eta}}^*(l+1|k)\| \\
&= \left\| \sum_{i=0}^l \delta f_h(\bar{\boldsymbol{\eta}}(i|k+1), \mathbf{u}^*(i+1|k), \hat{r}(k+1)) - \sum_{i=0}^l \delta f_h(\bar{\boldsymbol{\eta}}^*(i+1|k), \mathbf{u}^*(i+1|k), \hat{r}(k)) \right. \\
&\quad \left. - \bar{\boldsymbol{\eta}}^*(1|k) + \bar{\boldsymbol{\eta}}(0|k+1) \right\| \\
&\leq \sum_{i=0}^l \delta \|f_h(\bar{\boldsymbol{\eta}}(i|k+1), \mathbf{u}^*(i+1|k), \hat{r}(k+1)) - f_h(\bar{\boldsymbol{\eta}}^*(i+1|k), \mathbf{u}^*(i+1|k), \hat{r}(k))\| \\
&\quad + \|\bar{\boldsymbol{\eta}}(0|k+1) - \bar{\boldsymbol{\eta}}^*(1|k)\| \\
&\leq \delta \sqrt{\check{v}^2 + \check{\omega}^2 \hat{r}^2(k)} \sum_{i=0}^l \|\bar{\boldsymbol{\eta}}(i|k+1) - \bar{\boldsymbol{\eta}}^*(i+1|k)\| + (l-1)\check{\omega}|\hat{r}(k+1) - \hat{r}(k)| + \Delta(k),
\end{aligned}$$

where $\Delta(k) = \delta \|\omega(k)\| \sigma(k) + \check{d}$. Since $\hat{r}(k+1) \in \mathcal{R}(k)$, we have $|\hat{r}(k+1) - \hat{r}(k)| \leq \sigma(k) \leq \check{\sigma}$ and $\hat{k} \leq \check{r}$, implying

$$\|\bar{\boldsymbol{\eta}}(l+1|k+1) - \bar{\boldsymbol{\eta}}^*(l+1|k)\| \leq \check{L} \sum_{i=k+1}^l \|\bar{\boldsymbol{\eta}}(i|k+1) - \bar{\boldsymbol{\eta}}^*(i|k)\| + \check{\Delta},$$

where $\check{L} = \delta \sqrt{2(\check{v}^2 + \check{\omega}^2 \check{r}^2)}$ and $\check{\Delta} = T\check{\omega}\check{\sigma} + \delta\check{\omega}\check{\sigma} + \check{d}$. For all $l \in \mathbb{N}_{[1, T]}$, we derive the following upper bound for deviation between two predicted states based on the Gronwall–Bellman–Ou–Iang-type inequality [243, Theorem 2.1]

$$\|\bar{\boldsymbol{\eta}}(l|k+1) - \bar{\boldsymbol{\eta}}^*(l+1|k)\| \leq \check{\Delta} e^{(l-1)\check{L}}, \forall l \in \mathbb{N}_{[1, T]}. \quad (6.19)$$

The following theorem shows conditions under which the recursive feasibility of the formulated optimization problem can be guaranteed.

Theorem 6.1. *For the system (6.6), suppose that Assumptions 6.1–6.3 and 6.4 hold, and there exists a feasible solution for the MPC problem at time instant $k = 0$. Then the proposed MPC scheme, presented in Algorithm 6.1, is recursively feasible if the following conditions hold*

$$\xi_\alpha T \check{\Delta} e^{\check{L}(T-1)} \leq \varepsilon(\xi_x - 1), \quad (6.20a)$$

$$\sqrt{\lambda_{\max}(\mathbf{P})} e^{\xi_e \check{\sigma}} (T + \xi_x - 1) \leq T \xi_\alpha, \quad (6.20b)$$

$$\xi_\alpha \sqrt{\lambda_{\max}(\mathbf{P} - \bar{\mathbf{Q}})} \leq \sqrt{\lambda_{\min}(\mathbf{P})}. \quad (6.20c)$$

Proof. Let $\mathbf{u}_T^*(k) = \text{col}(\mathbf{u}^*(0|k), \mathbf{u}^*(1|k), \dots, \mathbf{u}^*(T-1|k))$ denote the optimal solution at time k . Correspondingly, under the optimal control input sequence $\mathbf{u}_T^*(k)$, the sequence of nominal states $\{\bar{\boldsymbol{\eta}}^*(l|k)\}_{l=0}^T$ is predicted by using the system model in (6.7) with online estimated parameter $\hat{r}(k)$ and $\bar{\boldsymbol{\eta}}^*(0|k) = \boldsymbol{\eta}(k)$. Similarly, we can obtain the corresponding nominal error state sequence $\{\bar{\mathbf{p}}_e^*(l|k)\}_{l=0}^T$. Then we construct a candidate solution at time $k+1$ as follows: $\bar{\mathbf{u}}_T(k+1) = \text{col}(\mathbf{u}^*(1|k), \mathbf{u}^*(2|k), \dots, \mathbf{u}^*(T-1|k), \tau_f(\bar{\mathbf{p}}_e(T|k+1), \hat{r}(k+1)))$. Based on the control input sequence $\bar{\mathbf{u}}_T(k+1)$, true state $\boldsymbol{\eta}(k+1)$ and parameter estimate $\hat{r}(k+1)$, the corresponding nominal system state $\bar{\boldsymbol{\eta}}(l|k+1)$, $l \in \mathbb{N}_{[0,T]}$ and error state $\bar{\mathbf{p}}_e(l|k+1)$ at time $k+1$ can be computed, where $\bar{\boldsymbol{\eta}}(0|k+1) = \boldsymbol{\eta}(k+1)$. To prove this theorem, we need to show that $\bar{\mathbf{u}}_T(k+1)$ is a feasible solution for the MPC problem in (6.16).

First, we show that the constraint (6.16d) is satisfied. It can be seen from (6.4) that $\|\bar{\mathbf{p}}_e(l|k+1) - \bar{\mathbf{p}}_e^*(l|k)\| \leq \|\bar{\boldsymbol{\eta}}(l|k+1) - \bar{\boldsymbol{\eta}}^*(l|k)\|$. Then for $\bar{\mathbf{p}}_e^*(l|k) \in \mathcal{X}(l|k)$, recalling (6.19)

$$\|\bar{\mathbf{p}}_e(l|k+1)\| \leq \alpha(k) \varepsilon \frac{\xi_x(T-l) + l}{T} + \check{\Delta} e^{\check{L}(l-1)}. \quad (6.21)$$

The above equation describes the upper bound of $\|\bar{\mathbf{p}}_e(l|k+1)\|$. In addition, it can be seen from (6.15) that, if $\bar{\mathbf{p}}_e(l|k+1) \in \mathcal{X}(l|k+1)$, $\bar{\mathbf{p}}_e(l|k+1)$ must be bounded by

$$\|\bar{\mathbf{p}}_e(l|k+1)\| \leq \alpha(k+1) \varepsilon \frac{\xi_x \cdot (T-l+1) + l - 1}{T}.$$

Therefore, the satisfaction of the constraint (6.16d) can be proved by showing that

$$\alpha(k+1) \varepsilon \frac{\xi_x \cdot (T-l+1) + l - 1}{T} \geq \alpha(k) \varepsilon \frac{\xi_x(T-l) + l}{T} + \check{\Delta} e^{\check{L}(l-1)}.$$

From $\alpha(k+1) \geq \alpha(k)$ we have

$$\begin{aligned} & \alpha(k+1)\varepsilon \frac{\xi_x(T-l+1) + l - 1}{T} - \alpha(k)\varepsilon \frac{\xi_x(T-l) + l}{T} \\ & \geq \alpha(k)\varepsilon \left(\frac{\xi_x(T-l+1) + l - 1}{T} + \frac{\xi_x(T-l) + l}{T} \right) \\ & = \alpha(k)\varepsilon \frac{\xi_x - 1}{T}. \end{aligned}$$

Using (6.14) and (6.20a) yields

$$\alpha(k)\varepsilon \frac{\xi_x - 1}{T} \geq \frac{\varepsilon(\xi_x - 1)}{\xi_\alpha T} \geq \check{\Delta} e^{\check{L}(T-1)}.$$

Consequently, we have

$$\begin{aligned} \|\bar{\mathbf{p}}_e(l|k+1)\| & \leq \alpha(k)\varepsilon \frac{\xi_x(T-l) + l}{T} + \check{\Delta} e^{\check{L}(l-1)}, \\ & \leq \alpha(k+1)\varepsilon \frac{\xi_x(T-l+1) + l - 1}{T}, \end{aligned}$$

implying that $\bar{\mathbf{p}}_e(l|k+1) \in \mathcal{X}(l|k+1)$ for $l \in \mathbb{N}_{[0, T-1]}$.

The next step is to show $\bar{\mathbf{p}}_e(T|k+1) \in \mathcal{X}(T|k+1)$. As shown in (6.21), $\|\bar{\mathbf{p}}_e(T-1|k+1)\| \leq \alpha(k)\varepsilon + \check{\Delta} e^{\check{L}(T-1)}$. Since $\alpha(k) \leq \frac{\varepsilon \xi_\alpha}{\xi_\alpha}$ and $\check{\Delta} e^{\check{L}(T-1)} \leq \frac{\varepsilon(\xi_x - 1)}{\xi_\alpha T}$, it can be derived from (6.20b) that

$$\|\bar{\mathbf{p}}_e(T-1|k+1)\| \leq \frac{\varepsilon}{\sqrt{\lambda_{\max}(\mathbf{P})}}.$$

As a result,

$$\|\bar{\mathbf{p}}_e(T-1|k+1)\|_{\mathbf{P}} \leq \sqrt{\lambda_{\max}(\mathbf{P})} \|\bar{\mathbf{p}}_e(T-1|k+1)\| \leq \varepsilon.$$

Therefore, we have $\bar{\mathbf{p}}_e(T-1|k+1) \in \Omega$. Moreover, Lemma 6.2 shows that

$$\begin{aligned} \|\bar{\mathbf{p}}_e(T|k+1)\|_{\mathbf{P}}^2 & \leq \bar{\mathbf{p}}_e^T(T-1|k+1)(\mathbf{P} - \bar{\mathbf{Q}})\bar{\mathbf{p}}_e^T(T-1|k+1) \\ & \leq \lambda_{\max}(\mathbf{P} - \bar{\mathbf{Q}}) \|\bar{\mathbf{p}}_e(T-1|k+1)\|^2 \end{aligned}$$

Then by (6.20c) one gets

$$\|\bar{\mathbf{p}}_e(T|k+1)\| \leq \sqrt{\frac{\lambda_{\max}(\mathbf{P} - \bar{\mathbf{Q}})}{\lambda_{\max}(\mathbf{P})}} \|\bar{\mathbf{p}}_e(T-1|k+1)\|$$

$$\leq \sqrt{\frac{\lambda_{\max}(\mathbf{P} - \bar{\mathbf{Q}})}{\lambda_{\max}(\mathbf{P})}} \varepsilon \leq \varepsilon / \xi_\alpha \leq \alpha(k) \varepsilon.$$

Hence, we arrive at $\bar{\mathbf{p}}_e(T|k+1) \in \mathcal{X}(T|k+1)$, implying that the constraint (6.16d) is satisfied.

The remainder of this proof is to show the satisfaction of constraint (6.16e). Since $\bar{\mathbf{p}}_e(T-1|k+1) \in \Omega$, $\tau_f(\bar{\mathbf{p}}_e(T-1|k+1), \hat{r}(k+1)) \in \mathcal{U}$ by Lemma 6.2. In addition, $\mathbf{u}^*(l|k) \in \mathcal{U}$ for all $l \in \mathbb{N}_{[0, T-1]}$. Therefore, it can be concluded that $\bar{\mathbf{u}}_T(k+1)$ is a feasible solution at time $k+1$, which proves Theorem 6.1. \square

6.4.3 Closed-loop stability

The following theorem states the closed-loop behaviors of the error dynamics in (6.17) under the proposed adaptive MPC scheme presented in Algorithm 6.1.

Theorem 6.2. *For the system (6.6), suppose that Assumptions 6.1–6.3 and 6.4 hold, and conditions in Theorem 6.1 are satisfied. Then the closed-loop system (6.17) is ISS.*

Proof. To prove the closed-loop stability, we need to show that the optimal value function $V_T(\mathbf{p}_e(k))$ is an ISS-Lyapunov function.

By (6.16) it can be seen that $V_T(\mathbf{p}_e(k)) \geq \|\mathbf{p}_e(k)\|_{\mathbf{Q}}^2 \geq \beta_1(\|\mathbf{p}_e(k)\|)$ with $\beta_1(\|\mathbf{p}_e(k)\|) = \lambda_{\min}(\mathbf{Q})\|\mathbf{p}_e(k)\|^2$. The next step is to find the function $\beta_2(\|\mathbf{p}_e(k)\|)$.

Let the optimal value function $V_j(\mathbf{p}_e(k))$, $j \in \mathbb{N}_{[0, T-1]}$ be defined by (6.16) with T replaced by j and $V_0(\mathbf{p}_e(k)) = \ell_f(\mathbf{p}_e(k))$. For all $\mathbf{p}_e(k) \in \Omega$, we have

$$\begin{aligned} V_{j+1}(\mathbf{p}_e(k)) - V_j(\mathbf{p}_e(k)) &\leq \ell_f(\bar{\mathbf{p}}_e^*(j+1|k)) - \ell_f(\bar{\mathbf{p}}_e^*(j|k)) + \ell(\bar{\mathbf{p}}_e^*(j|k), \tau_f(\bar{\mathbf{p}}_e^*(j|k), \hat{r}(k))) \\ &\leq 0, \end{aligned}$$

implying that

$$V_T(\mathbf{p}_e(k)) \leq V_0(\mathbf{p}_e(k)) = \ell_f(\mathbf{p}_e(k)) \leq \lambda_{\max}(\mathbf{P})\|\mathbf{p}_e(k)\|^2.$$

For $\mathbf{p}_e(k) \notin \Omega$, we firstly need to show that $V_T(\mathbf{p}_e(k))$ is bounded for all $k \geq 0$. Since $\bar{\boldsymbol{\eta}}^*(0|k) = \boldsymbol{\eta}(k)$, according to (6.19), one gets

$$\|\bar{\boldsymbol{\eta}}^*(k|k)\| \leq \|\bar{\boldsymbol{\eta}}^*(k|k-1)\| + \Delta(k) \leq \alpha(k-1) \frac{\xi_x(T-1) + 1}{T} + \check{\Delta}.$$

In addition, Assumption 6.2 shows that $\boldsymbol{\eta}_s(k)$ and $\mathbf{u}_s(k)$ are bounded for all $k \geq 0$. Therefore, $\bar{\mathbf{p}}_e(l|k)$ is bounded for all $k \geq 0$ and $l \in \mathbb{N}_{[0,T]}$. As a result, there exists a constant $\check{V} > 0$ such that $V_T(\mathbf{p}_e(k)) \leq \check{V}$ for all $\mathbf{p}_e(k) \notin \Omega$. Let $\mathcal{B}_{\xi_r} = \{\mathbf{p}_e \in \mathbb{R}^2 : \|\mathbf{p}_e\|^2 \leq \xi_r\}$ where $\xi_r > 0$ is a constant. Then for $\mathbf{p}_e(k) \notin \mathcal{B}_{\xi_r}$, we have $\|\mathbf{p}_e(k)\|^2 \geq \xi_r$ and $V_T(\mathbf{p}_e(k)) \leq \check{V}$, leading to $V_T(\mathbf{p}_e(k)) \leq \frac{\check{V}}{\xi_r} \|\mathbf{p}_e(k)\|^2$. By setting

$$\beta_2(\|\mathbf{p}_e(k)\|) = \max(\lambda_{\max}(\mathbf{P}), \frac{\check{V}}{\xi_r}) \|\mathbf{p}_e(k)\|^2,$$

one gets $V_T(\mathbf{p}_e(k)) \leq \beta_2(\|\mathbf{p}_e(k)\|)$ for all $k \geq 0$.

The next step is to find the difference between $V_T(\mathbf{p}_e(k))$ and $V_T(\mathbf{p}_e(k+1))$. Recalling the optimization problem in (6.16), one gets $V_T(\mathbf{p}_e(k+1)) - V_T(\mathbf{p}_e(k)) \leq \Lambda_1 + \Lambda_2 + \Lambda_3$, where

$$\begin{aligned} V_T(\mathbf{p}_e(k+1)) - V_T(\mathbf{p}_e(k)) &\leq \Lambda_1 + \Lambda_2 + \Lambda_3 \\ \Lambda_1 &= -\ell(\bar{\mathbf{p}}_e^*(0|k), \mathbf{u}^*(0|k)), \\ \Lambda_2 &= \sum_{l=0}^{T-1} (\ell(\bar{\mathbf{p}}_e(l|k+1), \mathbf{u}^*(l+1|k)) - \ell(\bar{\mathbf{p}}_e^*(l+1|k), \mathbf{u}^*(l+1|k))), \\ \Lambda_3 &= \ell(\bar{\mathbf{p}}_e(T-1|k+1), \tau_f(\bar{\mathbf{p}}_e(T-1|k+1), \hat{r}(k+1))) \\ &\quad + \ell_f(\bar{\mathbf{p}}_e(T|k+1)) - \ell_f(\bar{\mathbf{p}}_e^*(T|k)) \end{aligned}$$

The upper bound of $\Lambda_i, i = 1, 2, 3$ is derived in the following. Apparently,

$$\Lambda_1 \leq -\|\bar{\mathbf{p}}_e^*(0|k)\|_{\mathbf{Q}}^2 = -\|\mathbf{p}_e(k)\|_{\mathbf{Q}}^2 \leq \beta_3(\|\mathbf{p}_e(k)\|), \quad (6.22)$$

where $\beta_3(\|\mathbf{p}_e(k)\|) = \lambda_{\min}(\mathbf{Q})\|\mathbf{p}_e(k)\|^2$. In addition, using the triangle inequality leads to

$$\begin{aligned} \Lambda_2 &= \sum_{l=0}^{T-1} \|\bar{\mathbf{p}}_e(l|k+1)\|_{\mathbf{Q}}^2 - \|\bar{\mathbf{p}}_e^*(l+1|k)\|_{\mathbf{Q}}^2 \\ &\leq \sum_{l=0}^{T-1} \lambda_{\max}(\mathbf{Q}) (\|\bar{\mathbf{p}}_e^*(l|k+1)\| + \|\bar{\mathbf{p}}_e^*(l+1|k)\|) \cdot \|\bar{\mathbf{p}}_e(l|k+1) - \bar{\mathbf{p}}_e^*(l+1|k)\|. \end{aligned}$$

Since $\bar{\mathbf{p}}_e(l|k+1) \in \mathcal{X}(l|k+1)$ and $\bar{\mathbf{p}}_e^*(l|k) \in \mathcal{X}(l|k)$, substituting $\|\bar{\mathbf{p}}_e(l|k+1) - \bar{\mathbf{p}}_e^*(l|k)\| \leq$

$\check{\Delta}e^{\check{L}(l-1)}$ into the above inequality yields

$$\Lambda_2 \leq \sum_{l=0}^{T-1} \lambda_{\max}(\mathbf{Q}) \check{\Delta} \phi(l), \quad \phi(l) = \frac{e^{\xi_e \check{\sigma} + \check{L}(l-1)}}{T \xi_\alpha} (2(T-l)\xi_x + 2l + 1 - \xi_x).$$

In addition, because of $\bar{\mathbf{p}}_e(T-1|k+1) \in \Omega$, it follows from Assumption 6.3 that

$$\begin{aligned} \Lambda_3 &\leq \ell_f(\bar{\mathbf{p}}_e(T-1|k+1)) - \ell_f(\bar{\mathbf{p}}_e^*(T|k)) \\ &= \|\bar{\mathbf{p}}_e(T-1|k+1)\|_{\mathbf{P}}^2 - \|\bar{\mathbf{p}}_e^*(T|k)\|_{\mathbf{P}}^2. \end{aligned}$$

Analogously, the upper bound of Λ_3 can be derived as follows

$$\Lambda_3 \leq \lambda_{\max}(\mathbf{P}) \check{\Delta} \phi(T). \quad (6.23)$$

Then recalling (6.22)-(6.23) leads to

$$V_T(\mathbf{p}_e(k+1)) - V_T(\mathbf{p}_e(k)) \leq \beta_3(\|\mathbf{p}_e(k)\|) + \lambda_w,$$

where $\lambda_w = \check{\Delta}(\sum_{l=0}^{T-1} \lambda_{\max}(\mathbf{Q})\phi(l) + \lambda_{\max}(\mathbf{P})\phi(T))$. Therefore, it can be concluded that the optimal value function $V_T(\mathbf{p}_e(k))$ is an ISS-Lyapunov function, implying that the closed-loop system is ISS by [200, Theorem 1]. \square

Remark 6.3. *Theorems 6.1 and 6.2 presents the sufficient conditions for the recursive feasibility and closed-loop stability, which mainly depends on the upper bounds of the parametric uncertainty and additive disturbances. But the conditions (6.20a) and (6.20b) may result in a conservative bound on the admissible uncertainties. A potential solution to reduce the conservatism of the proposed method is to update the invariant set Ω with respect to the new estimation. Since the proposed estimator guarantees the estimation error to be non-increasing, it is possible to update the invariant set Ω such that the size of Ω is non-decreasing. But considering a time-varying invariant set will significantly increase the complexity of the proposed method, which may render the proposed method impractical. Therefore, the fixed invariant set is considered in this work. How to efficiently update the invariant set associated with the parameter estimation is a potential direction for our further research.*

6.5 Numerical Example

In this section, a numerical example is illustrated to validate the proposed adaptive MPC algorithm. The linear and angular velocities of the AGV are bounded by $\check{v} = 0.6$ m/s and $\check{\omega} = \pi/8$ rad/s. The objective is to track a lemniscate reference trajectory described by $x_s(t) = \sin(0.05t)$, $y_s(t) = \sin(0.1t)$, $\theta_s = \text{atan2}(\dot{x}_s(t), \dot{y}_s(t))$, where $\text{atan2}(\cdot, \cdot)$ is the four-quadrant inverse tangent function. The sampling interval is $\delta = 0.1$ s. In addition, $\mathcal{D} = \{d \in \mathbb{R}^3 : \|d\| \leq 0.004\}$ and $\mathcal{R}_0 = \{r \in \mathbb{R} : |r - \bar{r}_0| \leq 0.25\}$ with $\bar{r}_0 = 0.7$ m. The true value of the unknown parameter is $r^* = 0.47$ m. For the proposed estimator, $\hat{r}(0) = \bar{r}_0$ and $\hat{\sigma}(0) = 0.25$ m. For the proposed adaptive MPC scheme, the prediction horizon is chosen as $T = 5$. Set the weighting matrices as $Q = 0.02\mathbf{I}_2$ and $R = 0.1\mathbf{I}_2$. Based on Lemma 6.2, we compute the following parameters

$$\mathbf{P} = \begin{bmatrix} 0.4656 & 0 \\ 0 & 0.4656 \end{bmatrix}, \mathbf{K} = \begin{bmatrix} -0.4449 & 0 \\ 0 & -0.4449 \end{bmatrix}, \xi_u = 1, \varepsilon = 0.0996.$$

Then according to feasibility conditions (6.20a) - (6.20c) in Theorem 6.1, the tuning parameters for the robustness constraint are given as follows: $\xi_x = 2.0823$, $\xi_e = 0.0346$, $\xi_\alpha = 1.0457$.

In order to demonstrate the efficacy of the proposed method, we employ the robust MPC (RMPC) scheme, which can be regarded as a special case of the proposed adaptive MPC scheme, if not incorporating the parameter estimation, for the purpose of comparison. The results obtained by the proposed method are labeled as ALMPC. Starting from the point $\boldsymbol{\eta}(0) = [0.2, -0.2, \pi/2]^T$, the trajectories of the AGV's head point $\mathbf{p}_h(k)$ are shown in Figure 6.2, where the blue solid and red dash-dot lines denote the results by using the proposed adaptive MPC method and robust MPC method, respectively. Figure 6.3 shows the time evolution of the control inputs. It can be seen that the input constraint is satisfied by using both the adaptive MPC method and the robust MPC method. The comparison of tracking errors $\mathbf{p}_e(k)$ and input errors $\mathbf{u}_e(k)$ by using two methods is shown in Figure 6.4, and the trajectories of tracking errors $\mathbf{p}_e(k)$ are illustrated in Figure 6.5. As shown in these figures, it can be seen that the proposed adaptive MPC scheme can regulate the tracking error within a small region around the origin, which verifies our theoretical results. The results of parameter estimation are demonstrated in Figure 6.6, showing that the convergence of parameter estimates $\hat{r}(k)$ is achieved, while the estimated uncertainty set $\mathcal{R}(k)$ shrinks to a fixed set.

To further demonstrate the efficacy of the proposed method, we introduce the following

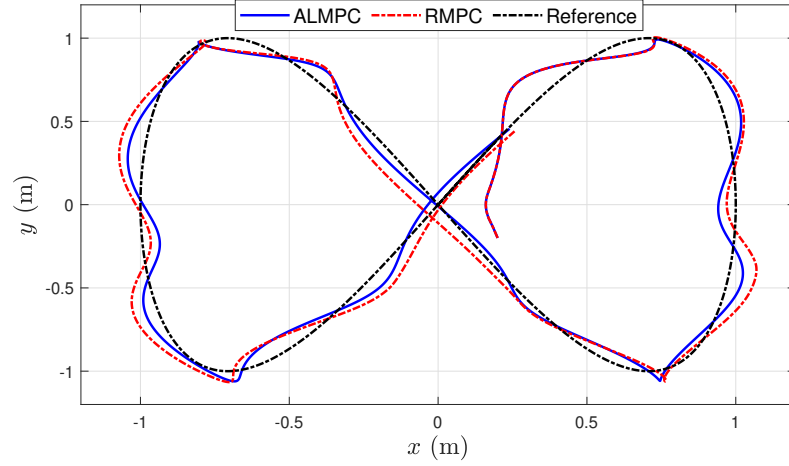


Figure 6.2: Trajectories of the AGV's head point $\mathbf{p}_h(k)$.

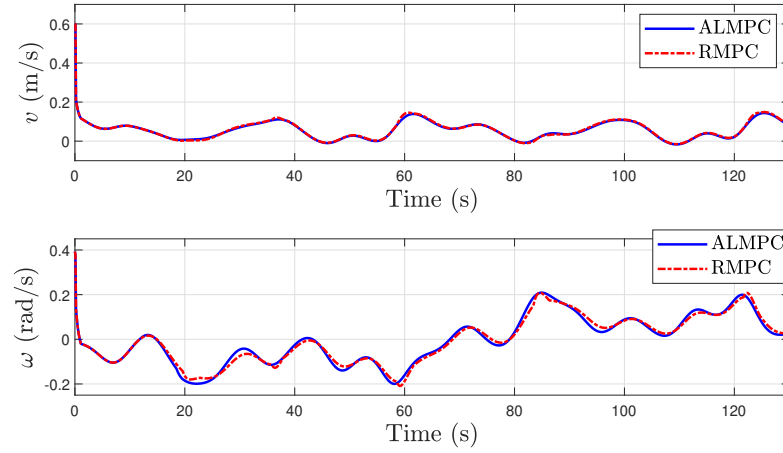


Figure 6.3: Control inputs $\mathbf{u}(k)$.

performance indexes:

$$J_p = \sum_{i=0}^M (\|\mathbf{p}_e(i)\|_{\mathbf{Q}}^2 + \|\mathbf{u}_e(i)\|_R^2), \quad \bar{V} = \sum_{i=0}^M V_T(V_T(\mathbf{p}_e(i))),$$

$$\text{MSE}_x = \left(\sum_{i=0}^M \|\mathbf{p}_e(i)\|^2 \right) / M, \quad \text{MSE}_u = \left(\sum_{i=0}^M \|\mathbf{u}_e(i)\|^2 \right) / M,$$

where M is the number of simulation steps. The comparison of system performance is illustrated in Table 6.1. Compared with the robust MPC method, the proposed adaptive MPC approach can reduce the cost and position tracking error by approximately 32.18%

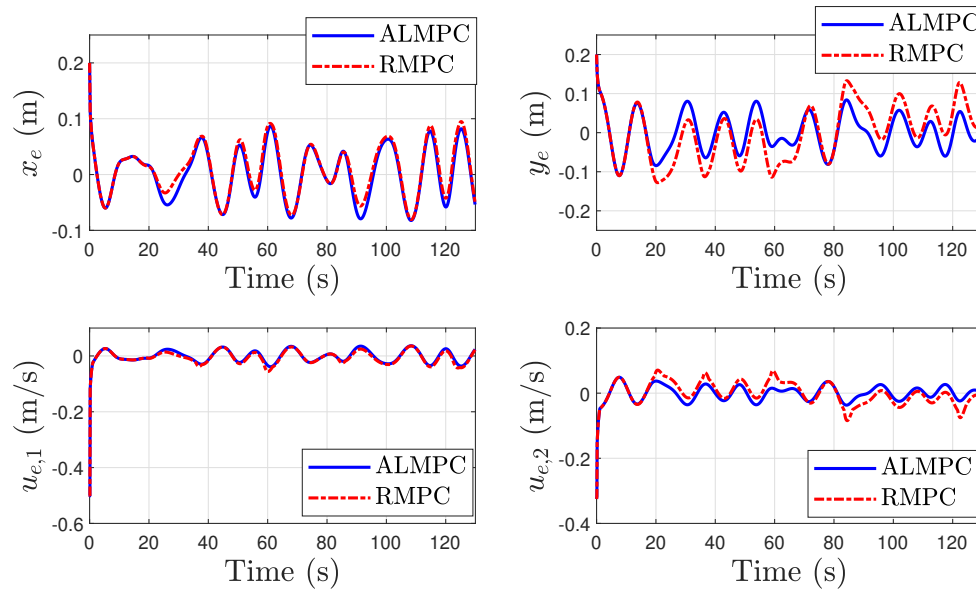


Figure 6.4: Tracking errors $\mathbf{p}_e(k)$ and input errors $\mathbf{u}_e(k)$.

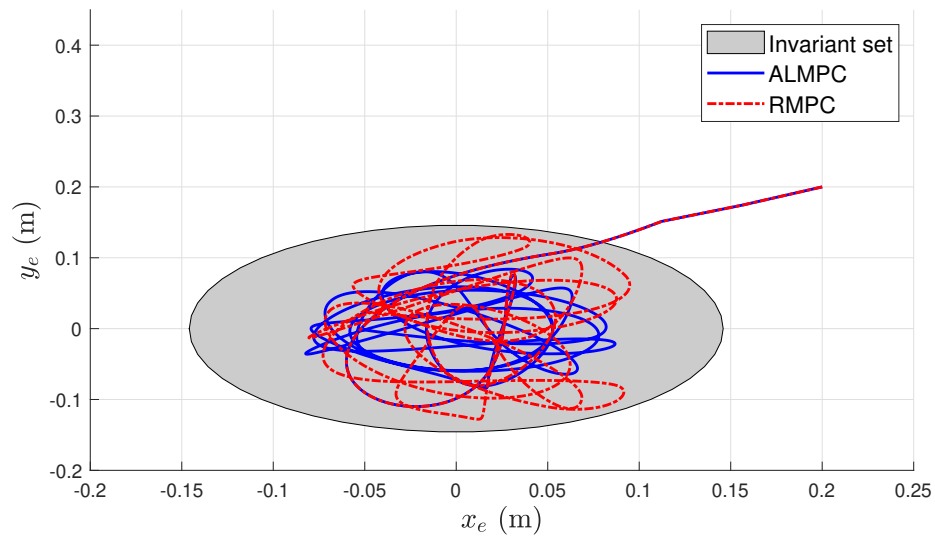


Figure 6.5: Trajectories of the tracking errors $\mathbf{p}_e(k)$.

and 34.5%, respectively. To summarize, the presented numerical example has demonstrated that the proposed adaptive MPC scheme can regulate the tracking error within a small region, while reducing the conservatism compared to the robust MPC scheme.

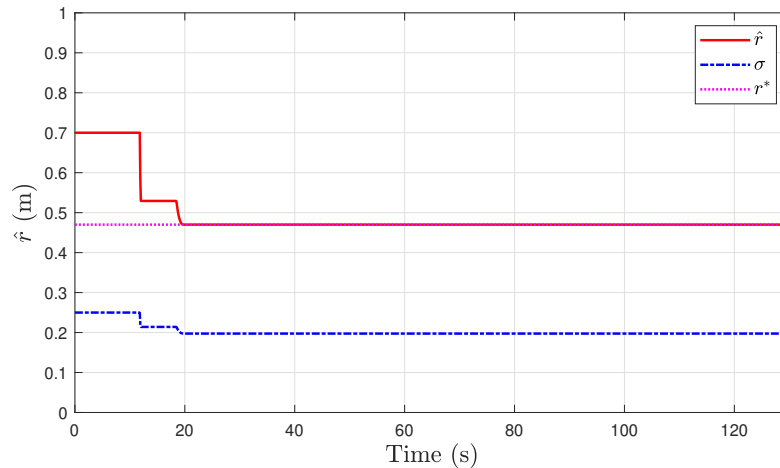


Figure 6.6: Parameter estimation $\hat{r}(k)$ and $\sigma(k)$.

Table 6.1: The comparison of system performance.

	J_p	MSE_x	MSE_u	\bar{V}
Adaptive MPC	0.3066	0.0045	0.0015	2.86
Robust MPC	0.4520	0.0068	0.0021	4.29

6.6 Conclusion

In this work, we have developed a novel adaptive MPC algorithm for the trajectory tracking of input constrained AGV systems subject to parametric uncertainties and additive disturbances. Based on the RLS technique, we first developed the online set-membership based parameter estimator being used to improve the prediction accuracy in MPC, where the estimation error was ensured to be non-increasing. This estimator also provided the sequence of bounding sets for the unknown parameter. These sets were employed to design the robustness constraint for handling uncertainties. The shape of the designed robustness constraint was computed offline based on the invariant set, whereas the shrinkage rate of this constraint was updated online associated with the estimated bounding set, thereby leading to the further reduced conservatism with slightly increased computational complexity compared with robust MPC. We also established sufficient conditions for guaranteeing the recursive feasibility and closed-loop stability. The numerical example and comparison study have demonstrated the advantages of the proposed method.

Chapter 7

Conclusion and Future Work

7.1 Conclusion

This dissertation investigates four problems in robust and adaptive MPC from theoretical and application points of view. New algorithms are developed to address these issues efficiently, and theoretical analysis of closed-loop stability and recursive feasibility of MPC algorithms are conducted rigorously.

Chapter 3 investigated adaptive MPC for constrained linear systems subject to multiplicative uncertainties. We have developed an RLS-based parameter estimator to update the point and set descriptions of uncertainties simultaneously. The estimated unknown parameters and uncertainty sets are employed in the construction of homothetic prediction tubes for robust constraint satisfaction. By deriving non-increasing properties on the proposed estimation routine, the resulting tube-based adaptive MPC scheme is recursively feasible under recursive model updates while providing less conservative performance compared with the robust tube MPC method. We have theoretically shown the perturbed closed-loop system is asymptotically stable under standard assumptions. The simplified version of the proposed adaptive MPC method was also given to provide a trade-off between conservatism and computational complexity. Numerical simulations and comparisons have been given to illustrate the efficacy of the proposed method.

Chapter 4 has explored the event-based adaptive MPC with aperiodic sampling. Specifically, we have developed an ST-AMPC approach for constrained discrete-time nonlinear systems subject to parametric uncertainties and additive disturbances. A real-time zonotope-based set-membership parameter estimator has been developed to refine a set-valued description of the time-varying parametric uncertainty based on the available mea-

surements. By approximating the set of reachable states between two successive triggering time instants, the proposed estimator can be used for dynamic systems sampled in an aperiodic manner, including the self-triggered scheduling. We have leveraged this estimation scheme to design a novel ST-AMPC approach that can further reduce the average sampling frequency while preserving comparable closed-loop performance. We have theoretically shown that, under some reasonable assumptions, the proposed ST-AMPC algorithm is recursively feasible, and the closed-loop system is ISpS at triggering time instants. Numerical experiments and comparisons have been conducted to demonstrate the efficacy of the proposed method.

Chapter 5 have studied the robust MPC theory and its application to quadrotor systems. In particular, we have proposed a robust NMPC scheme for the IBVS of quadrotors subject to external disturbances. A virtual camera approach has been used to define the image moments in the virtual camera plane to derive the decoupled image kinematics. Then by integrating the image kinematics and quadrotor dynamics, an NMPC scheme has been developed to fulfill the visibility constraint, where tightened state constraints are constructed based on the Lipschitz condition to tackle external disturbances. Sufficient conditions on guaranteeing recursive feasibility of the proposed robust NMPC-based IBVS scheme have been proposed. We have further proven that the quadrotor can be regulated to a small region around the desired position by using the proposed method. Simulation studies and experiment results have demonstrated the efficacy of the proposed robust NMPC based IBVS method.

In **Chapter 6**, we have developed a novel adaptive MPC algorithm for the trajectory tracking of input constrained AGV systems subject to parametric uncertainties and additive disturbances. Based on the RLS technique, a set-membership based parameter estimator has been developed to improve the prediction accuracy in MPC. In addition, we have developed a robustness constraint for the predicted states, where its shape is decided offline based on the RPI set, whereas its shrinkage rate is updated online according to the estimated upper bound of the estimation error. The resultant adaptive MPC scheme can efficiently handle uncertainties with reduced conservatism and slightly increased computational complexity compared with the robust MPC methods. Furthermore, we have proven that the proposed adaptive MPC algorithm is recursively feasible under some derived conditions, and the closed-loop system is ISS. Finally, a numerical example and comparison study are conducted to illustrate the efficacy of the proposed method.

7.2 Future Directions

Compound-triggered adaptive MPC for nonlinear systems

The current study of adaptive MPC conducts the system identification when receiving new measurements. Although enabling online model refinement in robust MPC potentially improves the closed-loop performance, the system identification process and the corresponding control parameter updates inevitably make the MPC problem significantly complicated. A potential solution is to reduce the redundant actions of system identification. Based on the proposed self-triggered adaptive MPC scheme in Chapter 4, it is possible to address this issue by designing suitable triggering conditions with respect to estimation accuracy and control performance. Under this triggering mechanism, we can also propose the appropriate exciting strategy to accelerate the system identification process. Therefore, one of the future directions is to design compound-triggered adaptive MPC for general nonlinear systems.

Distributed adaptive MPC for constrained large-scale nonlinear systems

In recent years, large-scale networked systems, such as road-traffic networks, water networks, and power networks, have attracted increasing attention. For those networked systems, it is relatively expensive to implement the centralized MPC method due to its large amount of dimensions. In contrast, distributed MPC is a desirable solution since it improves efficiency by dividing the large-scale system into interconnected subsystems based on communication networks. In addition, only the neighbor information of each agent can be assessed in the network system. In order to formulate the optimal control problem, it is necessary to estimate state information for those inaccessible agents. Hence distributed adaptive MPC is possibly a promising solution for controlling networked systems.

Data-driven MPC for constrained dynamic systems with external disturbances

In previous chapters, there exists a common assumption that the model structure is (partially) known. However, it is difficult to have accurate knowledge of the system structure in many practical applications, inherently making the aforementioned model-based adaptive MPC methods invalid. The data-driven control method is a promising solution to this problem since it aims to compute the optimal control input compatible with the collected data, thereby can be applied without the *a priori* knowledge of the system model. This has motivated the development of data-driven MPC (see Section 1.3.3 for details). But most

existing results are based on the fundamental lemma, and hence is only applicable to linear systems with the absence of measurement noises. Therefore, an interesting direction of our future work is to study data-driven MPC for nonlinear systems with the guarantee of closed-loop properties.

Appendix A

Publications

- **Refereed journal papers that have been published or accepted:**

- J1. Y. Shi and **K. Zhang**, “Advanced Model Predictive Control Framework for Autonomous Intelligent Mechatronic Systems: A Tutorial Overview and Perspectives,” *Annual Reviews in Control*, vol. 52, pp. 170–196, 2021.
- J2. **K. Zhang**, Q. Sun and Y. Shi, “Trajectory Tracking Control of Autonomous Ground Vehicles Using Adaptive Learning MPC,” *IEEE Transactions on Neural Networks and Learning Systems*, vol. 32, no. 12, pp. 5554–5564, 2021.
- J3. **K. Zhang**, Y. Shi and H. Sheng, “Robust Nonlinear Model Predictive Control Based Visual Servoing of Quadrotor UAVs,” *IEEE/ASME Transactions on Mechatronics*, vol. 26, no. 2, pp. 700–708, 2021.
- J4. **K. Zhang** and Y. Shi, “Adaptive Model Predictive Control for a Class of Constrained Linear Systems with Parametric Uncertainties,” *Automatica*, vol. 117, no. 7. pp. 108974, 2020.
- J5. Q. Sun, **K. Zhang** and Y. Shi, “Resilient Model Predictive Control of Cyber–Physical Systems Under DoS Attacks,” *IEEE Transactions on Industrial Informatics*, vol. 16, no. 7. pp. 4920–4927, 2020.
- J6. B. Mu, **K. Zhang**, F. Xiao and Y. Shi, “Event-Based Rendezvous Control for a Group of Robots With Asynchronous Periodic Detection and Communication Time Delays,” *IEEE Transactions on Cybernetics*, vol. 49, no. 7. pp. 2642–2651, 2019.
- J7. B. Mu, **K. Zhang** and Y. Shi, “Integral Sliding Mode Flight Controller Design for a Quadrotor and the Application in a Heterogeneous Multi-Agent System,” *IEEE Transactions on Industrial Electronics*, vol. 64, no. 12, pp. 9389–9398,

2017.

- J8. H. Wei, **K. Zhang** and Y. Shi, “Self-Triggered Min-Max DMPC for Asynchronous Multi-Agent Systems with Communication Delays,” *IEEE Transactions on Industrial Informatics*, accepted, 2021. DOI:10.1109/TII.2021.3127197.

• **Journal papers under review/revision:**

- J9. **K. Zhang** and Y. Shi, “Self-Triggered Adaptive Model Predictive Control of Constrained Nonlinear Systems: A Min-Max Approach,” *Automatica*, submitted, 2021.
- J10. **K. Zhang**, Y. Shi, H. Fang, A. Colombo, S. Thilo and S. Karnouskos “Advancements in Industrial Cyber-Physical Systems: An Overview and Perspectives,” *IEEE Transactions on Industrial Informatics*, submitted, 2021.

• **Refereed conference papers that have been published:**

- C1. H. Wei, **K. Zhang**, and Y. Shi. “Distributed Min–Max MPC for Dynamically Coupled Nonlinear Systems: A self-triggered approach,” In *Proceedings of The 21st IFAC World Congress (IFAC 2020)*, Berlin, Germany, July 12-17, 2020.
- C2. **K. Zhang**, C. Liu and Y. Shi, “Computationally Efficient Adaptive Model Predictive Control for Constrained Linear Systems with Parametric Uncertainties,” in *Proceedings of 2019 IEEE 28th International Symposium on Industrial Electronics (ISIE 2019)*, Vancouver, Canada, Jun. 12-14, 2019.
- C3. Y. Pei, **K. Zhang**, J. Pan and Y. Shi, “Nonlinear Model Predictive Tracking Control of Nonholonomic Wheeled Mobile Robot Using Modified C/GMRES Algorithm,” in *Proceedings of the 42nd Annual Conference of IEEE Industrial Electronics Society (IECON 2017)*, Beijing, China, Oct. 29-Nov. 1, 2017.
- C4. **K. Zhang**, J. Chen, Y. Chang and Y. Shi, “EKF-Bbased LQR Tracking Control of a Quadrotor Helicopter Subject to Uncertainties,” in *Proceedings of the 42nd Annual Conference of IEEE Industrial Electronics Society (IECON 2016)*, Florence, Italy, Oct. 24-27, 2016.

Bibliography

- [1] S Joe Qin and Thomas A Badgwell. A survey of industrial model predictive control technology. *Control Engineering Practice*, 11(7):733–764, 2003.
- [2] David Q Mayne. Model predictive control: Recent developments and future promise. *Automatica*, 50(12):2967–2986, 2014.
- [3] Grady Williams, Paul Drews, Brian Goldfain, James M Rehg, and Evangelos A Theodorou. Information-theoretic model predictive control: Theory and applications to autonomous driving. *IEEE Transactions on Robotics*, 34(6):1603–1622, 2018.
- [4] Alessandra Parisio, Evangelos Rikos, and Luigi Glielmo. A model predictive control approach to microgrid operation optimization. *IEEE Transactions on Control Systems Technology*, 22(5):1813–1827, 2014.
- [5] Jicheng Chen and Yang Shi. Stochastic model predictive control framework for resilient cyber-physical systems: review and perspectives. *Philosophical Transactions of the Royal Society A: Mathematical, Physical and Engineering Sciences*, 379(2207):20200371, 2021.
- [6] Qi Sun, Kunwu Zhang, and Yang Shi. Resilient model predictive control of cyber-physical systems under DoS attacks. *IEEE Transactions on Industrial Informatics*, 16(7):4920–4927, 2020.
- [7] Yang Shi and Kunwu Zhang. Advanced model predictive control framework for autonomous intelligent mechatronic systems: A tutorial overview and perspectives. *Annual Reviews in Control*, 52:170–196, 2021.
- [8] Frank Allgöwer and Alex Zheng. *Nonlinear Model Predictive Control*. Progress in Systems and Control Theory. Birkhäuser Verlag, 2000.

- [9] Basil Kouvaritakis and Mark Cannon. *Model Predictive Control: Classical, Robust and Stochastic*. Advanced Textbooks in Control and Signal Processing. Springer International Publishing, 2015.
- [10] Huiping Li and Yang Shi. *Robust Receding Horizon Control for Networked and Distributed Nonlinear Systems*, volume 83. Springer, 2016.
- [11] James Blake Rawlings, David Q Mayne, and Moritz Diehl. *Model Predictive Control: Theory, Computation, and Design*. Nob Hill, 2nd edition, 2020.
- [12] Shuyou Yu, Marcus Reble, Hong Chen, and Frank Allgöwer. Inherent robustness properties of quasi-infinite horizon nonlinear model predictive control. *Automatica*, 50(9):2269–2280, 2014.
- [13] Daniel Limón, T Alamo, Francisco Salas, and Eduardo F Camacho. Input to state stability of min-max MPC controllers for nonlinear systems with bounded uncertainties. *Automatica*, 42(5):797–803, 2006.
- [14] Davide Martino Raimondo, Daniel Limon, Mircea Lazar, Lalo Magni, and Eduardo Fernández Camacho. Min-max model predictive control of nonlinear systems: A unifying overview on stability. *European Journal of Control*, 15(1):5–21, 2009.
- [15] Peter J Campo and Manfred Morari. Robust model predictive control. In *Proceedings of the 1987 American control conference (ACC)*, pages 1021–1026, Minneapolis, MN, USA, 1987. IEEE.
- [16] Jay H Lee and Zhenghong Yu. Worst-case formulations of model predictive control for systems with bounded parameters. *Automatica*, 33(5):763–781, 1997.
- [17] P. O. M. Scokaert and D. Q. Mayne. Min-max feedback model predictive control for constrained linear systems. *IEEE Transactions on Automatic control*, 43(8):1136–1142, 1998.
- [18] Yaohui Lu and Yaman Arkun. Quasi-min-max MPC algorithms for LPV systems. *Automatica*, 36(4):527–540, 2000.
- [19] D Limon Marruedo, T Alamo, and EF Camacho. Input-to-state stable MPC for constrained discrete-time nonlinear systems with bounded additive uncertainties. In

Proceedings of the 41st IEEE Conference on Decision and Control (CDC), volume 4, pages 4619–4624, Las Vegas, NV, USA, 2002. IEEE.

- [20] Mircea Lazar, D Muñoz De La Peña, WPMH Heemels, and Teodoro Alamo. On input-to-state stability of min-max nonlinear model predictive control. *Systems & Control Letters*, 57(1):39–48, 2008.
- [21] Sergio Lucia, Tiago Finkler, and Sebastian Engell. Multi-stage nonlinear model predictive control applied to a semi-batch polymerization reactor under uncertainty. *Journal of Process Control*, 23(9):1306–1319, 2013.
- [22] Paul J Goulart, Eric C Kerrigan, and Jan M Maciejowski. Optimization over state feedback policies for robust control with constraints. *Automatica*, 42(4):523–533, 2006.
- [23] Dimetri Bertsekas and Ian Rhodes. Recursive state estimation for a set-membership description of uncertainty. *IEEE Transactions on Automatic Control*, 16(2):117–128, 1971.
- [24] Dimitri P Bertsekas and Ian B Rhodes. On the minimax reachability of target sets and target tubes. *Automatica*, 7(2):233–247, 1971.
- [25] L. Chisci, J. A. Rossiter, and G. Zappa. Systems with persistent disturbances: Predictive control with restricted constraints. *Automatica*, 37(7):1019–1028, 2001.
- [26] David Q Mayne and Wilbur Langson. Robustifying model predictive control of constrained linear systems. *Electronics Letters*, 37(23):1422–1423, 2001.
- [27] Ilya Kolmanovsky and Elmer G Gilbert. Theory and computation of disturbance invariant sets for discrete-time linear systems. *Mathematical Problems in Engineering*, 4(4):317–367, 1998.
- [28] David Q Mayne, María M Seron, and SV Raković. Robust model predictive control of constrained linear systems with bounded disturbances. *Automatica*, 41(2):219–224, 2005.
- [29] David Q Mayne, SV Raković, Rolf Findeisen, and Frank Allgöwer. Robust output feedback model predictive control of constrained linear systems: Time varying case. *Automatica*, 45(9):2082–2087, 2009.

- [30] David Q Mayne, Erric C Kerrigan, EJ Van Wyk, and Paola Falugi. Tube-based robust nonlinear model predictive control. *International Journal of Robust and Nonlinear Control*, 21(11):1341–1353, 2011.
- [31] Saša V Raković, Basil Kouvaritakis, Rolf Findeisen, and Mark Cannon. Homothetic tube model predictive control. *Automatica*, 48(8):1631–1638, 2012.
- [32] Saša V Raković, Basil Kouvaritakis, and Mark Cannon. Equi-normalization and exact scaling dynamics in homothetic tube model predictive control. *Systems & Control Letters*, 62(2):209–217, 2013.
- [33] Johannes Köhler, Raffaele Soloperto, Matthias A Muller, and Frank Allgower. A computationally efficient robust model predictive control framework for uncertain nonlinear systems. *IEEE Transactions on Automatic Control*, 2020.
- [34] Saša V Raković, William S Levine, and Behçet Açıkmese. Elastic tube model predictive control. In *Proceedings of the 2016 American Control Conference (ACC)*, pages 3594–3599. IEEE, 2016.
- [35] James Fleming, Basil Kouvaritakis, and Mark Cannon. Robust tube MPC for linear systems with multiplicative uncertainty. *IEEE Transactions on Automatic Control*, 60(4):1087–1092, 2014.
- [36] Saša V Rakovic and Miroslav Baric. Parameterized robust control invariant sets for linear systems: Theoretical advances and computational remarks. *IEEE Transactions on Automatic Control*, 55(7):1599–1614, 2010.
- [37] Saša V Rakovic, Basil Kouvaritakis, Mark Cannon, Christos Panos, and Rolf Findeisen. Parameterized tube model predictive control. *IEEE Transactions on Automatic Control*, 57(11):2746–2761, 2012.
- [38] Saša V Raković, Basil Kouvaritakis, Mark Cannon, and Christos Panos. Fully parameterized tube model predictive control. *International Journal of Robust and Nonlinear Control*, 22(12):1330–1361, 2012.
- [39] D Limon Marruedo, T Alamo, and EF Camacho. Input-to-state stable MPC for constrained discrete-time nonlinear systems with bounded additive uncertainties. In *Proceedings of the 2002 IEEE Conference on Decision and Control (CDC)*, volume 4, pages 4619–4624, Las Vega, USA, December 10-13, 2002. IEEE.

- [40] Gilberto Pin, Davide M Raimondo, Lalo Magni, and Thomas Parisini. Robust model predictive control of nonlinear systems with bounded and state-dependent uncertainties. *IEEE Transactions on Automatic Control*, 54(7):1681–1687, 2009.
- [41] Huiping Li and Yang Shi. Robust distributed model predictive control of constrained continuous-time nonlinear systems: A robustness constraint approach. *IEEE Transactions on Automatic Control*, 59(6):1673–1678, 2013.
- [42] Matthias Lorenzen, Mark Cannon, and Frank Allgöwer. Robust MPC with recursive model update. *Automatica*, 103:461–471, 2019.
- [43] Johannes Köhler, Peter Kötting, Raffaele Soloperto, Frank Allgöwer, and Matthias A Müller. A robust adaptive model predictive control framework for nonlinear uncertain systems. *International Journal of Robust and Nonlinear Control*, 2020.
- [44] Kunwu Zhang and Yang Shi. Adaptive model predictive control for a class of constrained linear systems with parametric uncertainties. *Automatica*, 117:108974, 2020.
- [45] A.A. Feldbaum. *Optimal Control Systems*. Academic Press, New York, 1965.
- [46] Miroslav Krstić, Ioannis Kanellakopoulos, and Petar V. Kokotović. *Nonlinear and Adaptive Control Design*. A Wiley-Interscience publication. Wiley, 1995.
- [47] Karl J Åström and Björn Wittenmark. *Adaptive Control*. Courier Corporation, 2013.
- [48] Tor Aksel N Heirung, B Erik Ydstie, and Bjarne Foss. Dual adaptive model predictive control. *Automatica*, 80:340–348, 2017.
- [49] Graham C Goodwin and Kwai Sang Sin. *Adaptive Filtering Prediction and Control*. Courier Corporation, 2014.
- [50] Håkan Hjalmarsson. From experiment design to closed-loop control. *Automatica*, 41(3):393–438, 2005.
- [51] Ali Mesbah. Stochastic model predictive control with active uncertainty learning: A survey on dual control. *Annual Reviews in Control*, 45:107–117, 2018.
- [52] Hasmet Genceli and Michael Nikolaou. New approach to constrained predictive control with simultaneous model identification. *AIChE Journal*, 42(10):2857–2868, 1996.

- [53] Manoj Shouche, Hasmet Genceli, Premkiran Vuthandam, and Michael Nikolaou. Simultaneous constrained model predictive control and identification of DARX processes. *Automatica*, 34(12):1521–1530, 1998.
- [54] Manoj S Shouche, Hasmet Genceli, and Michael Nikolaou. Effect of on-line optimization techniques on model predictive control and identification (MPCI). *Computers & Chemical Engineering*, 26(9):1241–1252, 2002.
- [55] Premkiran Vuthandam and Michael Nikolaou. Constrained MPCI: A weak persistent excitation approach. *AIChE Journal*, 43(9):2279–2288, 1997.
- [56] Alex Alexandridis and Haralambos Sarimveis. Nonlinear adaptive model predictive control based on self-correcting neural network models. *AIChE Journal*, 51(9):2495–2506, 2005.
- [57] Eleni Aggelogiannaki and Haralambos Sarimveis. Multiobjective constrained MPC with simultaneous closed-loop identification. *International Journal of Adaptive Control and Signal Processing*, 20(4):145–173, 2006.
- [58] Jan Rathouský and Vladimír Havlena. MPC-based approximate dual controller by information matrix maximization. *International Journal of Adaptive Control and Signal Processing*, 27(11):974–999, 2013.
- [59] Eva Žáčková, Samuel Prívará, and Matej Pčolka. Persistent excitation condition within the dual control framework. *Journal of Process Control*, 23(9):1270–1280, 2013.
- [60] Giancarlo Marafioti, Robert R Bitmead, and Morten Hovd. Persistently exciting model predictive control. *International Journal of Adaptive Control and Signal Processing*, 28(6):536–552, 2014.
- [61] Antonio Ferramosca, Daniel Limon, Alejandro Hernán González, Darci Odloak, and EF Camacho. MPC for tracking zone regions. *Journal of Process Control*, 20(4):506–516, 2010.
- [62] Alejandro H González, Antonio Ferramosca, Germán A Bustos, Jacinto L Marchetti, Mirko Fiacchini, and Darci Odloak. Model predictive control suitable for closed-loop re-identification. *Systems & Control Letters*, 69:23–33, 2014.

- [63] Bernardo Hernandez and Paul Trodden. Persistently exciting tube MPC. In *Proceedings of the 2016 American Control Conference (ACC)*, pages 948–953, Boston, MA, USA, July 6-8, 2016. IEEE.
- [64] Bernardo A Hernandez Vicente and Paul A Trodden. Stabilizing predictive control with persistence of excitation for constrained linear systems. *Systems & Control Letters*, 126:58–66, 2019.
- [65] Sven Brüggemann and Robert R Bitmead. Model predictive control with forward-looking persistent excitation. *arXiv preprint arXiv:2004.01625*, 2020.
- [66] Morten Hovd and Robert R Bitmead. Interaction between control and state estimation in nonlinear MPC. *IFAC Proceedings Volumes*, 37(9):119–124, 2004.
- [67] Tor Aksel N Heirung, Bjarne Foss, and B Erik Ydstie. MPC-based dual control with online experiment design. *Journal of Process Control*, 32:64–76, 2015.
- [68] Avishai Weiss and Stefano Di Cairano. Robust dual control MPC with guaranteed constraint satisfaction. In *Proceedings of 53rd IEEE Conference on Decision and Control (CDC)*, pages 6713–6718, Los Angeles, CA, USA, 2014. IEEE.
- [69] Boris Houska, Dries Telen, Filip Logist, and Jan Van Impe. Self-reflective model predictive control. *SIAM Journal on Control and Optimization*, 55(5):2959–2980, 2017.
- [70] Xuhui Feng and Boris Houska. Real-time algorithm for self-reflective model predictive control. *Journal of Process Control*, 65:68–77, 2018.
- [71] Tor Aksel N Heirung, Tito LM Santos, and Ali Mesbah. Model predictive control with active learning for stochastic systems with structural model uncertainty: Online model discrimination. *Computers & Chemical Engineering*, 128:128–140, 2019.
- [72] Raffaele Soloperto, Johannes Köhler, and Frank Allgöwer. Augmenting MPC schemes with active learning: Intuitive tuning and guaranteed performance. *IEEE Control Systems Letters*, 4(3):713–718, 2020.
- [73] David Q Mayne and H Michalska. Adaptive receding horizon control for constrained nonlinear systems. In *Proceedings of 32nd IEEE Conference on Decision and Control (CDC)*, pages 1286–1291, San Antonio, TX, USA, December 15-17, 1993. IEEE.

- [74] Jing Sun, Hyeonjun Park, Ilya Kolmanovsky, and Richard Choroszuca. Adaptive model predictive control in the IPA-SQP framework. In *Proceedings of the 52nd IEEE Annual Conference on Decision and Control (CDC)*, pages 5565–5570, Florence, Italy, December 10-13, 2013. IEEE.
- [75] Arthur Earl Bryson. *Applied Optimal Control: Optimization, Estimation and Control*. CRC Press, 1975.
- [76] Veronica Adetola and Martin Guay. Adaptive receding horizon control of nonlinear systems. *IFAC Proceedings Volumes*, 37(13):787–792, 2004.
- [77] Bing Zhu and Xiaohua Xia. Lyapunov-based adaptive model predictive control for unconstrained non-linear systems with parametric uncertainties. *IET Control Theory & Applications*, 10(15):1937–1943, 2016.
- [78] Bing Zhu and Xiaohua Xia. Adaptive model predictive control for unconstrained discrete-time linear systems with parametric uncertainties. *IEEE Transactions on Automatic Control*, 61(10):3171–3176, 2016.
- [79] Abhishek Dhar and Shubhendu Bhasin. Novel adaptive MPC design for uncertain MIMO discrete-time LTI systems with input constraints. In *Proceedings of 2018 European Control Conference (ECC)*, pages 319–324, Limassol, Cyprus, 2018. IEEE.
- [80] Abhishek Dhar and Shubhendu Bhasin. Adaptive MPC for uncertain discrete-time LTI MIMO systems with incremental input constraints. *IFAC-PapersOnLine*, 51(1):329–334, 2018.
- [81] Jung-Su Kim, Tae-Woong Yoon, Ali Jadbabaie, and Claudio De Persis. Input-to-state stable finite horizon MPC for neutrally stable linear discrete-time systems with input constraints. *Systems & Control Letters*, 55(4):293–303, 2006.
- [82] J-S Kim, T-W Yoon, Hyungbo Shim, and Jin Heon Seo. Switching adaptive output feedback model predictive control for a class of input-constrained linear plants. *IET Control Theory & Applications*, 2(7):573–582, 2008.
- [83] Tae-Woong Yoon, Jung-Su Kim, and A Stephen Morse. Supervisory control using a new control-relevant switching. *Automatica*, 43(10):1791–1798, 2007.

- [84] Stefano Di Cairano. Indirect adaptive model predictive control for linear systems with polytopic uncertainty. In *Proceedings of the 2016 American Control Conference (ACC)*, pages 2948–2953, Boston, MA, USA, July 6-8, 2016. IEEE.
- [85] Jamal Daafouz and Jacques Bernussou. Parameter dependent lyapunov functions for discrete time systems with time varying parametric uncertainties. *Systems & control letters*, 43(5):355–359, 2001.
- [86] Donglei Fan and Stefano Di Cairano. Further results and properties of indirect adaptive model predictive control for linear systems with polytopic uncertainty. In *Proceedings of the 2016 American Control Conference (ACC)*, pages 2948–2953, Boston, MA, USA, July 6-8, 2016. IEEE.
- [87] Abhishek Dhar and Shubhendu Bhasin. Tube based adaptive model predictive control. In *Proceedings of 2019 IEEE 58th Conference on Decision and Control (CDC)*, pages 451–456, Nice, France, 2019. IEEE.
- [88] Abhishek Dhar and Shubhendu Bhasin. Indirect adaptive MPC for discrete-time LTI system with robust constraint satisfaction. In *Proceedings of 2020 American Control Conference (ACC)*, pages 2407–2412, Denver, CO, USA, 2020. IEEE.
- [89] Wilbur Langson, Ioannis Chrysochoos, SV Raković, and David Q Mayne. Robust model predictive control using tubes. *Automatica*, 40(1):125–133, 2004.
- [90] Alberto Bemporad, Francesco Borrelli, and Manfred Morari. Min-max control of constrained uncertain discrete-time linear systems. *IEEE Transactions on Automatic Control*, 48(9):1600–1606, 2003.
- [91] Bing Zhu, Zewei Zheng, and Xiaohua Xia. Constrained adaptive model-predictive control for a class of discrete-time linear systems with parametric uncertainties. *IEEE Transactions on Automatic Control*, 65(5):2223–2229, 2019.
- [92] Hossein Bolandi and Saman Saki. Design of adaptive model predictive control for a class of uncertain non-linear dynamic systems: stability, convergence, and robustness analysis. *IET Control Theory & Applications*, 13(15):2376–2386, 2019.
- [93] Anil Aswani, Humberto Gonzalez, S Shankar Sastry, and Claire Tomlin. Provably safe and robust learning-based model predictive control. *Automatica*, 49(5):1216–1226, 2013.

- [94] Sven Brüggemann, Corrado Possieri, Jorge I Poveda, and Andrew R Teel. Robust constrained model predictive control with persistent model adaptation. In *Proceedings of 2016 IEEE 55th Conference on Decision and Control (CDC)*, pages 2364–2369, Las Vegas, NV, USA, 2016. IEEE.
- [95] K Hariprasad and Sharad Bhartiya. Adaptive robust model predictive control of nonlinear systems using tubes based on interval inclusions. In *Proceedings of 2014 IEEE 53rd Conference on Decision and Control (CDC)*, pages 2032–2037, Los Angeles, CA, USA, 2014. IEEE.
- [96] Hiroaki Fukushima, Tae-Hyoung Kim, and Toshiharu Sugie. Adaptive model predictive control for a class of constrained linear systems based on the comparison model. *Automatica*, 43(2):301–308, 2007.
- [97] Hiroaki Fukushima and Robert R Bitmead. Robust constrained predictive control using comparison model. *Automatica*, 41(1):97–106, 2005.
- [98] T-H Kim and Toshiharu Sugie. Adaptive receding horizon predictive control for constrained discrete-time linear systems with parameter uncertainties. *International Journal of Control*, 81(1):62–73, 2008.
- [99] Darryl DeHaan and Martin Guay. Adaptive robust MPC: A minimally-conservative approach. In *Proceedings of 2007 American Control Conference (ACC)*, pages 3937–3942, New York, NY, USA, 2007. IEEE.
- [100] D DeHaan, V Adetola, and M Guay. Adaptive robust MPC: An eye towards computational simplicity. *IFAC Proceedings Volumes*, 40(12):228–233, 2007.
- [101] Veronica Adetola and Martin Guay. Robust adaptive MPC for systems with exogenous disturbances. *IFAC Proceedings Volumes*, 42(11):249–254, 2009.
- [102] Veronica Adetola, Darryl DeHaan, and Martin Guay. Adaptive model predictive control for constrained nonlinear systems. *Systems & Control Letters*, 58(5):320–326, 2009.
- [103] Veronica Adetola and Martin Guay. Robust adaptive MPC for constrained uncertain nonlinear systems. *International Journal of Adaptive Control and Signal Processing*, 25(2):155–167, 2011.

- [104] Martin Guay and Veronica Adetola. Adaptive economic optimising model predictive control of uncertain nonlinear systems. *International Journal of Control*, 86(8):1425–1437, 2013.
- [105] Guilherme AA Gonçalves and Martin Guay. Robust discrete-time set-based adaptive predictive control for nonlinear systems. *Journal of Process Control*, 39:111–122, 2016.
- [106] Xiaofeng Wang, Yu Sun, and Kun Deng. Adaptive model predictive control of uncertain constrained systems. In *Proceedings of 2014 American Control Conference (ACC)*, pages 2857–2862, Portland, OR, USA, 2014. IEEE.
- [107] Xiaofeng Wang, Lixing Yang, Yu Sun, and Kun Deng. Adaptive model predictive control of nonlinear systems with state-dependent uncertainties. *International Journal of Robust and Nonlinear Control*, 27(17):4138–4153, 2017.
- [108] Sixing Zhang, Li Dai, and Yuanqing Xia. Adaptive MPC for constrained systems with parameter uncertainty and additive disturbance. *IET Control Theory & Applications*, 13(15):2500–2506, 2019.
- [109] Marko Tanaskovic, Lorenzo Fagiano, Roy Smith, and Manfred Morari. Adaptive receding horizon control for constrained MIMO systems. *Automatica*, 50(12):3019–3029, 2014.
- [110] Monimoy Bujarbaruah, Xiaojing Zhang, and Francesco Borrelli. Adaptive MPC with chance constraints for fir systems. In *Proceedings of 2018 Annual American Control Conference (ACC)*, pages 2312–2317, Milwaukee, WI, USA, 2018. IEEE.
- [111] Monimoy Bujarbaruah and Charlott Vallon. Exploiting model sparsity in adaptive MPC: A compressed sensing viewpoint. In *Proceedings of the 2nd Conference on Learning for Dynamics and Control (L4DC)*, pages 137–146, 2020.
- [112] Marko Tanaskovic, Lorenzo Fagiano, and Vojislav Gligorovski. Adaptive model predictive control for linear time varying MIMO systems. *Automatica*, 105:237–245, 2019.
- [113] Monimoy Bujarbaruah, Xiaojing Zhang, Ugo Rosolia, and Francesco Borrelli. Adaptive MPC for iterative tasks. In *Proceedings of 2018 IEEE Conference on Decision and Control (CDC)*, pages 6322–6327, iami Beach, FL, USA, December 17-19, 2018. IEEE.

- [114] Ugo Rosolia and Francesco Borrelli. Learning model predictive control for iterative tasks. a data-driven control framework. *IEEE Transactions on Automatic Control*, 63(7):1883–1896, 2017.
- [115] Matthias Lorenzen, Frank Allgöwer, and Mark Cannon. Adaptive model predictive control with robust constraint satisfaction. In *Proceedings of the 20th World Congress of the International Federation of Automatic Control (IFAC)*, pages 3313–3318, Toulouse, France, July 9-14, 2017. Elsevier.
- [116] Johannes Köhler, Elisa Andina, Raffaele Soloperto, Matthias A Müller, and Frank Allgöwer. Linear robust adaptive model predictive control: Computational complexity and conservatism. In *Proceedings of 2019 IEEE 58th Conference on Decision and Control (CDC)*, pages 1383–1388, Nice, France, 2019. IEEE.
- [117] Xiaonan Lu and Mark Cannon. Robust adaptive tube model predictive control. In *2019 American Control Conference (ACC)*, pages 3695–3701, Philadelphia, PA, USA, 2019. IEEE.
- [118] Xiaonan Lu, Mark Cannon, and Denis Koksal-Rivet. Robust adaptive model predictive control: Performance and parameter estimation. *International Journal of Robust and Nonlinear Control*, 2019.
- [119] Luigi Chisci, Andrea Garulli, Antonio Vicino, and Giovanni Zappa. Block recursive parallelotopic bounding in set membership identification. *Automatica*, 34(1):15–22, 1998.
- [120] Monimoy Bujarbaruah, Xiaojing Zhang, Marko Tanaskovic, and Francesco Borrelli. Adaptive stochastic MPC under time varying uncertainty. *IEEE Transactions on Automatic Control*, 2020.
- [121] Marcello Farina, Luca Giulioni, and Riccardo Scattolini. Stochastic linear model predictive control with chance constraints—a review. *Journal of Process Control*, 44:53–67, 2016.
- [122] Zhong-Sheng Hou and Zhuo Wang. From model-based control to data-driven control: Survey, classification and perspective. *Information Sciences*, 235:3–35, 2013.
- [123] Lukas Hewing, Kim P Wabersich, Marcel Menner, and Melanie N Zeilinger. Learning-based model predictive control: Toward safe learning in control. *Annual Review of Control, Robotics, and Autonomous Systems*, 3:269–296, 2020.

- [124] Michel Verhaegen and Vincent Verdult. *Filtering and System Identification: A Least Squares Approach*. Cambridge university press, 2007.
- [125] Alessandro Chiuso and Gianluigi Pillonetto. System identification: A machine learning perspective. *Annual Review of Control, Robotics, and Autonomous Systems*, 2:281–304, 2019.
- [126] Wouter Favoreel, Bart De Moor, and Michel Gevers. SPC: Subspace predictive control. *IFAC Proceedings Volumes*, 32(2):4004–4009, 1999.
- [127] Peter Van Overschee and BL De Moor. *Subspace Identification for Linear Systems: Theory, Implementation, Applications*. Springer Science & Business Media, 2012.
- [128] Ramesh Kadali, Biao Huang, and Anthony Rossiter. A data driven subspace approach to predictive controller design. *Control Engineering Practice*, 11(3):261–278, 2003.
- [129] Balázs Kulcsár, Jan-Willem van Wingerden, Jianfei Dong, and Michel Verhaegen. Closed-loop subspace predictive control for hammerstein systems. In *Proceedings of the 48th IEEE Conference on Decision and Control held jointly with 2009 28th Chinese Control Conference (CDC-CCC)*, pages 2604–2609. IEEE, 2009.
- [130] Biao Huang and Ramesh Kadali. *Dynamic Modeling, Predictive Control and Performance Monitoring: A Data-Driven Subspace Approach*. Springer, 2008.
- [131] Xiaohui Lu, Hong Chen, Bingzhao Gao, Zhenwei Zhang, and Weiwei Jin. Data-driven predictive gearshift control for dual-clutch transmissions and FPGA implementation. *IEEE Transactions on Industrial Electronics*, 62(1):599–610, 2014.
- [132] Xiaorui Wang, Biao Huang, and Tongwen Chen. Data-driven predictive control for solid oxide fuel cells. *Journal of Process Control*, 17(2):103–114, 2007.
- [133] Saba Sedghizadeh and Soosan Beheshti. Data-driven subspace predictive control: Stability and horizon tuning. *Journal of the Franklin Institute*, 355(15):7509–7547, 2018.
- [134] Gianluigi Pillonetto, Francesco Dinuzzo, Tianshi Chen, Giuseppe De Nicolao, and Lennart Ljung. Kernel methods in system identification, machine learning and function estimation: A survey. *Automatica*, 50(3):657–682, 2014.

- [135] Juš Kocijan, Roderick Murray-Smith, Carl Edward Rasmussen, and Agathe Girard. Gaussian process model based predictive control. In *Proceedings of the 2004 American control conference (ACC)*, volume 3, pages 2214–2219. IEEE, 2004.
- [136] Alexandra Grancharova, Juš Kocijan, and Tor A Johansen. Explicit stochastic predictive control of combustion plants based on gaussian process models. *Automatica*, 44(6):1621–1631, 2008.
- [137] Gang Cao, Edmund MK Lai, and Fakhurul Alam. Gaussian process model predictive control of unmanned quadrotors. In *Proceedings of 2016 2nd International conference on control, automation and robotics (ICCAR)*, pages 200–206. IEEE, 2016.
- [138] Jan M Maciejowski and Xiaoke Yang. Fault tolerant control using Gaussian processes and model predictive control. In *Proceedings of 2013 Conference on Control and Fault-Tolerant Systems (SysTol)*, pages 1–12. IEEE, 2013.
- [139] Yunpeng Pan, Xinyan Yan, Evangelos A Theodorou, and Byron Boots. Prediction under uncertainty in sparse spectrum gaussian processes with applications to filtering and control. In *Proceedings of International Conference on Machine Learning (ICML)*, pages 2760–2768. PMLR, 2017.
- [140] Sanket Kamthe and Marc Deisenroth. Data-efficient reinforcement learning with probabilistic model predictive control. In *Proceedings of International Conference on Artificial Intelligence and Statistics (AISTATS)*, pages 1701–1710. PMLR, 2018.
- [141] Edgar D Klenske, Melanie N Zeilinger, Bernhard Schölkopf, and Philipp Hennig. Gaussian process-based predictive control for periodic error correction. *IEEE Transactions on Control Systems Technology*, 24(1):110–121, 2015.
- [142] Lukas Hewing, Juraj Kabzan, and Melanie N Zeilinger. Cautious model predictive control using gaussian process regression. *IEEE Transactions on Control Systems Technology*, 28(6):2736–2743, 2019.
- [143] T Peterson, E Hernandez, Y Arkun, and FJ Schork. Nonlinear predictive control of a semi batch polymerization reactor by an extended DMC. In *Proceedings of 1989 American Control Conference (ACC)*, pages 1534–1539. IEEE, 1989.
- [144] Evelio Hernandaz and Yaman Arkun. Neural network modeling and an extended dmc algorithm to control nonlinear systems. In *Proceedings of 1990 American Control Conference (ACC)*, pages 2454–2459. IEEE, 1990.

- [145] JM Zamarreno and P Vega. Neural predictive control. application to a highly nonlinear system. *Engineering Applications of Artificial Intelligence*, 12(2):149–158, 1999.
- [146] Stephen Piche, Bijan Sayyar-Rodsari, Doug Johnson, and Mark Gerules. Nonlinear model predictive control using neural networks. *IEEE Control Systems Magazine*, 20(3):53–62, 2000.
- [147] Dongbing Gu and Huosheng Hu. Neural predictive control for a car-like mobile robot. *Robotics and Autonomous Systems*, 39(2):73–86, 2002.
- [148] RK Al Seyab and Yi Cao. Nonlinear system identification for predictive control using continuous time recurrent neural networks and automatic differentiation. *Journal of Process Control*, 18(6):568–581, 2008.
- [149] Yunpeng Pan and Jun Wang. Model predictive control of unknown nonlinear dynamical systems based on recurrent neural networks. *IEEE Transactions on Industrial Electronics*, 59(8):3089–3101, 2011.
- [150] Hong-Gui Han, Lu Zhang, Ying Hou, and Jun-Fei Qiao. Nonlinear model predictive control based on a self-organizing recurrent neural network. *IEEE Transactions on Neural Networks and Learning Systems*, 27(2):402–415, 2015.
- [151] Chao Huang, Xiangyu Wang, Liang Li, and Xiang Chen. Multistructure radial basis function neural-networks-based extended model predictive control: Application to clutch control. *IEEE/ASME Transactions on Mechatronics*, 24(6):2519–2530, 2019.
- [152] Enrico Terzi, Lorenzo Fagiano, Marcello Farina, and Riccardo Scattolini. Learning-based predictive control for linear systems: A unitary approach. *Automatica*, 108:108473, 2019.
- [153] Amr Alanwar, Yvonne Stürz, and Karl Henrik Johansson. Robust data-driven predictive control using reachability analysis. *arXiv preprint arXiv:2103.14110*, 2021.
- [154] Jan C Willems. The behavioral approach to open and interconnected systems. *IEEE Control Systems Magazine*, 27(6):46–99, 2007.
- [155] Jan C Willems, Paolo Rapisarda, Ivan Markovskiy, and Bart LM De Moor. A note on persistency of excitation. *Systems & Control Letters*, 54(4):325–329, 2005.

- [156] Ivan Markovsky, Jan C Willems, Sabine Van Huffel, and Bart De Moor. *Exact and approximate modeling of linear systems: A behavioral approach*. SIAM, 2006.
- [157] Ivan Markovsky, Jan C Willems, Paolo Rapisarda, and Bart LM De Moor. Algorithms for deterministic balanced subspace identification. *Automatica*, 41(5):755–766, 2005.
- [158] Ivan Markovsky. A missing data approach to data-driven filtering and control. *IEEE Transactions on Automatic Control*, 62(4):1972–1978, 2016.
- [159] Hua Yang and Shaoyuan Li. A data-driven predictive controller design based on reduced hankel matrix. In *Proceedings of 2015 10th Asian Control Conference (ASCC)*, pages 1–7. IEEE, 2015.
- [160] Jeremy Coulson, John Lygeros, and Florian Dörfler. Data-enabled predictive control: In the shallows of the DeePC. In *Proceedings of 2019 18th European Control Conference (ECC)*, pages 307–312. IEEE, 2019.
- [161] Jeremy Coulson, John Lygeros, and Florian Dörfler. Regularized and distributionally robust data-enabled predictive control. In *Proceedings of 2019 IEEE 58th Conference on Decision and Control (CDC)*, pages 2696–2701. IEEE, 2019.
- [162] Jeremy Coulson, John Lygeros, and Florian Dörfler. Distributionally robust chance constrained data-enabled predictive control. *arXiv preprint arXiv:2006.01702*, 2020.
- [163] Linbin Huang, Jianzhe Zhen, John Lygeros, and Florian Dörfler. Quadratic regularization of data-enabled predictive control: Theory and application to power converter experiments. *arXiv preprint arXiv:2012.04434*, 2020.
- [164] Linbin Huang, Jianzhe Zhen, John Lygeros, and Florian Dörfler. Robust data-enabled predictive control: Tractable formulations and performance guarantees. *arXiv preprint arXiv:2105.07199*, 2021.
- [165] Peyman Mohajerin Esfahani and Daniel Kuhn. Data-driven distributionally robust optimization using the wasserstein metric: Performance guarantees and tractable reformulations. *Mathematical Programming*, 171(1):115–166, 2018.
- [166] Julian Berberich, Johannes Köhler, Matthias A Muller, and Frank Allgower. Data-driven model predictive control with stability and robustness guarantees. *IEEE Transactions on Automatic Control*, 66(4):1702–1717, 2020.

- [167] Julian Berberich, Johannes Köhler, Matthias A Müller, and Frank Allgöwer. Data-driven tracking MPC for changing setpoints. *IFAC-PapersOnLine*, 53(2):6923–6930, 2020.
- [168] Julian Berberich, Johannes Köhler, Matthias A Müller, and Frank Allgöwer. Robust constraint satisfaction in data-driven mpc. In *Proceedings of 2020 59th IEEE Conference on Decision and Control (CDC)*, pages 1260–1267. IEEE, 2020.
- [169] Julian Berberich, Johannes Köhler, Matthias A Müller, and Frank Allgöwer. Linear tracking MPC for nonlinear systems part ii: The data-driven case. *arXiv preprint arXiv:2105.08567*, 2021.
- [170] Julian Berberich, Johannes Köhler, Matthias A Müller, and Frank Allgöwer. On the design of terminal ingredients for data-driven MPC. *arXiv preprint arXiv:2101.05573*, 2021.
- [171] Joscha Bongard, Julian Berberich, Johannes Köhler, and Frank Allgöwer. Robust stability analysis of a simple data-driven model predictive control approach. *arXiv preprint arXiv:2103.00851*, 2021.
- [172] Chaohong Cai and Andrew R Teel. Input–output-to-state stability for discrete-time systems. *Automatica*, 44(2):326–336, 2008.
- [173] Julian Berberich, Carsten W Scherer, and Frank Allgöwer. Combining prior knowledge and data for robust controller design. *arXiv preprint arXiv:2009.05253*, 2020.
- [174] Felix Fiedler and Sergio Lucia. On the relationship between data-enabled predictive control and subspace predictive control. *arXiv preprint arXiv:2011.13868*, 2020.
- [175] Florian Dörfler, Jeremy Coulson, and Ivan Markovskiy. Bridging direct & indirect data-driven control formulations via regularizations and relaxations. *arXiv preprint arXiv:2101.01273*, 2021.
- [176] Vishaal Krishnan and Fabio Pasqualetti. On direct vs indirect data-driven predictive control. *arXiv preprint arXiv:2103.14936*, 2021.
- [177] PCN Verheijen, GR da Silva, and M Lazar. Data-driven predictive control with estimated prediction matrices and integral action. *arXiv preprint arXiv:2104.04972*, 2021.

- [178] W. P. M. H. Heemels, Karl Henrik Johansson, and Paulo Tabuada. An introduction to event-triggered and self-triggered control. In *Proceedings of 51st IEEE Conference on Decision and Control (CDC)*, pages 3270–3285, Maui, Hawaii, USA, December 10-13, 2012. IEEE.
- [179] S Joe Qin and Thomas A Badgwell. A survey of industrial model predictive control technology. *Control Engineering Practice*, 11(7):733–764, 2003.
- [180] Huiping Li and Yang Shi. Event-triggered robust model predictive control of continuous-time nonlinear systems. *Automatica*, 50(5):1507–1513, 2014.
- [181] Huiping Li, Weisheng Yan, Yang Shi, and Yintao Wang. Periodic event-triggering in distributed receding horizon control of nonlinear systems. *Systems & Control Letters*, 86:16–23, 2015.
- [182] Changxin Liu, Huiping Li, Yang Shi, and Demin Xu. Co-design of event trigger and feedback policy in robust model predictive control. *IEEE Transactions on Automatic Control*, 65(1):302–309, 2019.
- [183] Kazumune Hashimoto, Shuichi Adachi, and Dimos V Dimarogonas. Self-triggered model predictive control for nonlinear input-affine dynamical systems via adaptive control samples selection. *IEEE Transactions on Automatic Control*, 62:177–189, 2016.
- [184] Li Dai, Yulong Gao, Lihua Xie, Karl Henrik Johansson, and Yuanqing Xia. Stochastic self-triggered model predictive control for linear systems with probabilistic constraints. *Automatica*, 92:9–17, 2018.
- [185] Jicheng Chen, Qi Sun, and Yang Shi. Stochastic self-triggered MPC for linear constrained systems under additive uncertainty and chance constraints. *Information Sciences*, 459:198–210, 2018.
- [186] Zhongqi Sun, Li Dai, Kun Liu, Dimos V Dimarogonas, and Yuanqing Xia. Robust self-triggered MPC with adaptive prediction horizon for perturbed nonlinear systems. *IEEE Transactions on Automatic Control*, 64(11):4780–4787, 2019.
- [187] Huiping Li, Weisheng Yan, and Yang Shi. Triggering and control codesign in self-triggered model predictive control of constrained systems: With guaranteed performance. *IEEE Transactions on Automatic Control*, 63(11):4008–4015, 2018.

- [188] Changxin Liu, Huiping Li, Jian Gao, and Demin Xu. Robust self-triggered min–max model predictive control for discrete-time nonlinear systems. *Automatica*, 89:333–339, 2018.
- [189] Florian David Brunner, W. P. M. H. Heemels, and Frank Allgöwer. Robust self-triggered MPC for constrained linear systems. In *Proceedings of 2014 European Control Conference (ECC)*, pages 472–477. IEEE, 2014.
- [190] Florian David Brunner, Maurice Heemels, and Frank Allgöwer. Robust self-triggered MPC for constrained linear systems: A tube-based approach. *Automatica*, 72:73–83, 2016.
- [191] Nikolai Michailovich Filatov and Heinz Unbehauen. *Adaptive Dual Control: Theory and Applications*, volume 302. Springer Science & Business Media, 2004.
- [192] Edison Tse and Yaakov Bar-Shalom. An actively adaptive control for linear systems with random parameters via the dual control approach. *IEEE Transactions on Automatic Control*, 18(2):109–117, 1973.
- [193] Bingxian Mu, Kunwu Zhang, and Yang Shi. Integral sliding mode flight controller design for a quadrotor and the application in a heterogeneous multi-agent system. *IEEE Transactions on Industrial Electronics*, 64(12):9389–9398, 2017.
- [194] Xiao Liang, Yongchun Fang, Ning Sun, and He Lin. A novel energy-coupling-based hierarchical control approach for unmanned quadrotor transportation systems. *IEEE/ASME Transactions on Mechatronics*, 24(1):248–259, 2019.
- [195] Linxing Xu, Hongjun Ma, Dong Guo, Anhuan Xie, and Dalei Song. Backstepping sliding-mode and cascade active disturbance rejection control for a quadrotor UAV. *IEEE/ASME Transactions on Mechatronics*, 2020.
- [196] Qi Lu, Beibei Ren, and Siva Parameswaran. Uncertainty and disturbance estimator-based global trajectory tracking control for a quadrotor. *IEEE/ASME Transactions on Mechatronics*, 25(3):1519–1530, 2020.
- [197] Shida Liu, Zhongsheng Hou, Taotao Tian, Zhidong Deng, and Zhenxuan Li. A novel dual successive projection-based model-free adaptive control method and application to an autonomous car. *IEEE Transactions on Neural Networks and Learning Systems*, 30(11):3444–3457, 2019.

- [198] Yutaka Kanayama, Yoshihiko Kimura, Fumio Miyazaki, and Tetsuo Noguchi. A stable tracking control method for an autonomous mobile robot. In *Proceedings of 1990 IEEE International Conference on Robotics and Automation (ICRA)*, Tsukuba, Japan, May 13-18, 1990.
- [199] Zhongping Jiang and Henk Nijmeijer. Tracking control of mobile robots: A case study in backstepping. *Automatica*, 33(7):1393–1399, 1997.
- [200] Zhong-Ping Jiang and Yuan Wang. Input-to-state stability for discrete-time nonlinear systems. *Automatica*, 37(6):857–869, 2001.
- [201] Eduardo D Sontag and Yuan Wang. New characterizations of input-to-state stability. *IEEE Transactions on Automatic Control*, 41(9):1283–1294, 1996.
- [202] Daniel Limón, Teodoro Alamo, Francisco Salas, and Eduardo F Camacho. Input to state stability of min–max MPC controllers for nonlinear systems with bounded uncertainties. *Automatica*, 42(5):797–803, 2006.
- [203] Sasa V Rakovic, Eric C Kerrigan, Konstantinos I Kouramas, and David Q Mayne. Invariant approximations of the minimal robust positively invariant set. *IEEE Transactions on Automatic Control*, 50(3):406–410, 2005.
- [204] David Q Mayne. Control of constrained dynamic systems. *European Journal of Control*, 7(2-3):87–99, 2001.
- [205] Franco Blanchini and Stefano Miani. *Set-Theoretic Methods in Control*. Springer, 2008.
- [206] Teodoro Alamo, José M Bravo, and Eduardo F Camacho. Guaranteed state estimation by zonotopes. *Automatica*, 41(6):1035–1043, 2005.
- [207] Maria Pia Saccomani, Stefania Audoly, and Leontina D’Angiò. Parameter identifiability of nonlinear systems: the role of initial conditions. *Automatica*, 39(4):619–632, 2003.
- [208] Richard M Johnstone, C Richard Johnson Jr, Robert R Bitmead, and Brian DO Anderson. Exponential convergence of recursive least squares with exponential forgetting factor. *Systems & Control Letters*, 2(2):77–82, 1982.

- [209] Sachin S Sapatnekar, Pravin M Vaidya, and Sung-Mo Kang. Feasible region approximation using convex polytopes. In *Proceedings of 1993 IEEE International Symposium on Circuits and Systems (ISCAS)*, pages 1786–1789, Chicago, IL, USA, May 3-6, 1993. IEEE.
- [210] Bert Pluymers, John A Rossiter, Johan A K Suykens, and Bart De Moor. The efficient computation of polyhedral invariant sets for linear systems with polytopic uncertainty. In *Proceedings of the 2005 American Control Conference 2005 (ACC)*, pages 804–809, Portland, OR, USA, June 8-10, 2005. IEEE.
- [211] J. Löfberg. Yalmip: A toolbox for modeling and optimization in matlab. In *Proceedings of 2004 IEEE International Symposium on Computer Aided Control System Design (CACSD)*, Taipei, Taiwan, 2004.
- [212] Dewei Li and Yugeng Xi. The feedback robust MPC for LPV systems with bounded rates of parameter changes. *IEEE Transactions on Automatic Control*, 55(2):503–507, 2010.
- [213] Jian Wan, Sanjay Sharma, and Robert Sutton. Guaranteed state estimation for nonlinear discrete-time systems via indirectly implemented polytopic set computation. *IEEE Transactions on Automatic Control*, 63(12):4317–4322, 2018.
- [214] Iain Dunning, Joey Huchette, and Miles Lubin. JuMP: A modeling language for mathematical optimization. *SIAM Review*, 59(2):295–320, 2017.
- [215] Richard H Byrd, Jorge Nocedal, and Richard A Waltz. KNITRO: An integrated package for nonlinear optimization. In *Large-Scale Nonlinear Optimization*, pages 35–59. Springer, 2006.
- [216] Júlio Hoffmann. GeoStats. jl–high-performance geostatistics in julia. *Journal of Open Source Software*, 3(24):692, 2018.
- [217] Farid Kendoul. Survey of advances in guidance, navigation, and control of unmanned rotorcraft systems. *Journal of Field Robotics*, 29(2):315–378, 2012.
- [218] François Chaumette and Seth Hutchinson. Visual servo control part i: Basic approaches. *IEEE Robotics & Automation Magazine*, 13(4):82–90, 2006.
- [219] Hui Xie. *Dynamic visual servoing of rotary wing unmanned aerial vehicles*. PhD thesis, University of Alberta, 2016.

- [220] Mickaël Sauvée, Philippe Poignet, Etienne Dombre, and Estelle Courtial. Image based visual servoing through nonlinear model predictive control. In *Proceedings of the 45th IEEE Conference on Decision and Control (CDC)*, pages 1776–1781, San Diego, CA, USA, December 13-15, 2006. IEEE.
- [221] Jian Gao, Alison A Proctor, Yang Shi, and Colin Bradley. Hierarchical model predictive image-based visual servoing of underwater vehicles with adaptive neural network dynamic control. *IEEE Transactions on Cybernetics*, 46(10):2323–2334, 2015.
- [222] Huaiyuan Sheng, Eric Shi, and Kunwu Zhang. Image-based visual servoing of a quadrotor with improved visibility using model predictive control. In *Proceedings of 2019 IEEE 28th International Symposium on Industrial Electronics (ISIE)*, Vancouver, Canada, June 12-14, 2019.
- [223] Amir Hajiloo, Mohammad Keshmiri, Wen-Fang Xie, and Ting-Ting Wang. Robust online model predictive control for a constrained image-based visual servoing. *IEEE Transactions on Industrial Electronics*, 63(4):2242–2250, 2015.
- [224] Shahab Heshmati-Alamdari, George K Karavas, Alina Eqtami, Michael Drossakis, and Kostas J Kyriakopoulos. Robustness analysis of model predictive control for constrained image-based visual servoing. In *Proceedings of 2014 IEEE International Conference on Robotics and Automation (ICRA)*, pages 4469–4474, Hong Kong, China, 2014. IEEE.
- [225] Changxin Liu, Jian Gao, Huiping Li, and Demin Xu. Aperiodic robust model predictive control for constrained continuous-time nonlinear systems: An event-triggered approach. *IEEE transactions on cybernetics*, 48(5):1397–1405, 2017.
- [226] Samir Bouabdallah. *Design and control of quadrotors with application to autonomous flying*. PhD thesis, Epfl, 2007.
- [227] Hui Xie and Alan F Lynch. Input saturated visual servoing for unmanned aerial vehicles. *IEEE/ASME Transactions on Mechatronics*, 22(2):952–960, 2016.
- [228] Dongliang Zheng, Hesheng Wang, Jingchuan Wang, Siheng Chen, Weidong Chen, and Xinwu Liang. Image-based visual servoing of a quadrotor using virtual camera approach. *IEEE/ASME Transactions on Mechatronics*, 22(2):972–982, 2016.

- [229] Omar Tahri and Francois Chaumette. Point-based and region-based image moments for visual servoing of planar objects. *IEEE Transactions on Robotics*, 21(6):1116–1127, 2005.
- [230] Hanna Michalska and David Q Mayne. Robust receding horizon control of constrained nonlinear systems. *IEEE Transactions on Automatic Control*, 38(11):1623–1633, 1993.
- [231] Hong Chen and Frank Allgöwer. A quasi-infinite horizon nonlinear model predictive control scheme with guaranteed stability. *Automatica*, 34(10):1205–1217, 1998.
- [232] Hassan K Khalil and Jessy W Grizzle. *Nonlinear Systems*, volume 3. Prentice hall Upper Saddle River, NJ, 2002.
- [233] Taeyoung Lee, Melvin Leok, and N Harris McClamroch. Nonlinear robust tracking control of a quadrotor UAV on SE (3). *Asian Journal of Control*, 15(2):391–408, 2013.
- [234] G. Bradski. The OpenCV Library. *Dr. Dobb's Journal of Software Tools*, 2000.
- [235] Joel A E Andersson, Joris Gillis, Greg Horn, James B Rawlings, and Moritz Diehl. CasADi – A software framework for nonlinear optimization and optimal control. *Mathematical Programming Computation*, 11:1–36, 2019.
- [236] Wilko Schwarting, Javier Alonso-Mora, and Daniela Rus. Planning and decision-making for autonomous vehicles. *Annual Review of Control, Robotics, and Autonomous Systems*, 1:187–210, 2018.
- [237] Jong-Min Yang and Jong-Hwan Kim. Sliding mode control for trajectory tracking of nonholonomic wheeled mobile robots. *IEEE Transactions on Robotics and Automation*, 15(3):578–587, 1999.
- [238] Felipe N Martins, Wanderley C Celeste, Ricardo Carelli, Mário Sarcinelli-Filho, and Teodiano F Bastos-Filho. An adaptive dynamic controller for autonomous mobile robot trajectory tracking. *Control Engineering Practice*, 16(11):1354–1363, 2008.
- [239] Zhongqi Sun, Li Dai, Kun Liu, Yuanqing Xia, and Karl Henrik Johansson. Robust MPC for tracking constrained unicycle robots with additive disturbances. *Automatica*, 90:172–184, 2018.

- [240] Dongbing Gu and Huosheng Hu. Receding horizon tracking control of wheeled mobile robots. *IEEE Transactions on Control Systems Technology*, 14(4):743–749, 2006.
- [241] Qi Sun, Jicheng Chen, and Yang Shi. Integral-type event-triggered model predictive control of nonlinear systems with additive disturbance. *IEEE Transactions on Cybernetics*, 2020.
- [242] Guojie Tan, Changyun Wen, and Yeng Chai Soh. Identification for systems with bounded noise. *IEEE Transactions on Automatic Control*, 42(7):996–1001, 1997.
- [243] Wing-Sum Cheung and Jingli Ren. Discrete non-linear inequalities and applications to boundary value problems. *Journal of Mathematical Analysis and Applications*, 319(2):708–724, 2006.